UNIVERSITY OF CALGARY

Src Regulation of von Hippel-Lindau Tumour Suppressor Protein

by

Mary Trieu-Huy Chou

A THESIS

SUBMITTED TO THE FACULTY OF GRADUATE STUDIES

IN PARTIAL FULFILMENT OF THE REQUIREMENTS FOR THE

DEGREE OF DOCTOR OF PHILOSOPHY

DEPARTMENT OF BIOCHEMISTRY AND MOLECULAR BIOLOGY

CALGARY, ALBERTA

September, 2009

UNIVERSITY OF
CALGARY

Abstract

The von Hippel-Lindau (VHL) protein is a tumour suppressor that, when mutated and inactivated, has been associated with renal and CNS cancer development. The VHL tumour suppressor protein normally plays an important role in targeting the HIF-1α (hypoxia inducible factor-1α) transcription factor for degradation, a primary positive regulator of vascular endothelial growth factor (VEGF) production. In this thesis, I report that VHL destabilization can be induced by Src kinase, and may be involved in other cancers including breast cancer. Src is a cytoplasmic tyrosine kinase whose oncogenic potency has been linked to its elevated activity in many cancers. I have found that Src can trigger a drastic reduction in VHL stability even under normoxic conditions, through phosphorylation of VHL tyrosine residue 185, ubiquitination, and proteasome-mediated degradation of VHL. I have also found that E3 ligases Hakai and c-Cbl promote VHL protein destabilization (and destabilization of the VHL ligase complex). In contrast, VHL ligase complex assembly proteins such as elongin C and Cul2 may antagonize the VHL protein destabilization. The Src-induced degradation of VHL protein, ultimately leads to increased HIF-1α protein levels and transcriptional activity. In this manner, Src regulation of VHL protein stability may play an important role in promoting VEGF expression, tumour angiogenesis, and cancer progression.

Acknowledgements

I would like to thank Dr. Don Fujita for his support and mentorship throughout my program. Thank you to past and present members of the Fujita lab, SACRI, and department, whom I have been fortunate to come to know, and who have enriched my PhD journey in so many ways. In particular, I would like to thank Drs. Jeff Bjorge, and Josephine Anthony for their collaborations and helpful discussions. Also thank you Drs. Elana Cherry, Andrew Jakymiw, Shudong Zhu, Ivan Babic, Lisa Yu, and Arja Kaipainen, for your scientific and technical advice, and friendship. Thank you to my supervisory committee, Dr. Shirin Bonni, Dr. Marvin Fritzler, and Dr. Dallan Young for volunteering your time and expertise. I am deeply appreciative of your suggestions and guidance during my program. Also, thank you to my external thesis defense examiners, Dr. Roseline Godbout and Dr. Carrie Shemanko.

I am grateful to Dr. Stephen Lee for providing me with the Flag-VHL-GFP expression vector, Dr. Roland Wenger for the 3xHRE-Luc reporter plasmid, Dr. Joan Brugge for the anti-Src 327 monoclonal hybridoma, Dr. Cora-Jean S. Edgell for the EA.hy926 endothelial cell line, and Dr. Steve Robbins for the 4G10 monoclonal antibody. Thank you to Dr. Michael Ohh and Dr. Kamala Patel for their helpful discussions. Also Drs. Bo young Ahn, Alex Klimowicz, Jennifer Rahn, Stuart Netherton, Laura Gauthier, Laura Zachowski, Cathlin Mutch, Patricia Tang, Tien Phan, and Elizabeth Long, thank you for your friendship.

Finally, this thesis would not have been realized without the steadfast support and encouragement of my family. Mom and Dad, your love and sacrifice are my inspiration. Little sis' Nancy, your boldness and cheer energize me through all.

Dedication

To my family.

And to my early role models Dr. and Mrs. Dale and Carol Bray,

and Mr. and Mrs. Clive and Marie Roberts.

Table of Contents

List of Tables

List of Figures and Illustrations

List of Symbols, Abbreviations and Nomenclature

Symbol	Definition
ATCC	American Type Culture Collection
ARNT	aryl hydrocarbon receptor nuclear translocator
BHK	baby hamster kidney
c-Met	hepatocyte growth factor receptor
CAM	chorioallantoic membrane
CNS	central nervous system
CSF-1R	colony stimulating factor-1 receptor
CSK	C-terminal Src kinase
DMSO	dimethylsulphoxide
ECM	extracellular matrix
EGFR	epidermal growth factor receptor
ELISA	enzyme-linked immunsorbent assay
EPO	erythropoietin
ExPASy	Expert Protein Analysis System
FDA	Food and Drug Administration
FGFR	fibroblast growth factor receptor
GST	glutathione-S-transferase
HEK	human embryonic kidney
HIF	hypoxia inducible factor
HRE	hypoxia response element
ODD	oxygen-dependent degradation
PAGE	polyacrylamide gel electrophoresis
PCR	polymerase chain reaction
PTP	protein tyrosine phosphatase
RT-PCR	reverse transcriptase-polymerase chain reaction
RCC 786-O	renal cell carcinoma cell line 786-O
SCID	severe combined immunodeficiency
SDS	sodium dodecyl sulfate
SH2	Src homology 2 domain
SIB	Swiss Institute of Bioinformatics
TMB	3,3′,5,5′-tetramethylbenzidine
UCP	ubiquitin-conjugating protein
VDU	VHL-interacting deubiquitinating enzyme
VEC	VHL-elongin-Cullin complex
VEGF	vascular endothelial growth factor
VHL	von Hippel-Lindau
VHLaK	VHL-associated KRAB-A domain-containing protein

CHAPTER ONE: INTRODUCTION

1.1 Src oncoprotein

There are nine members of the Src family of kinases (Brown and Cooper, 1996). These proteins can be divided into two classes - those with broad patterns of expression such as Src, Fyn and Yes, and those with more restricted patterns of expression, such as Yrk, Hck, Fgr, Blk, Lck, and Lyn. Perhaps due to the overlapping patterns of expression and potential functional redundancy of these kinases, evaluation of Src function through gene targeting in mice has produced only limited information. Although Src is expressed in most cell-types, targeted disruption of Src leads to one major phenotype - osteopetrosis or a failure to resorb bone due to an intrinsic defect in osteoclasts (Soriano *et al.*, 1991;Boyce *et al.*, 1992). Osteoclasts express high levels of Src and the lack of this molecule leads to dramatic defects in the ability of this cell-type to resorb bone and organize its actin cytoskeleton (Horne *et al.*, 1992;Lowell *et al.*, 1996;Schwartzberg *et al.*, 1997).

The Src family of non-receptor tyrosine kinases is defined by a common modular structure (Brown and Cooper, 1996) (Figure 1). The N-termini of all family members are myristoylated, a fatty acid modification that is determined by the first seven amino acids of the molecule and causes association with the plasma membrane (Resh, 1994). Downstream of the myristoylation sequence lies a short (50 to 80 amino acid) sequence that varies highly among the various family members and is termed the unique domain.

The next section of the protein consists of two distinct regions shared not only with other Src family kinases, but also with a variety of unrelated proteins involved in signal transduction (Pawson and Gish, 1992). These are the Src Homology or SH3 and SH2 domains. The importance of these domains was first suggested by mutants in Src and in non-Src family tyrosine kinases that displayed a variety of host range and conditional transforming phenotypes (Parsons and Weber, 1989;Pawson and Gish, 1992).

It was subsequently demonstrated that these regions encode protein interaction domains. SH3 domains interact with specific proline-rich sequences that fold in a left-handed helix (Cicchetti *et al.*, 1992;Ren *et al.*, 1993). The SH2 domains, bind to phosphorylated tyrosine residues in the context of specific amino acid sequences (Pawson and Gish, 1992;Songyang *et al.*, 1993;Songyang *et al.*, 1995). Using peptide libraries, a consensus binding sequence for Src's SH2 domain was determined to be pYEEI (Songyang *et al.*, 1993). Interestingly, specific *in vivo* interactions may not fit this consensus sequence perfectly - the SH2 domain of Src binds to the platelet-derived growth factor receptor at the sequence pYIpYV (Mori *et al.*, 1993). In this case, phosphorylation of the tyrosine at the +2 position may facilitate binding in the absence of acidic residues.

The C-terminal half of the molecule consists of the kinase or SH1 domain. Certain residues within this domain are strictly conserved among all kinases and are important for the binding of ATP and the phosphotransfer reaction (Hunter and Cooper, 1985). Mutation of these residues can inactivate the kinase (Parsons and Weber, 1989). Other residues within the kinase domain contribute to the enzymatic efficiency. In particular, the major autophosphorylation site (Tyr 419) is located within the kinase

domain in a region termed the activation loop, that has been shown to contain phosphorylated residues in its activated version (Smart *et al.*, 1981). Mutation of the autophosphorylation site (Tyr 419) leads to decreased kinase activity (Kmiecik and Shalloway, 1987;Piwnica-Worms *et al.*, 1987). In addition, a Glu378Gly kinase domain mutation or an Ile441Phe kinase domain mutation also leads to a constitutively activated kinase (avian Src Glu378 corresponding to human c-Src Glu381, and avian Src Ile441 corresponding to human c-Src Ile444), however the mechanism of this activation is unclear (Levy *et al.*, 1986).

Much of the evidence supporting a role for Src as a potential oncogene in human cancer are derived from experiments utilizing v-Src protein or other activated forms of Src to induce cellular transformation, tumourigenicity, tumour progression, and metastasis in experimental animals. The v-Src gene encoded by Rous sarcoma virus was the first transmissible gene found to induce tumours. Early observations of Rous sarcoma virus as a transmissible agent that would produce tumours in chickens were published by Peyton Rous (Rous, 1910). The cellular homologue of v-Src, c-Src, was subsequently found in normal cells and shown to be protooncogenic (Stehelin *et al.*, 1976;Czernilofsky *et al.*, 1980). The structure of the two proteins is similar, but the regulatory carboxyl terminus of v-Src is truncated (resulting in activation), and numerous differences in amino acid sequence throughout the protein exist (enhancing activation) (Jove and Hanafusa, 1987). While the two proteins perform the same function, the kinase activity of v-Src and its capacity to transform are much higher than c-Src. Moreover, cellular transformation by v-Src has been reported to produce a 10-fold elevation in protein phosphorylation over that produced by c-Src. Despite relatively modest protein

expression levels in cells, v-Src invariably results in high levels of cellular transformation as distinguished by altered cellular morphology, cytoskeletal reorganization, proliferation under low serum conditions, and anchorage independent growth. The end result of these changes *in vitro* is the enhanced tumourigenicity *in vivo*. The phosphorylation of numerous cellular substrates on tyrosine residues by v-Src is likely responsible for the effects on cellular transformation. These phosphorylation events are presumed to affect proteins that regulate cell growth and differentiation and include, among others, growth factor receptors, members of signal transduction cascades, and transcription factors (Brown and Cooper, 1996;Thomas and Brugge, 1997).

1.1.1 Mechanisms of Src tyrosine kinase activation

Cumulative evidence supports a role for Src in the development, growth, progression, and metastasis of a number of human cancers including those of the colon, breast, pancreas, and brain. Both Src protein levels, and, to a greater degree, Src protein kinase activity, are frequently elevated in human neoplastic tissues when compared to adjacent normal tissues. Src activation and recruitment to signalling complexes has important implications for cellular fate. It has been well-documented that Src protein levels and Src kinase activity are significantly elevated in human breast cancers (Verbeek *et al.*, 1996;Egan *et al.*, 1999), colon cancers (Bolen *et al.*, 1987a;Cartwright *et al.*, 1990;Irby *et al.*, 1999), and pancreatic cancers (Visser *et al.*, 1996;Lutz *et al.*, 1998). Furthermore, activation of Src by growth factors and growth factor receptors, such as PDGF(R), EGF(R), and HER2/Neu, has been shown to promote cell proliferation (Alonso *et al.*, 1995).

Several mechanisms for high levels of Src activation in human cancer have been proposed (Figure 2). This suggests that the process is multifactorial (Bolen *et al.*, 1987b;Ottenhoff-Kalff *et al.*, 1992;Mao *et al.*, 1997). First, Src can be activated by receptor tyrosine kinases such as EGFR (epidermal growth factor receptor), Her2/Neu, and c-Met (hepatocyte growth factor) (Maa *et al.*, 1995;Mao *et al.*, 1997). These receptors have been known to promote cancer progression, and, in turn, may activate Src. It has been suggested that the association between c-Src and these receptor tyrosine kinases is instrumental in some forms of malignant transformation (Luttrell *et al.*, 1994). The specific activity of Src protein kinase may be increased by direct or indirect interaction with receptor tyrosine kinases, such as EGFR (Luttrell *et al.*, 1994;Mao *et al.*, 1997;Tice *et al.*, 1999), PDGFR (platelet-derived growth factor receptor) (Courtneidge *et al.*, 1993), FGFR (fibroblast growth factor receptor) (LaVallee *et al.*, 1998), CSF-1R (colony stimulating factor-1 receptor (Courtneidge *et al.*, 1993;Levitzki, 1996), HER2/neu (Luttrell *et al.*, 1994), and c-Met (hepatocyte growth factor receptor) (Rahimi *et al.*, 1998). For example, it has been demonstrated that the combination of EGFR and Src expression in fibroblasts leads to synergistic levels of tumourigenicity when compared with expression of EGFR or Src alone (Maa *et al.*, 1995;Mao *et al.*, 1997). Another publication commented on the topic of how co-overexpression of Src and EGFR can collaborate in tumour progression, resulting in particularly aggressive tumours (Bao *et al.*, 2003). The underlying mechanism involves inhibition of the normal c-Cbl regulated process of ligand-induced receptor down-regulation. In response to activation of c-Src, c-Cbl protein undergoes tyrosine phosphorylation that promotes its ubiquitination and proteasomal destruction. Consequently, ubiquitination of EGFR by c-

Cbl is restrained in Src-transformed cells, and receptor sorting to endocytic compartments is impaired. Thus, by promoting destruction of c-Cbl, c-Src enables EGFR to evade desensitization, which could explain Src-EGFR cooperation in oncogenesis. Observations such as these provide strong evidence that Src does not act alone, but may require partnerships for full expression of activity.

Another mechanism for Src activation may involve reductions in the levels or activity of Csk, the enzyme known to phosphorylate the negative regulatory tyrosine residue of c-Src (Tyr 530) (Masaki *et al.*, 1999). In hepatocarcinomas, Src activity has been shown to be correlated with decreased Csk levels (Masaki *et al.*, 1999). Although this mode of activation is anticipated, it does not account for all of the activated Src kinase in human tumours. Enhanced activity of phosphatases (such as PTP1B and Syp/SH-PTP2) is known to dephosphorylate the negative regulatory Tyr 530 and also causes Src activation (Peng and Cartwright, 1995;Egan *et al.*, 1999;Bjorge *et al.*, 2000). Moreover, studies of human breast cancer cell lines demonstrated that phosphatases could activate Src by dephosphorylating the regulatory Tyr 530 (Egan *et al.*, 1999;Bjorge *et al.*, 2000). Thus, several modes of post-translational activation exist for Src.

Furthermore, Src activation can result from genetic mutation of the *src* gene. One naturally occurring human mutation has been reported (Irby *et al.*, 1999). Using a very sensitive, mutant allele-specific assay, a single base pair C-T transition was found in a subset of colon cancer liver metastases and advanced colon cancer primary lesions (Irby *et al.*, 1999). This mutation was identified in codon 531 and resulted in truncation of the Src protein leading to Src activation. This Src 531 mutation was shown to be modestly transforming in focus formation assays and to lead to increased levels of metastatic lung

colonization. Thus, these data support a genetic link between Src activation and cancer development, progression, and metastasis.

Therefore, Src can contribute to cancer development and progression, when overexpressed, activated, or mutated. Src protein levels and/or Src protein kinase activity are frequently elevated in human cancers and cell lines, including those of the breast (Verbeek *et al.*, 1996;Egan *et al.*, 1999), colon (Bolen *et al.*, 1987a;Cartwright *et al.*, 1990;Irby *et al.*, 1999;Zhu *et al.*, 2007), brain (Ding *et al.*, 2003;Weissenberger *et al.*, 2004), and pancreas (Visser *et al.*, 1996;Lutz *et al.*, 1998). Indeed, our laboratory has previously reported elevated levels of endogenous Src activity in breast and colon cancer cells, ranging from 1.7 to 17.3 fold (Egan *et al.*, 1999;Zhu *et al.*, 2007), and that Src kinase can be activated by high levels of the protein tyrosine phosphatase PTP1B in breast and colon cancer cells (Egan *et al.*, 1999;Bjorge *et al.*, 2000;Zhu *et al.*, 2007).

1.2 von Hippel-Lindau tumour suppressor protein and tumour angiogenesis

1.2.1 von Hippel-Lindau disease history

VHL disease is a familial cancer syndrome that was first described in the literature by a German ophthalmologist Eugen von Hippel, a Swedish neuropathologist Arvid Lindau, and a British surgeon E. Treacher Collins at the turn of the 20th century (Maher and Kaelin, Jr., 1997). VHL disease is estimated to affect 1 in 36,000 individuals, displaying no ethnic, racial, cultural, or sexual bias, and is characterized by the presence of hypervascular tumours in multiple organs, including the central nervous system (cerebellum, brainstem, and spinal cord), retina, pancreas, adrenal gland, endolymphatic sac of the inner ear, epididymis (male), and kidneys (Ohh *et al.*, 1999).

Although most of the tumours associated with VHL disease are benign, kidney cancer is malignant and is of the clear cell type, which accounts for 75 % of kidney cancers. Kidney cancer remains the principal cause of morbidity and mortality for VHL patients (Kaelin, Jr., 2002;Ohh and Kaelin, Jr., 2003).

VHL disease is caused by the inheritance of a defective copy of the VHL gene (Latif *et al.*, 1993). Tumours arise in VHL kindred when the remaining wild-type allele is mutated or lost in a susceptible cell. Thus, on a cellular level, VHL disease has an autosomal recessive pattern of inheritance requiring inactivation of both alleles. However, clinically, it is perceived as an autosomal-dominant disease because the occurrence of the second inactivating mutation on the wild-type allele is highly likely (Ohh and Kaelin, Jr., 2003). VHL inactivation has been established as an early and requisite step in renal clear-cell carcinoma (RCC) pathogenesis, as the loss of heterozygosity in the remaining wild-type VHL allele in the proximal renal tubular epithelial cells has been documented in early premalignant renal cysts in VHL patients (Lubensky *et al.*, 1996). In keeping with the two-hit model of Knudson (Knudson, Jr., 1971), biallelic inactivation of the VHL gene is also observed in the majority of sporadic RCC, establishing VHL as a critical gatekeeper of the renal epithelium.

The VHL gene consists of three exons, producing an mRNA of 4.5 kb. The mRNA can be translated into two proteins due to an alternative in-frame, internal translational initiation start site at codon 54 (Iliopoulos *et al.*, 1998;Schoenfeld *et al.*, 1998;Blankenship *et al.*, 1999) (Figure 3). The larger product is a 213-amino-acid protein of approximately 24 to 30 kDa (VHL p30) including an N-terminal pentameric acidic repeat domain, and the shorter product is an 18- to 19-kDa isoform (VHL p19) of

160 amino acids, lacks the N-terminal acidic repeat domain. Both protein isoforms have been found to behave similarly in most functional assays, and are often referred to generically as pVHL. Notably, almost all disease-associated *VHL* mutations map to the region of VHL shared by both long and short VHL isoforms, suggesting that the short form of VHL possesses significant tumour suppressor activity *in vivo*. Reconstitution of RCC cells with either VHL30 or VHL19 suppressed tumour development in a nude mouse xenograft assay (Iliopoulos *et al.*, 1995;Gnarra *et al.*, 1996;Schoenfeld *et al.*, 1998;Blankenship *et al.*, 1999). These observations led to the belief that VHL30 and VHL19 have overlapping functions as tumour suppressors.

However, some findings challenge this notion. Firstly, *VHL* mutations associated with tumour development have been identified throughout the *VHL* open reading frame, including several mutations within the first 53 amino acids that are predicted to produce functional VHL19 (Crossey *et al.*, 1994;Zbar *et al.*, 1996;van der *et al.*, 1998). Secondly, VHL30 and VHL19 were shown to have different subcellular localization profiles. VHL can shuttle back and forth between the nucleus and the cytoplasm, with the bulk of the protein located in the cytoplasm under steady-state conditions (Iliopoulos *et al.*, 1995;Bonicalzi *et al.*, 2001;Groulx and Lee, 2002). Under low pH conditions, a greater fraction of VHL is sequestered in nucleoli (Mekhail *et al.*, 2004;Mekhail *et al.*, 2005) VHL30 is found in the nuclear, cytosolic, and membranous [associated with endoplasmic reticulum (ER)] fractions, but VHL19 is excluded from the membrane fraction (Zbar *et al.*, 1996;Corless *et al.*, 1997;Ohh *et al.*, 1998). The functional significance of VHL30 association with ER is still debatable, however, it may be related to the ability of VHL30, but not VHL19, to bind fibronectin and its requirement to promote the assembly of

fibronectin extracellular matrix (ECM) (Ohh *et al.*, 1998;Esteban-Barragan *et al.*, 2002). VHL30 long form is also more tightly associated with microtubules in the cytoplasm than the short form (Iliopoulos *et al.*, 1998;Hergovich *et al.*, 2003). Stickle *et al.* (Stickle *et al.*, 2004) have shown that mutant VHL-expressing RCC cells, with intact hypoxia-inducible factor (HIF) regulation but defective fibronectin ECM assembly, formed tumours in an SCID mouse xenograft assay, underscoring a significance for proper fibronectin ECM in the development of RCC. In addition, phosphorylation of the N-terminal acidic domain, which is lacking in VHL19, by casein kinase 2 was shown to prevent the binding of VHL30 to fibronectin (Lolkema *et al.*, 2005). This result suggests that, although the first 53 amino acids of VHL30 are required for binding fibronectin, phosphorylation of this region either prevents the recruitment of fibronectin or releases bound fibronectin in the ER. Indeed, there still remains much to be studied with regard to the question of whether VHL19 can support a tumour-suppressor role, and differences in the tumour suppressor roles of VHL30 versus VHL19.

VHL disease is classified into categories, depending on a patient's likelihood of developing phaeochromocytoma (Ohh and Kaelin, Jr., 2003). Type 1 patients have a low risk of developing phaeochromocytoma (of the adrenal medulla), but present with RCC. Type 2 patients have a high risk of developing phaeochromocytoma, with type 2A patients having a low risk of developing RCC but with type 2B patients having a high risk of developing RCC. Type 1, type 2A, and type 2B patients also develop the two cardinal features of VHL disease: cerebellar and retinal hemangioblastomas. Type 2C patients develop phaeochromocytoma exclusively. The mutations associated with type 1

disease are deletions, microinsertions, and nonsense mutations, whereas type 2 patients typically present with missense mutations.

Conventional knockout of VHL in mice results in embryonic lethality due to defective placental vasculature, precluding the study of VHL inactivation/disease in adults (Gnarra *et al.*, 1997). Therefore, to generate a mouse model to study VHL disease, Rankin *et al.* (2006) used the phosphoenolpyruvate carboxykinase (PEPCK) promoter to generate transgenic mice in which Cre-recombinase was expressed in renal proximal tubules and hepatocytes. Conditional inactivation of VHL in PEPCK-Cre mice resulted in glomerular and tubular renal cysts, increased serum erythropoietin (EPO) levels, and polycythemia (Rankin *et al.*, 2006). Notably, elevation of EPO level was limited to the liver, whereas HIF downstream genes carbonic anhydrase 9 and multidrug resistance gene 1 were increased in the renal cortex. Development of renal cysts in mice with VHL inactivation is similar to the human condition wherein loss of VHL has been observed in preneoplastic cysts (Lubensky *et al.*, 1996), and suggests that other genetic events are required for the progression of premalignant cysts to RCC.

Restoration of *VHL* function in *VHL−/−* clear cell renal carcinoma cells is sufficient to inhibit their growth as tumours in xenograft assays in nude mice (Iliopoulos *et al.*, 1995;Gnarra *et al.*, 1996). Therefore, *VHL* inactivation appears to play a role in tumour maintenance as well as in tumour initiation. Reintroduction of wildtype *VHL* into *VHL−/−* clear cell renal carcinoma cells usually does not grossly affect cell proliferation under serum-rich conditions. Under low-serum conditions, *VHL−/−* clear cell renal carcinoma cells fail to exit the cell cycle properly compared with their wildtype counterparts (Pause *et al.*, 1998), and VHL inhibits cell growth at high cell density

(confluence) (Baba *et al.*, 2001;Davidowitz *et al.*, 2001). *VHL−/−* clear cell renal carcinoma cells also display features suggestive of an epithelial-to-mesenchymal transition. Restoration of VHL function promotes the reacquisition of epithelial markers, especially when cells are grown under low-serum conditions (Davidowitz *et al.*, 2001). VHL-defective renal carcinoma cells display abnormalities in cytoskeletal architecture (actin, vinculin, and tubulin), cell-cell adhesion, integrin expression, and extracellular matrix formation, all of which can be corrected upon reintroduction of wild-type VHL. These abnormalities appear to be at least partially HIF-independent, and genetic studies in *Caenorhabditis elegans* strongly suggest a role for VHL in extracellular matrix control independent of its role in HIF regulation (Bishop *et al.*, 2004).

VHL also plays a role in the control of renal cell apoptosis. For example, loss of *VHL* sensitizes clear cell renal carcinoma cells to UV-induced apoptosis (Schoenfeld *et al.*, 2000b), but protects them from apoptosis induced by TNF (Caldwell *et al.*, 2002;Galban *et al.*, 2003;Qi and Ohh, 2003). The former correlates with a failure to induce p21 and p27 properly in response to UV damage (Schoenfeld *et al.*, 2000b); the latter appears to be multifactorial and may involve VHL-dependent changes in NFκB activity (Qi and Ohh, 2003;An and Rettig, 2005).

1.2.2 The VEC complex and ubiquitin-mediated destruction

The full proteasome-dependent protein degradation pathway was seminally delineated by Hershko, Ciechanover, and Rose (Hershko *et al.*, 1983). Activated ubiquitin bound via its COOH terminus to the thiol site of an E1 ubiquitin-activating enzyme, is first transferred to another sulfhydryl site on E2 ubiquitin-conjugating

enzyme. Ubiquitin is then further transferred from E2-bound thiol esters to the target substrate in the presence of E3 ubiquitin ligase. The E3 catalyzed reaction is repeated on the target substrate, resulting in polyubiquitination. This ubiquitin chain is recognized in the opening of the proteasome, and the protein enters and is degraded in the proteasome. Therefore, the work of Hershko, Ciechanover, and Rose was able to elucidate the components involved in cellular proteasome-dependent degradation cellular protein degradation, which can be summarized in an equation schematic as follows:

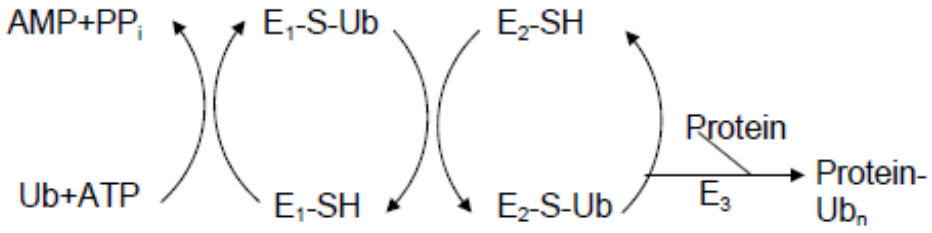

Specifically, VHL (VHL30 or VHL19) is a component of the E3 ubiquitin ligase complex called VEC, consisting of elongin B, elongin C, Rbx1 (also known as ROC1/Hrt1), and Cullin 2 (Cul2) (Ohh and Kaelin, Jr., 2003). Structurally and functionally, VEC is analogous to the Skp1/Cdc53/F-box protein (SCF) complex. VHL consists of two functional domains: an α domain and a β domain (Stebbins *et al.*, 1999). The α domain is required for binding elongin C, which binds to Cul2 to nucleate the VEC complex. The β domain acts as a substrate-recognition/docking site. Disease-associated mutations in VHL kindred frequently map to surface residues on either domain, suggesting that these domains are important for the tumour suppressor function of VHL. Rbx1, which is recruited by Cul2, is thought to recognize a cognate E2 ubiquitin-conjugating enzyme required for the E3 ligase function of VEC (Stebbins *et al.*, 1999).

Several putative target substrates of VEC, including atypical protein kinase C (Okuda *et al.*, 1999), VHL-interacting deubiquitinating enzyme (Li *et al.*, 2002), and the seventh (Rpb7) and the large (Rbp1) subunits of RNA polymerase II (Na *et al.*, 2003), have been identified. Interestingly, though, not every protein bound by VHL is subjected to polyubiquitination. These include SP1 transcription factor (Cohen *et al.*, 1979), VHL-associated KRAB-A domain–containing protein transcription repressor (Li *et al.*, 2003), microtubules (Hergovich *et al.*, 2003), and fibronectin (Ohh *et al.*, 1998;Hoffman *et al.*, 2001). These findings have led to the notion that VHL has multiple functions from transcription, to cytoskeletal organization, to ECM assembly through ubiquitin-dependent and ubiquitin-independent mechanisms. Although these are intriguing possibilities, especially with growing evidence supporting the role of VHL in the assembly of fibronectin ECM, the extent of the physiological relevance of these functions for the tumour-suppressor activity of VHL remains to be further studied.

What is widely accepted as a bona fide VEC substrate is the α subunit of HIF (Maxwell *et al.*, 1999;Ohh *et al.*, 2000). HIF is the major transcription factor that transactivates a number (more than 60 and growing) of hypoxia-inducible genes, including vascular endothelial growth factor (VEGF; also known as vascular permeability factor), erythropoietin (EPO), and glucose transporter-1(GLUT1), to promote angiogenesis, production of oxygen-carrying erythrocytes, and anaerobic metabolism, respectively, in adaptation to reduced oxygen tension (Semenza, 1999;Zhu and Bunn, 2001) (Figure 4). There are three members of the HIF family (HIF-1, HIF-2, and HIF-3) in humans (Maynard and Ohh, 2004). HIF is a heterodimeric complex consisting of α and β subunits. The β subunit [also known as aryl hydrocarbon receptor nuclear

translocator (ARNT)] is abundantly expressed independent of oxygen tension, whereas the α subunit is oxygen labile. Specifically, the α subunit is ubiquitinated on a stretch of residues within its oxygen-dependent degradation (ODD) domain and, consequently, is targeted for degradation through the 26S proteasome (Huang *et al.*, 1998). Under hypoxia, HIF-α is stabilized and binds to the common ARNT to form an active HIF complex, which binds to hypoxia response elements (HREs) within the promoter/enhancer of hypoxia-inducible genes. Thus, HIF regulation occurs at the level of the α subunit.

VHL, through its substrate-binding β domain, recruits the HIF-α subunit for oxygen-dependent ubiquitination (Tanimoto *et al.*, 2000). In the presence of oxygen, HIF-α is hydroxylated on conserved prolines (P) at positions 402 and 564 (the number according to HIF-1α) within the ODD domain by prolyl hydroxylase domain (PHD)–containing enzymes (Jaakkola *et al.*, 2001;Ivan *et al.*, 2001). P564 hydroxylation is both necessary and sufficient for the binding of HIF-α ODD to VHL. Thus, ubiquitin-mediated destruction of HIF-α only occurs in the presence of oxygen. Accordingly, under hypoxia, HIF-α is no longer prolyl hydroxylated and thus escapes recognition by VHL. The now stable HIF-α dimerizes with HIF-β (ARNT) to bind HREs to trigger transcriptional activation of various hypoxia-inducible genes.

In addition, a conserved C-terminal asparagine at position 803 on HIF-1α is hydroxylated by the factor-inhibiting HIF-1 enzyme in the presence of oxygen (Lando *et al.*, 2002). Unlike prolyl hydroxylation, which induces VHL binding to HIF-α, asparagyl hydroxylation prevents the recruitment of p300/CBP transcriptional coactivators to HIF-

α. Therefore, asparagyl hydroxylation of HIF-1α attenuates the transcription of HIF target genes (Dames *et al.*, 2002). This would suggest that there are, at a minimum, two mechanisms that negatively regulate the expression of hypoxia-inducible genes under normoxia 1) oxygen-dependent ubiquitination of HIF-α through VEC and 2) the inhibition of p300/CBP recruitment in remaining HIF-α that has evaded destruction by VEC.

1.2.3 Tumour angiogenesis, Src, and VHL, in tumour progression

Angiogenesis is a process that is of critical importance to tumourigenesis and tumour metastasis, as well as to the growth and maintenance of normal vasculature. Both the processes of angiogenesis and tumourigenic proliferation are key events essential for the successful growth of vascularized tumours. Indeed, inhibition of neovascularization has been shown to abolish or slow tumour growth in various experimental models (Ruegg *et al.*, 1998;Bergers *et al.*, 1999). Angiogenesis plays both beneficial and detrimental roles in normal and disease processes. For example, abnormally enhanced angiogenic responses are observed during conditions such as diabetic retinopathy and rheumatoid arthritis (Folkman, 1995). On the other hand, promotion of the angiogenic response has been demonstrated to be beneficial in treating ischemic conditions, such as myocardial ischemia/infarction (Isner and Asahara, 1999). Thus, a comprehensive understanding of the molecular mechanisms underlying the angiogenic response may help in preventing and treating many diseases displaying aberrant angiogenesis.

The process of angiogenesis is complex and multistage. Endothelial cells undergo a transition from quiescent to a proliferative state, loosen the cell-cell contacts within the

vascular wall, detach from the parent vessels, and migrate directionally. Vasodilation, mediated by nitric oxide, and increased vascular permeability, which allows for extravasation of plasma proteins serving as a provisional scaffold for migrating endothelial cells, are initial components of the angiogenic program. Further steps in the formation of functional vessels include lumen formation and vessel stabilization (Carmeliet, 2000). In conjunction with other endothelial-specific signalling systems such as angiopoietins and Tie receptors, VE-cadherin/β-catenin, and $a_v\beta_3$ integrins, vascular endothelial growth factor receptors (VEGFRs) relay the signals essential for stimulation of vessel growth.

Elevated Src activity has been reported to upregulate vascular endothelial growth factor (VEGF) production in several normal and tumourigenic cells types (Mukhopadhyay *et al.*, 1995;Ellis *et al.*, 1998;Wiener *et al.*, 1999). Src has also been shown to be required for VEGF-mediated vascular permeability (Weis *et al.*, 2004). Collectively, these and other findings support a role for Src in promoting tumour angiogenesis and cancer progression.

Several lines of evidence support the significance of the VHL regulation of angiogenesis in cancer. VHL-associated tumours are highly vascularized, displaying overproduction of angiogenic peptides, such as VEGF, which is one of many HIF-regulated genes. In addition, VHL-defective cells express inordinately high levels of numerous hypoxia inducible transcripts even under normoxic conditions (Stratmann *et al.*, 1997). Reconstitution of cells devoid of VHL with wild-type VHL restored the cells' ability to regulate or, more precisely, downregulate the expression of hypoxia-inducible genes in the presence of oxygen (Stratmann *et al.*, 1997).

VEGF production is normally regulated by changes in tissue oxygenation. Under normoxic conditions, the von Hippel-Lindau protein (VHL, an E3 ligase) is capable of physically binding to and triggering proteasome-mediated destruction of a proline-hydroxylated form of hypoxia inducible factor-1α (HIF-1α), the regulatable component of the HIF-1 transcription factor heterodimer. Therefore, in the presence of VHL, HIF-1α is targeted for proteasome-mediated degradation (Semenza and Wang, 1992;Guillemin and Krasnow, 1997;Semenza, 2000). However, under hypoxic conditions, such as those existing within interior regions of solid tumours, hydroxylation of HIF-1α is inhibited, thus preventing VHL binding to HIF-1α and preventing HIF-1α degradation in these tumour cells. The HIF-1 transcription factor is then able to recognize the VEGF promoter and upregulate VEGF transcription. VEGF is a potent stimulator of angiogenesis, playing an important role in facilitating tumour progression and metastasis (Cavallaro and Christofori, 2000;Neufeld *et al.*, 2001). VEGF produced and secreted from the tumour cells is able to bind to cell surface receptors on endothelial cells, stimulating endothelial cell proliferation and angiogenesis, and contributing to further tumour progression and metastasis. Importantly, functional inactivation of the VHL tumour suppressor protein through germline mutations has been documented in highly vascular tumours which overproduce VEGF, such as renal carcinomas, phaeochromocytomas, and central nervous system hemangioblastomas (Latif *et al.*, 1993;Chen *et al.*, 1995;Zbar *et al.*, 1996;Neumann and Bender, 1998;Kaelin, Jr., 2002;Kaelin, Jr., 2007).

1.3 Overview of the project

Mutation or inactivation of tumour suppressor proteins can often result in disease and cancer progression. Thus, characterizing the inappropriate modifications of molecules such as VHL and understanding the functional consequence of these changes on protein function, are key towards deciphering the elaborate code dictating cellular biochemistry. Such information could reveal new targets for directed therapy of cancer and diseases resulting from deregulated signalling pathways.

1.3.1 Hypothesis

In some tumour cells VEGF is produced even under normoxic condition. However, details of the Src-induced mechanisms or pathways responsible for this effect have not been extensively studied. My preliminary evidence led me to reason that Src can potentially stimulate VEGF synthesis under normoxic conditions in malignant breast cancer cells, through the targeted phosphorylation and ubiquitin-targeted destruction of VHL tumour suppressor protein, which is a major regulator of VEGF synthesis.

1.3.2 Objective

My overall objective is to investigate the mechanisms involved in Src-mediated reduction in levels of VHL tumour suppressor protein. This is an important avenue of investigation, the results of which might explain why high Src activity is often highly correlated with tumour progression and metastasis in breast cancer and other cancers. The conclusions arising from this research plan may also elucidate why Src is such a potent oncoprotein, since such Src-mediated effects would give a selective growth advantage to cells even under normoxic conditions because of their resulting increased VEGF production. The findings from this project will also reveal important mechanisms

that could be targeted for reducing Src-dependant tumour angiogenesis and cancer progression.

In this thesis, I report that elevated Src activity in breast cancer and other cell lines can drastically reduce VHL stability, half-life, and tumour suppressive function even under normoxic conditions (Figure 5). Specifically, Src activation results in increased tyrosine phosphorylation of VHL, and ubiquitination of VHL, which promotes degradation of VHL by 26S proteasomes. The results of this project demonstrate that a dramatic reduction of VHL levels mediated by Src can contribute to increased cellular synthesis of VEGF, via increased levels and activity of HIF-1α protein. Overall this thesis describes the finding of an important mechanism of Src-dependent destruction of VHL protein involved in promoting tumour angiogenesis and cancer progression.

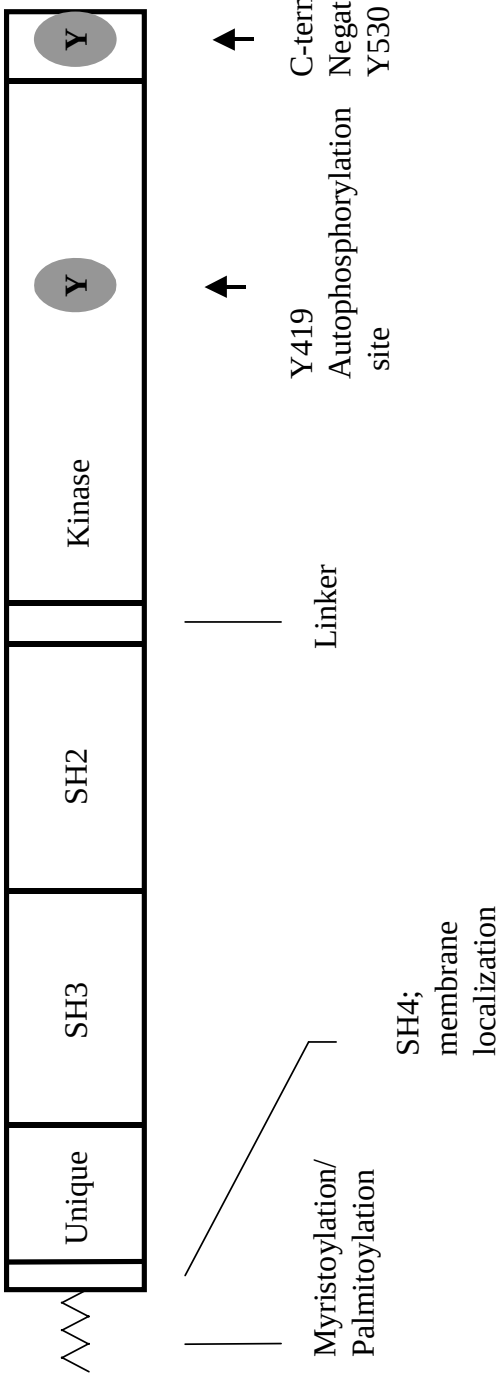
Unique
SH3
SH2
Kinase
Y
Y
Myristoylation/
Palmitoylation
SH4;
membrane
localization
Linker
Y419
Autophosphorylation
site
C-terminal
Negative regulatory
Y530

Figure 1. The domain structure of Src protein tyrosine kinases.

Src protein tyrosine kinase family members all contains six distinct functional regions: an N-terminal Src homology (SH) 4 domain, which directs myristoylation (also directs palmitoylation in the case of several of the Src family kinase members), a unique domain, an SH3 domain, an SH2 domain, a catalytic kinase domain, and a short C-terminal negative regulatory tail that functions in negative regulation of Src activity.

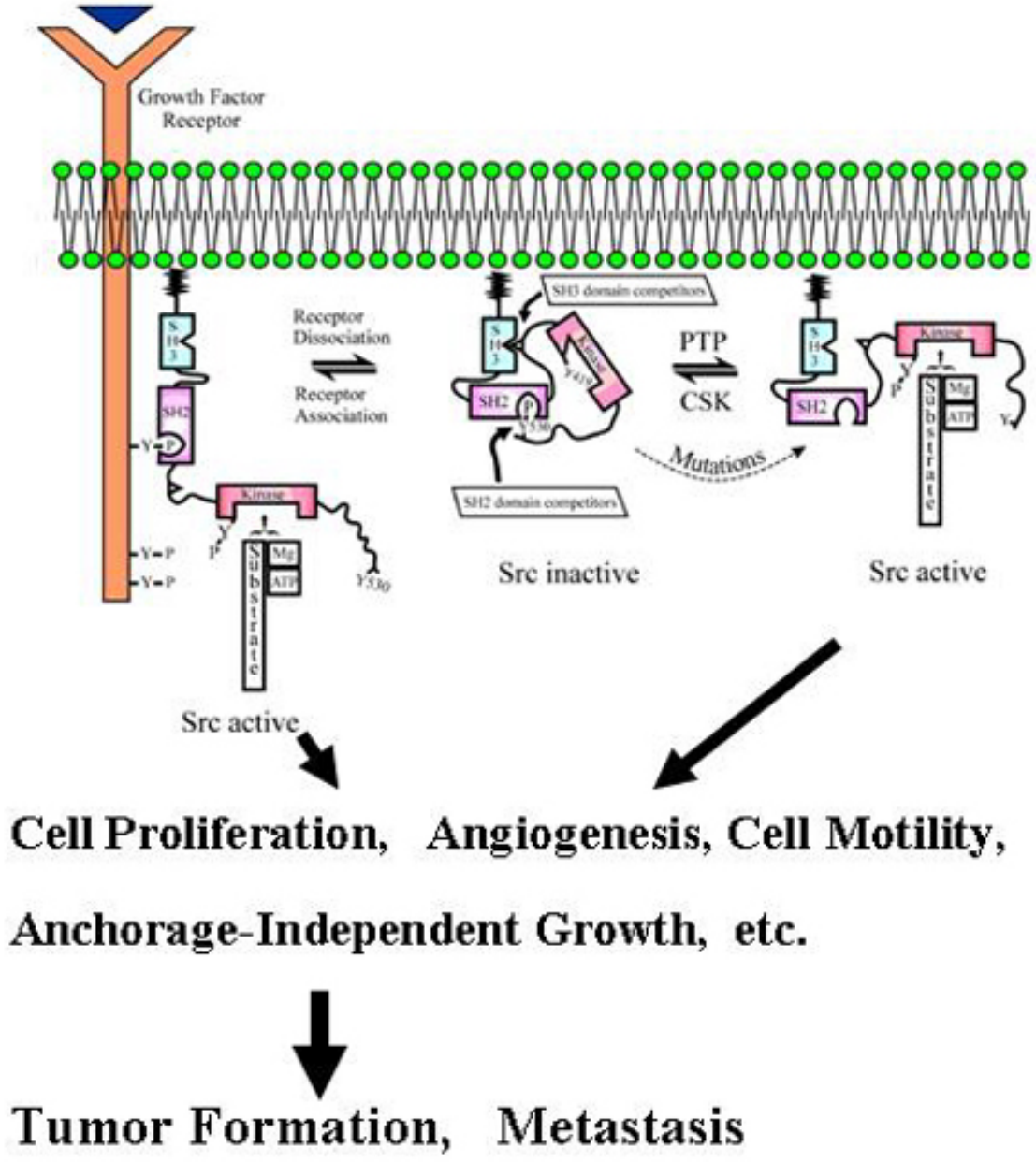

(Figure courtesy of J.D. Bjorge and D.J. Fujita.)

Figure 2. Mechanism of Src activation: aberrant Src activation can lead to tumour growth and metastasis.

The structural model in the centre represents Src in the inactive conformation, in which the C-terminal regulatory Tyr530 (human c-Src) is phosphorylated and bound to the SH2 domain, positioning the SH3 domain such that it can interact with the linker region. The structures on the left and right represent Src in the active conformation in which the intramolecular interactions with the SH2 and SH3 domains are disrupted. The mechanisms of activation of Src include protein tyrosine phosphatases (PTPs), mutations, and ligand displacement. Tyr419 is the autophosphorylation site in the activation loop of Src. The CSK (C-terminal Src kinase) phosphorylates Src on Tyr530 and restores Src to its inactive conformation.

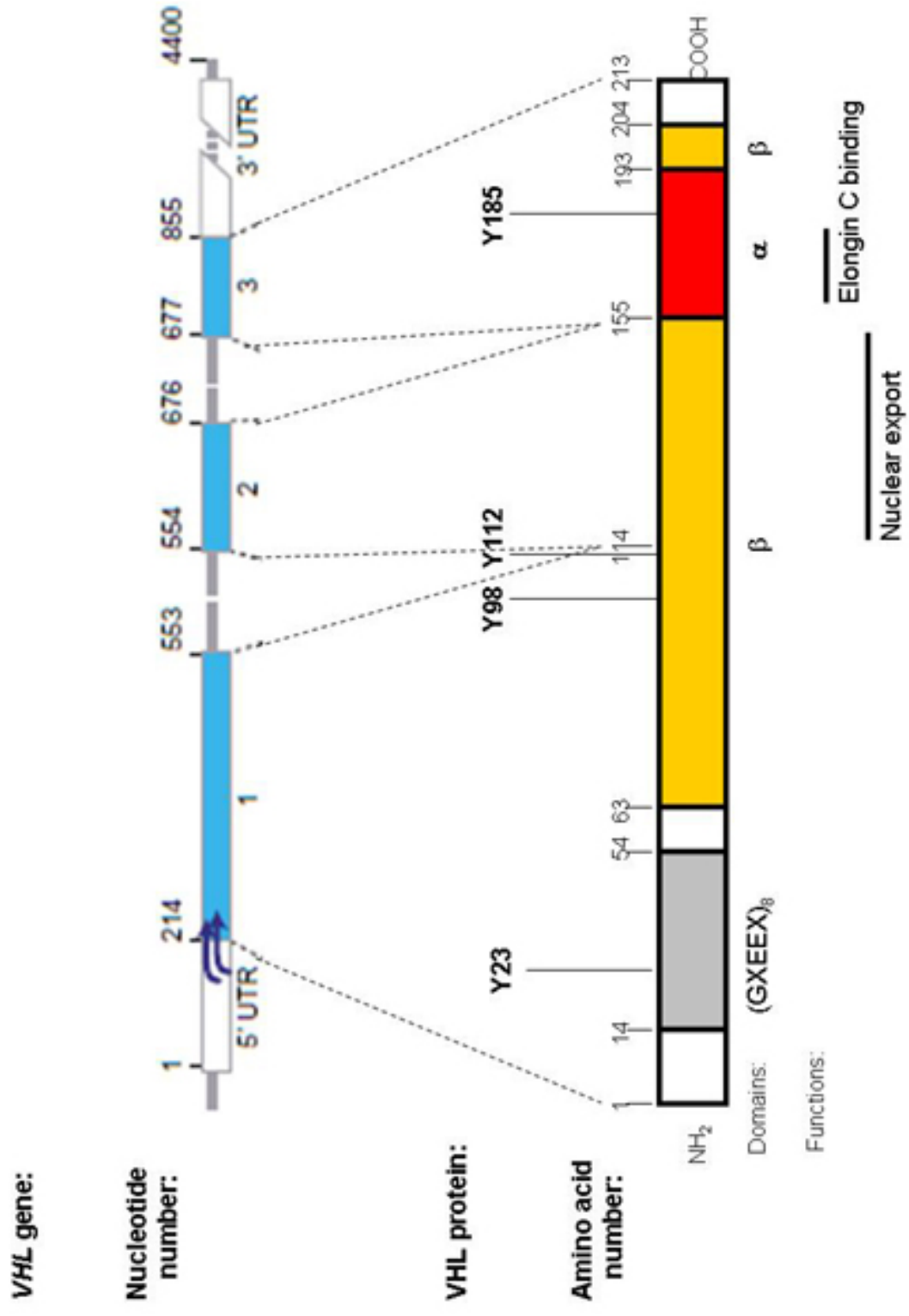
VHL gene:
Nucleotide number:
VHL protein:
Amino acid number:
1
214
553
554
676
677
855
4400
5' UTR
3' UTR
1
2
3
Y23
Y98
Y112
Y185
1
14
54
63
114
155
193
204
213
NH2
COOH
Domains:
(GXEEX)8
β
α
β
Functions:
Elongin C binding
Nuclear export

Figure 3. Schematic of VHL gene and protein.

(A) The *VHL* gene structure. The VHL mRNA is coded from three exons. There are two methionine (Met) start codons, one at codon 1 and a second one in-frame at codon 54. (B) The VHL protein regions. The VHL α region is able to bind proteins that are able to act as assembly proteins in the VHL ligase complex, such as elongin C that enhances recruitment of E2 ubiquitin-conjugating enzyme in to the VHL complex. The VHL β region is able to bind the target for protein degradation. (Figure modified from Richards, 2001.)

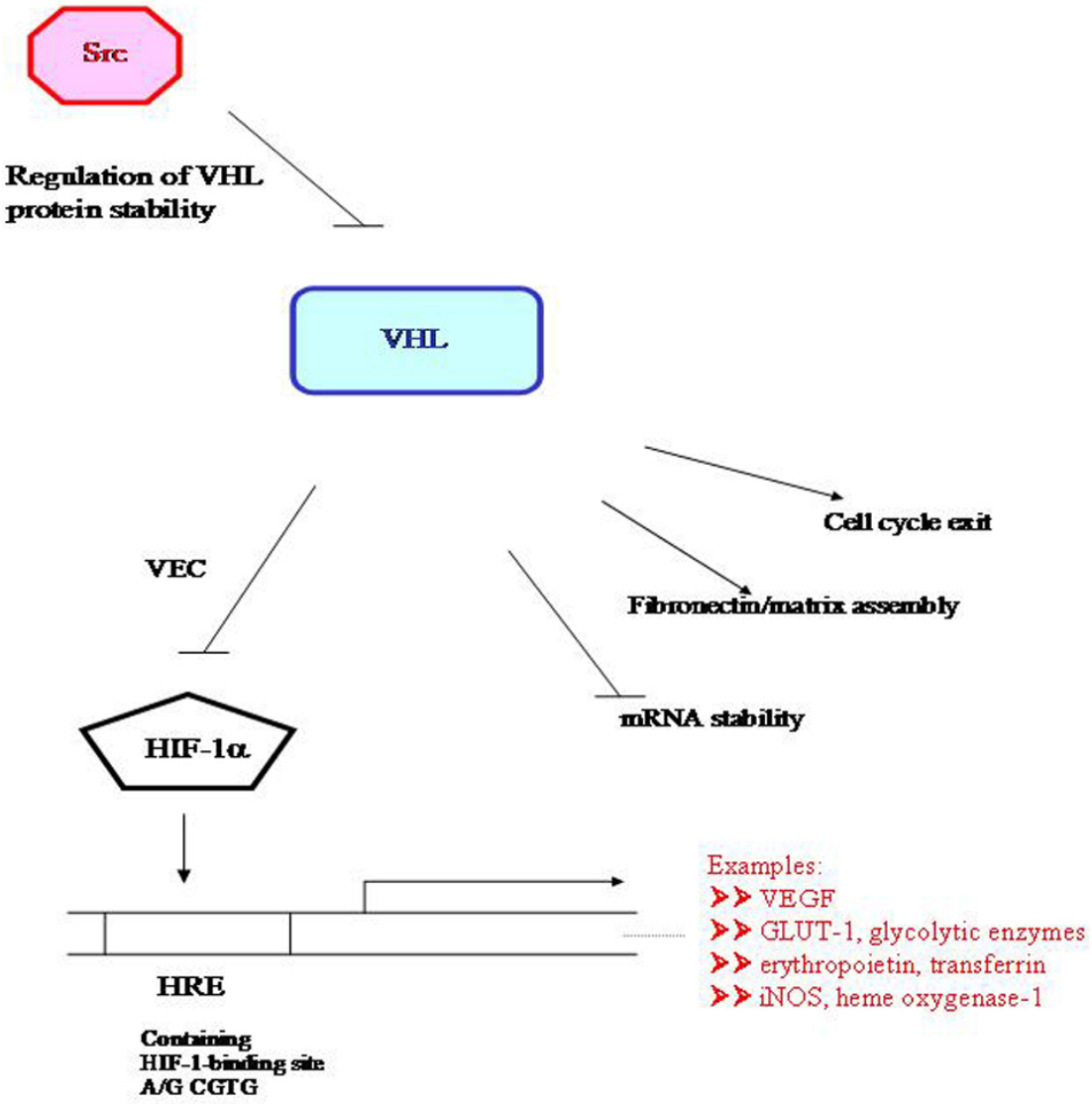

Figure 4. Schematic of the cellular functions of VHL.

VHL has various cellular roles including downregulation of HIF-1α and HRE (hypoxia response element) genes, decreasing mRNA stability, binding to fibronectin and promoting the assembly of fibronectin extracellular matrix (ECM), and promoting cell cycle exit.

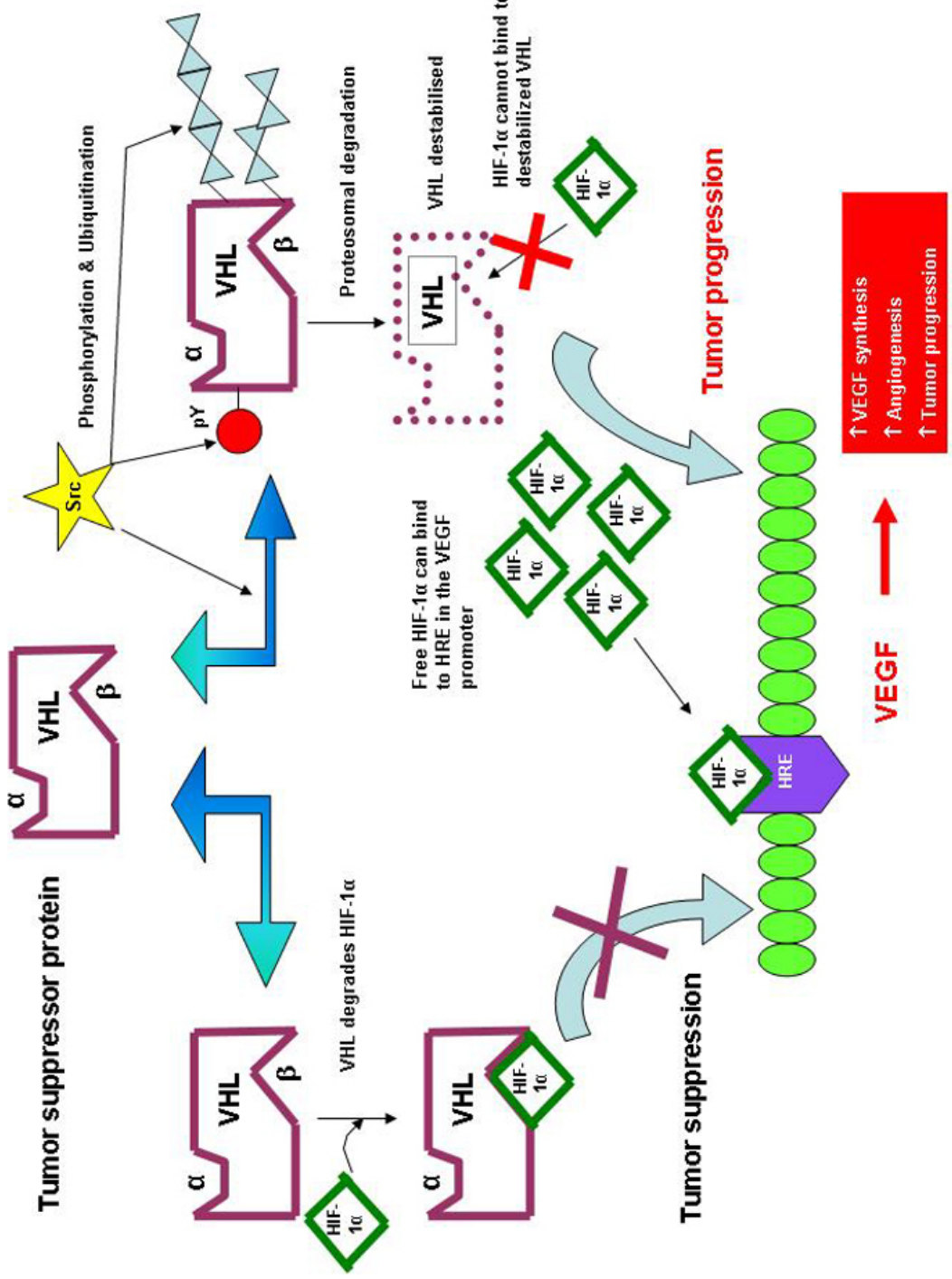
Tumor suppressor protein
α
VHL
β
Phosphorylation & Ubiquitination
Src
pY
α
VHL
β
Proteosomal degradation
VHL destabilised
VHL
HIF-1α cannot bind to destabilized VHL
HIF-1α
Free HIF-1α can bind to HRE in the VEGF promoter
HIF-1α
HIF-1α
HIF-1α
HIF-1α
Tumor progression
VHL degrades HIF-1α
α
VHL
β
HIF-1α
α
VHL
HIF-1α
Tumor suppression
HIF-1α
HRE
VEGF
↑ VEGF synthesis
↑ Angiogenesis
↑ Tumor progression

Figure 5. Model of Src downregulation of von Hippel-Lindau tumour suppressor protein.

Src tyrosine phosphorylation VHL allows tagging and recruitment of VHL for proteolysis by an E3 ligase complex. Also, post-translational modification of VHL may displace VHL from the VHL E3 ligase complex (thereby facilitating ubiquitin tagging and recruitment of VHL for proteolysis by E3 ligase complexes and/or facilitating VHL protein instability). Consequently, a build up of increased levels of HIF-1α upregulates VEGF production, and ultimately increases tumour angiogenesis, and increases the potential for tumour malignancy.

CHAPTER TWO: MATERIALS AND METHODS

2.1 Cell culture

The mammalian cell lines, unless otherwise stated, were maintained in Dulbecco's modified Eagle's medium (DMEM) (Gibco Invitrogen) containing 10 % fetal bovine serum, and antibiotics (100 units/mL penicillin, 100 μg/mL streptomycin, and 0.25 μg/mL amphotericin) (Gibco Invitrogen) at 37 ^{o}C in 5 % CO_2. Cell lines MCF-10A, BT-483, SK-BR-3, Hs 578T, MDA-MB-435S, and RCC 786-O were obtained from American Type Culture Collection (ATCC). Human mammary epithelial control cell lines MCF-10A was grown at 37 ^{o}C in 5 % CO_2, and were maintained in DMEM/Ham's F12 (1:1, Gibco Invitrogen) supplemented with 5 % horse serum (Sigma), 2 mM L-glutamine (Gibco Invitrogen), 20 ng epidermal growth factor (Gibco Invitrogen), 100 ng/mL cholera toxin (Calbiochem), 0.01 mg/mL insulin (Sigma), 500 ng/mL hydrocortisone (Sigma), and antibiotics (100 units/mL penicillin, 100 μg/mL streptomycin, and 0.25 μg/mL amphotericin) (Gibco Invitrogen).

2.2 Antibodies and reagents

Unless otherwise specified antibodies were used at 10 μg/mL final concentration in Western blot incubations. Anti-Src 327 monoclonal antibody Cruz (used at 1:500 dilution for Western blotting) was purified from a hybridoma provided by Dr. Joan Brugge (Harvard Medical School). Anti –Src phosphotyrosine 419 antibody (used at

1:1000 dilution for Western blotting) was purchased from Cell Signalling. Anti-VHL (FL 1-181) rabbit polyclonal antibody was purchased from Santa Cruz (used at 1:1000 dilution for Western blotting), and anti-VHL (1g32) mouse monoclonal antibody (used at 1:200 for Western blotting) was purchased from BD Biosciences Pharmingen. Anti-Flag M2 mouse monoclonal antibody (used at 1:500 dilution for Western blotting) and anti-Flag M2 affinity gel (monoclonal antibody covalently conjugated to agarose beads) were purchased from Sigma. Anti-HIF-1α mouse monoclonal antibody (used at 1:200 for Western blotting) was purchased from BD Biosciences Transduction Laboratories. Anti-VEGF (A-20) rabbit polyclonal antibody (used at 1:1000 dilution for Western blotting), and anti-GFP (FL) rabbit polyclonal antibody (used at 1:1000 dilution for Western blotting) were purchased from Santa Cruz. Isotype control IgG antibodies were purchased from Santa Cruz. Anti-α-tubulin (DM1A, CP06) mouse monoclonal antibody (used at 1:1000 dilution for Western blotting) was purchased from Calbiochem. Anti-phosphotyrosine (4G10) mouse monoclonal antibody (used at 1:1000 dilution for Western blotting) and anti c-Cbl (7G10) mouse monoclonal antibody (used at 1:1000 dilution for Western blotting) were provided by Dr. Stephen Robbins (University of Calgary). Anti-ubiquitin (Ubi-1) mouse monoclonal antibody (used at 1:200 for Western blotting) was purchased from Zymed Invitrogen. Anti-HA (HA.C5) mouse monoclonal antibody (used at 1:200 for Western blotting) and anti-GST (3G10/1B3) mouse monoclonal antibody (used at 1:200 dilution for Western blotting) were purchased from Abcam. Anti-Hakai (ZMD.288) rabbit polyclonal antibody (used at 1:200 for Western blotting) was purchased from Zymed Invitrogen. Anti-elongin C rabbit polyclonal antibody (used at 1:1000 dilution for Western blotting) and anti-Rbx1 (N-15) rabbit

polyclonal antibody (used at 1:1000 dilution for Western blotting). And anti-Cul2 mouse monoclonal antibody (used at 1:200 for Western blotting) was purchased from BD Biosciences Pharmingen.

MG-132 and PP2 were purchased from Calbiochem. Cycloheximide was purchased from Sigma. Unless otherwise indicated, general laboratory chemicals were purchased from Sigma, Gibco Invitrogen, BDH, Fisher, or EMD chemicals.

2.3 Plasmids

The human wildtype Src expression construct was made by subcloning human Src cDNA into the pCI mammalian expression vector (pCI-CMVp, Promega). The Flag-tagged VHL-GFP expression plasmid (pcDNA3.1-CMVp-Flag-VHL-GFP) and Flag-GFP-GFP control expression plasmid (pcDNA3.1-CMVp-Flag-GFP -GFP) were kindly provided by Dr. Stephen Lee (University of Ottawa), and have been described previously (Groulx *et al.*, 2000). HA-Ubiquitin expression plasmid (pMT123-CMVp-HA-Ubiquitinx8) was kindly provided by Dr. G. Steven Martin (University of California, Berkely). HREx3-Luciferase reporter plasmid (pGL3-HREx3-SV40p-Luciferase) was a gift from Dr. Roland Wenger (University of Zurich). The LNCX-β-galactosidase expression plasmid (LNCX-CMVp-β-galactosidase) was from Clontech. Wildtype Hakai and RING finger domain mutant C309A Hakai expression constructs were provided by Dr. Yasuyuki Fujita (MRC Laboratory, University College London, UK). Wildtype c-Cbl and RING finger domain mutant C381A c-Cbl expression constructs were provided by Dr. Stephen Robbins (University of Calgary).

Active Src mutant Y530F and the kinase dead Src K298M were generated in the laboratory of Dr. D.J. Fujita (University of Calgary) using QuickChange® site-directed mutagenesis (Stratagene). Mutant Y185F VHL was generated using QuickChange® site-directed mutagenesis (Stratagene).

2.4 Transfections and cell lysis

Cells were grown in six-well plates or 60 mm plates to 70-80 % confluency. Transfections were performed with LipofectAmine 2000 (Invitrogen) or FuGENE 6 (Roche Molecular Biochemicals) according to manufacturer's instructions. Unless otherwise specified, 1 μg DNA per plasmid type was used for each transfection. For FuGENE 6 transient transfections, transient transfections were conducted using 2 μg plasmid to 3 μL FuGENE 6 transfection reagent ratios as per manufacturer's instructions. The cell culture medium was changed once to growth medium containing 10 % FBS and antibiotics 16 h after transfection.

48 h post-transfection, the cells were lysed in 1 % NP-40 lysis buffer (150 mM NaCl, 50 mM Tris pH 7.5, 1 % Nonidet P-40, 2 mM EDTA, 50 μg/mL leupeptin, 10 μg/mL aprotinin, 200 μM sodium orthovanadate, 4 mg/mL p-nitrophenyl phosphate). Plates were placed on ice, the cells were first washed gently with cold PBS, then cold lysis buffer was added to the plates. After 20 min on ice, the cells were lifted by scraping with a rubber cell scraper and further lysed by pipetting up and down. The cell lysate was then transferred to a microfuge tube and vortexed for 10 seconds then centrifuged in a microfuge at 4 ^{o}C, at 14 000 rpm for 12 min. The supernatant was transferred to a new

tube and the protein concentration was determined by using the Bio-Rad Bradford assay system and the samples were stored at –80 ^{o}C.

2.5 Preparation of conjugated antibody-agarose beads

Two mg antibody was mixed with protein A agarose beads in a 15 mL conical Falcon tube. The antibody-protein A agarose bead mixture was incubated for 1 h at room temperature with rotation. The beads were then washed twice with 10 volumes of 0.2 M sodium borate (pH 9.0), and pelleted in between each wash by centrifugation at 3000 x g for 5 min. The beads were then resuspended in 10 volumes of 0.2 M sodium borate (pH 9.0). Dimethylpimelimidate (Sigma) was added to a final concentration of 20 mM dimethylpimelimidate, and the mixture was then incubated for 30 min at room temperature with rotation. Finally, the conjugation reaction was then stopped by washing the beads once in 0.2 M ethanolamine (pH 8.0), and then incubating the beads in 0.2 M ethanolamine (pH 8.0) for 2 h at room temperature with rotation.

2.6 Immunoprecipitation

Transfected cells were washed with PBS on ice, and were then scraped in 1 % NP-40 lysis buffer. The scraped cells were briefly vortexed, and then incubated on ice for 20 min. Cell extracts were then clarified by centrifugation in a microfuge at 4 ^{o}C, at 14 000 rpm for 12 min. Cell extract samples for immunoprecipitation were pre-cleared using 10 μl packed Protein A/G beads (1:1) and mixing on a rotator at 4 ^{o}C for 30 min. Centrifugation at 14 000 rpm at 4 ^{o}C for 2 min was then conducted and the pre-cleared cell extract supernatant was collected. In the case of immunoprecipitations to detect

ubiquitination and phosphorylation, immunoprecipitations were conducted on boiled SDS lysates (2 % SDS, 50 mM Tris pH6.8 lysis buffer). Immunoprecipitations were performed by adding 3 μg of IP antibody per 1 mg cell extract sample. Total volume was adjusted to 1 mL with lysis buffer, and the samples were placed on ice for 2 h. Subsequently, a 50 % slurry of protein A/G Plus beads (Santa Cruz Biotechnology, Inc), Protein A (Bio-Rad Laboratories Inc) agarose, or Protein G agarose (Calbiochem) (v/v) 15 μL packed agarose beads bed volume in 15 μL lysis buffer. Then the IP mixture was incubated on a rotator, at 4 ^{o}C for 2 h or overnight. The immune complexes were washed 3 times with lysis buffer (pelleted by a 2 min centrifugation at 14 000 rpm in a microfuge at 4 ^{o}C, in between each wash). The samples were then resuspended in Laemmli sample buffer (62.5 mM Tris pH 6.8, 2 % SDS, 10 % glycerol, 0.005 % bromophenol blue, and 5 % 2-mercaptoethanol), boiled for 5 min, and resolved by SDS-PAGE.

2.7 SDS-PAGE

Separation of proteins was performed by SDS-PAGE essentially as described by Laemmli (Laemmli, 1970). Unless otherwise stated, 50 μg of protein were prepped for loading per well of the SDS-PAGE gels. Protein samples were first denatured by boiling for 5 min in Laemmli sample buffer. Denatured samples were loaded into a SDS-PAGE stacking gel which consisted of a 5 % (v/v) concentration of 30 % (w/v) acrylamide/0. 8 % (w/v) bisacrylamide solution (37.5:1) (National Diagnostics), and 125 mM Tris-HCl pH 6.8 with 0.1 % SDS, 0.1 % ammonium persulfate (BDH Chemicals), and 0.1 % TEMED (EM Science). The stacking gel was layered onto a SDS-PAGE separating gel ranging in concentration of the acrylamide/bis solution from 8 % to 15 % dependent upon

the size of protein to be resolved. The separating gel with the desired concentration of acrylamide/bis solution was comprised of 375 mM Tris-HCl pH 8.8, 0.1 % SDS, 0.1 % ammonium persulfate, and 0.1 % TEMED. Electrophoretic separation of proteins was performed using the Mini-protean II Dual Slab Cell apparatus (Bio-Rad Laboratories Inc). The running buffer contained 25 mM Tris-HCl pH 8.3, 250 mM glycine, and 0.1 % SDS. Electrophoresis was performed at a constant voltage of 110 for 1.5 to 2.5 hours. Rainbow coloured protein molecular weight markers (Amersham Biosciences Inc) were also resolved in each SDS-PAGE, and these molecular weight markers ranged in size from 14.3 to 220 kDa.

2.8 Western blotting

Proteins resolved by SDS-PAGE were transferred to Protran pure nitrocellulose transfer and immobilization membrane (Schleicher and Schuell) using a Bio-Rad mini Trans Blotter apparatus (Bio-Rad Laboratories Inc). Transfers were typically performed for 1 hour at 100 volts at 4 ^{o}C, or overnight at 20 volts at 4 ^{o}C. The transfer buffer was composed of 25 mM Tris-HCl pH 8.3, 192 mM glycine, 0.01 % SDS, and 20 % methanol. The transfers were then disassembled and membranes were rinsed with double distilled water (ddH2O), and were subsequently blocked with a 5 % BSA solution in PBS-T (137 mM NaCl, 2.7 mM KCl, 1.5 mM KH_2PO_4, 8.1 mM Na_2HPO_4, pH 7.5, and 0.1 % Tween-20) for 1 h at room temperature, or overnight at 4 ^{o}C. Membranes were then probed with appropriate primary antibodies at concentrations of 1/200 to 1/10,000 (depending on the antibody source and manufacturers suggested concentrations for Western analysis) in 5 % BSA in PBS-T. Primary antibody incubations were either

overnight at 4 ^{o}C, or 1.5 hour at room temperature. Membranes were then washed three times for 5 min in PBS-T, and then incubated with 1/5,000 dilution of horseradish peroxidase (HRP) conjugated anti-mouse (Amersham) or anti-rabbit secondary antibody (Amersham) in 5 % BSA in PBS-Tfor 1 hour at room temperature. Membranes were washed three times for 5 min each time in PBS-T. Immunodetected proteins were visualized using Amersham enhanced chemiluminescence (ECL) detection reagent according to manufacturer's instructions (Amersham).

2.9 Stripping and reprobing of membranes

To remove primary and secondary antibodies from immunoblots, membranes were immersed in stripping buffer (100 mM 2-mercaptoethanol, 2 % SDS, 62.5 mM Tris-HCl pH 6.7) and incubated in a 60 ^{o}C shaking water bath for 30 min. The membranes were then washed two times 10 min each with PBS-T at room temperature. ECL detection was performed to confirm removal of bound antibodies. Membranes were blocked again for 1h at room temperature using 5 % BSA in PBS-T. Immunoblotting was performed as described above.

2.10 ELISA

Microtiter plates (Immulon II plates, Dynatech Laboratories Inc.) were coated with 50 μL conditioned media per well and incubated overnight at 4 ^{o}C. The conditioned media solution (antigen) was then removed from the wells by flicking. 200 uL/well of blocking buffer (PBS containing 3 % BSA) was then added to block non-specific protein binding, and the wells were incubated for 1 h at room temperature. The blocking buffer

was then removed from the wells by flicking, and the wells were washed once with PBS. Subsequently, 50 uL/well of 3 ug/mL anti –VEGF polyclonal antibody in PBS containing 3 % BSA was added, and the wells were incubated for 1 h at room temperature. The primary antibody solution was then removed from the wells by flicking, and the wells were washed three times with PBS containing 0.05 % Tween-20. 50 uL/well of horseradish peroxidase conjugated secondary antibody diluted 1:500 in PBS containing 3 % BSA was added, and the wells were incubated for 1 h at room temperature. The secondary antibody solution was then removed from the wells by flicking, and the wells were washed three times with PBS containing 0.05 % Tween-20. Finally, 50 uL of substrate solution was added to each well. [Substrate solution consisted of 0.1 mL stock 1 mg 3,3′,5,5′-tetramethylbenzidine (TMB) (Sigma) in 0.1 mL dimethylsulphoxide added to 9.9 mL of 0.1 M sodium acetate (pH 6.0): 0.01 % hydrogen peroxide.] The substrate solution reaction was allowed to incubate in the microtiter wells for 15 minutes at room temperature. Then 50 uL of stop solution (1 M H_2SO_4) was added to each well. Positive reactions were visualized by colour change from pale blue to yellow. The results were read on a microtiter plate reader at 450 nm.

2.11 Sequence analysis

PattInProt v5.4 and NetPhos software programs accessible via the The ExPASy (**Ex**pert **P**rotein **A**nalysis **Sy**stem) proteomics server of the Swiss Institute of Bioinformatics (SIB) were used to analyze protein sequences for consensus sequences. Gene Construction Kit 2 program (Textco Inc.) was used to analyze cDNA sequences and aid in primer design for PCR reactions for construct generation. The NetPrimer software

program accessible via the Premier Biosoft International homepage (http://www.premierbiosoft.com/products/products.html) was used to design and analyse primers for PCR reactions.

2.12 GST-Src domain fusion construction

The Src domain cDNA fragments of interest were generated by restriction digestion from pBA3CS, which contained full-length wild type human c-Src cDNA. pGEX-SH3-SH2 contains human c-Src SH3 and SH2 domains (nucleotides 170-775, amino acids 57-258) obtained by restriction digestion using NotI and EcoNI. The Src cDNA fragment was then treated with Klenow to blunt their ends before ligation in-frame into pGEX-2T (AMRAD Corporation). pGEX-SH3 contains the human c-Src SH3 domain (nt 170-420, aa 57-140) obtained by restriction digestion using NotI and NarI. The pGEX-SH2 construct was obtained by PCR amplification of the human c-Src SH2 region (nt 424-786, aa 142-262) using the sense strand primer 5'GGAATTCGCCCTCCGACTCCATC3' and the antisense strand primer 5'GAAACTCGAGGCATCCTTGGCCAG3'. The primers were designed with an EcoRI site and an XhoI site (at the 5' end of the sense primer and 5'end of the antisense primer, respectively). The PCR amplified SH2 domain cDNA was cut with EcoRI and XhoI, allowing for directional and in-frame ligation with the EcoRI/XhoI cut vector, pGEX-4T-3 (AMRAD Corporation). The ligated DNA was transformed into competent *E.*coli BL21 and resulting colonies screened for the presence of the inserts. Positive clones with the inserts were sequenced using the University of Calgary Sequencing Facility to confirm in-frame insertion and that no other mutations were present.

2.13 GST-VHL fusion construction

Nested C-terminal deletions of VHL were generated by PCR for construction of constructs to express GST-VHL fusion proteins. Wildtype pcDNA3.1-Fl-VHL-GFP was used as the template in PCR reactions. For construction of the pGEX-VHL wildtype 213 amino acids (aa), the sense primer 5'-AATATGAATTCCGGA**ATG**CCCCGGAGG-3' (the *EcoRI* site is underlined and the start codon is in bold) and the antisense primer 5'-AATATTAGTCGAC**TCA**ATCTCCCATCCGTTG-3' (the *SalI* site is underlined and the stop codon is in bold) were used for PCR amplification of wildtype full-length VHL 1-213 aa. For construction of pGEX-VHL 184 aa, the sense primer 5'-AATATGAATTCCGGA**ATG**CCCCGGAGG-3' (the *EcoRI* site is underlined and the start codon is in bold) and the antisense primer 5'-AATATTAGTCGAC**TCA**GAGCGACCTGACGATG -3' (the *SalI* site is underlined and the stop codon is in bold) were used for PCR amplification of the VHL 1-184 aa region. For construction of pGEX-VHL 111 aa, the sense primer 5'-AATATGAATTCCGGA**ATG**CCCCGGAGG-3' (the *EcoRI* site is underlined and the start codon is in bold) and the antisense primer 5'-AATATTAGTCGAC**TCA**GCTGTGGATGCGGCG-3' (the *SalI* site is underlined and the stop codon is in bold) were used for PCR amplification of the VHL 1-111 aa region. For construction of pGEX-VHL 97 aa, the sense primer 5'-AATATGAATTCCGGA**ATG**CCCCGGAGG-3' (the *EcoRI* site is underlined and the start codon is in bold) and the antisense primer 5'-AATATTAGTCGAC**TCA**GGGCTGCGGCTCGC-3' (the *SalI* site is underlined and the

stop codon is in bold) were used for PCR amplification of the VHL 1-97 aa region. The PCR fragments were restriction digested with *EcoR1* and *Sal1*. The PCR inserts were then ligated into *EcoR1* and *Sal1* digested pGEX-4T-3 (AMRAD Corporation). The ligated DNA were then transformed into competent *E.coli* BL21, and the resulting colonies screened for the presence of the inserts. Positive clones with the inserts were sequenced using the University of Calgary Sequencing Facility to confirm in-frame insertion and that no other mutations were present.

2.14 GST-fusion protein expression

Each pGEX-fusion construct-containing *E. coli* BL21 clone was cultured in 10 mL 2x YTA broth (16g/L tryptone, 10g/L yeast extract, 5 g/L NaCl, 100 μg/mL ampicillin, pH 7.0) overnight at 30 ^{o}C, shaking at 250 rpm. The starter culture was diluted 1:100 into 400 mL of fresh 2xYTA broth and grown at 30 ^{o}C, shaking at 250 rpm, until A_{600} reached 0.5-2. The culture was then induced by the addition of isopropyl-β-D-thiogalactoside to a final concentration of 0.2 mM for 3 h at 30 ^{o}C, shaking at 250 rpm. GST-Src fusion protein harvesting and purification were carried out following the pGEX GST fusion gene system supplier's recommended instructions (Pharmacia Biotech). Briefly, bacterial cultures were pelleted by centrifugation at 4,000 rpm in a Sorval GS rotor, for 20 min; and the bacterial pellet was resuspended in 20 mL of 1xPBS (including 2 μg/mL antipain, 2 μg/mL leupeptin, and 1mM DTT). The bacterial cells were then sonicated for 3x30 sec at 50 % output control. Following addition of Triton-X 100 to 1 % (v/v) final concentration, the cell suspension was centrifuged at 4 ^{o}C, at 10,000 rpm in an SS-34 rotor, for 20 min. Fusion protein was adsorbed in a batchwise fashion by

addition of 0.02 volumes of washed glutathione sepharose 4B beads, and incubation with gentle mixing at 4 ^{o}C, for 60 min to overnight. The fusion protein-bound beads were then collected by centrifugation at 500 x g for 5 min, and washed 3 times with PBS. Small aliquots of the fusion protein-bound beads were stored in PBS containing 10 % glycerol. For yielding protein for quantitation, the fusion protein samples were eluted from the glutathione sepharose 4B beads using 50 mM Tris-HCl (pH 8.0) containing 10 mM reduced glutathione.

2.15 Baculovirus Src kinase phosphorylation of GST-VHL

10 μg of GST alone, GST-VHL wildtype full-length 213 aa, or GST-VHL N-terminal proteins bound to glutathione sepharose 4B beads (10 μL bed volume), were each incubated for 30 min at 30^{o}C with 100 ng of purified baculovirus expressed c-Src in 25 μL of kinase buffer (50 mM Hepes pH 7.4, 150 mM NaCl, 1 mM DTT, 5 mM $MgCl_2$, 30 μM ATP, 200 μM sodium orthovanadate, and 4 mg/mL p-nitrophenolphosphate). The reaction was terminated by the addition of 35 μL of 2X SDS-PAGE sample buffer and boiling for 8 min. The phosphorylated proteins were resolved by 10 % SDS-PAGE, after which the gel was fixed (in 40 % methanol, 7 % acetic acid), stained in Coomassie blue (0.25 % Coomassie blue, 40 % methanol, 7 % acetic acid), and destained (in 50 % methanol, 12.5 % acetic acid).

2.16 GST-fusion binding experiments

GST-fusion binding experiments were conducted as described Figure 6. Four GST-VHL expression constructs were generated: GST-VHL wildtype (213 aa), GST-

VHL N-terminal 184 aa, GST-VHL N-terminal 111 aa, and GST-VHL N-terminal 97 aa. GST proteins were produced in BL21 *E. coli*, harvested and purified by binding to glutathione sepharose 4B beads. Then, the GST proteins bound to glutathione beads were phosphorylated in kinase reactions in two groups (one group in the absence of baculovirus Src, the other group in the presence of baculovirus Src) in a ratio of 1 pmol baculovirus Src to 100 pmol GST protein target. Kinase reactions were conducted in kinase buffer (50 mM Hepes pH 7.4, 150 mM NaCl, 1 mM DTT, 5 mM $MgCl_2$, 30 μM ATP, 200 μM sodium orthovanadate, and 4 mg/mL p-nitrophenolphosphate) at 30 °C for 30 minutes. Subsequently, the two groups of glutathione bead-bound GST proteins, phosphorylated or not phosphorylated, were tested for their ability to bind candidate E3 ubiquitin ligases in GST-pull-down experiments, by pull-downs from lysates expressing Y530F Src or K298M Src respectively. Equimolar amounts of the various GST-VHL domain fusion proteins (500 pmol) bound to glutathione-sepharose beads were used in pull-down incubations (at 4 °C for 3 hours) with equal amounts of cell extracts (500 μg). The fusion protein complexes were pelleted by centrifugation and washed three times with lysis buffer. The washed fusion protein pellets were boiled in 2X Laemmli's sample buffer, resolved on 10 % acrylamide SDS-PAGE gels, and transferred to nitrocellulose. Afterward, immunoblotting was performed using antibodies for candidate VHL-interacting proteins of interest, and results were developed by using enhanced chemiluminescence (Amersham).

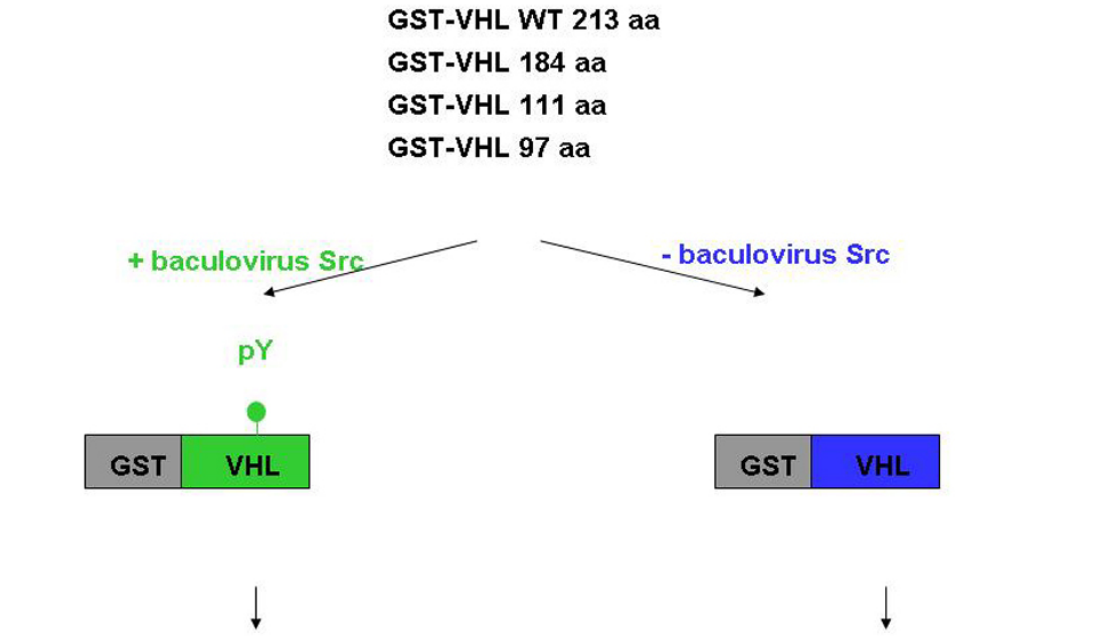

GST-VHL Pull-downs from HEK 293 cell lysate (Y530F Src or K298M Src expressing);

WB for interacting protein.

Figure 6. Flow chart of GST-VHL pulldown experiments studying the effect of Src phosphorylation of VHL on binding of E3 ligases to VHL.

GST, GST-VHL wildtype full-length 213 aa, and GST-VHL N-terminal proteins were produced, bound to glutathione sepharose beads, and purified. The GST-VHL fusion protein beads were then phosphorylated in the presence or absence of baculovirus Src. The GST-VHL fusion protein beads were subsequently used in pull-down incubations (500 pmol equimolar amounts each), with equal amounts of protein lysate (500 μg protein lysate each) from HEK 293T cells expressing activated Src or kinase dead Src, for pull-downs using baculovirus Src phosphorylated (+) GST-VHL beads or non-baculovirus Src phosphorylated (-) GST-VHL beads respectively). The pull-down complexes were resolved on 10 % acrylamide SDS-PAGE gels and transferred to nitrocellulose. Immunoblotting was then performed using antibodies for candidate VHL-interacting proteins of interest.

2.17 Site-directed mutagenesis

To generate the Y185F VHL construct (pcDNA3.1-Flag-Y185F VHL-GFP), the QuikChange™ Site-Directed Mutagenesis method (Stratagene) was used. The mutagenic primers sense 5'-CATCGTCAGGTCGCTC**TTC**GAAGATCTGGAAGACC-3' and antisense 5'-GGTCTTCCAGATCTTC**GAA**GAGCGACCTGACGATG-3' (site mutation bolded and underlined) were synthesized by the University Core DNA Services at the University of Calgary. The PCR mutagenesis reactions were as follows: 50 ng of template (pcDNA3.1-Flag-wildtype VHL-GFP) with 150 ng of each mutagenic primer was added to 1X Pfu reaction buffer (20 mM Tris-HCl, 10 mM KCl, 10 mM $(NH_4)_2SO_4$, 2 mM $MgSO_4$, 0.1 % Triton-X-100, 0.1 μg/μL BSA; pH 8.75), and 0.2 mM each dNTP. One unit of PfuTurbo ™ DNA polymerase (Stratagene) was then added, and the tubes mixed by vortexing and then centrifuged briefly. The tubes were then heated to 95°C for 1 min. The reaction was allowed to proceed for 18 cycles using the following parameters: denaturation was at 95°C for 50 s, annealing was at 60 °C for 50 s, extension was at 68 °C for 10 min. The tubes then underwent one final extension cycle at 68 °C for 10 min. After the cycling reactions, the samples were cooled to 4 °C. Then 10 units of the restriction enzyme *DpnI* was added to the mixture, and the samples were then incubated at 37 °C for 2 hours. Two μL of the *DpnI* digested DNA was used to transform 50 μL of competent *E. coli* DH5-α. After overnight growth at 37 °C on LB ampicillin containing agar plates, colonies were screened for the presence of the mutation by sequencing. Colonies were only screened if the control reaction which lacked mutagenic primers did not result in any colonies (i.e. this indicated that the *DpnI* reaction was effective). Basically, three candidate positive colonies were chosen and grown overnight

in 2 mL of LB with appropriate antibiotic (100 μg/mL of ampicillin). The next day the plasmid DNA was purified by plasmid mini-prep method (Qiagen). The purified plasmids were then sequenced using the University of Calgary DNA Sequencing Facility to confirm the presence of only the directed mutation. Upon verification of the mutation, the expression constructs were then purified using the Endo-free plasmid maxi-prep kit from Qiagen and subsequently used for cell transfection experiments.

2.18 Extraction of RNA from cells

Cells grown in 10-cm culture dishes were lysed using 600 μL of Buffer RLT (Qiagen) per plate. The cell lysates were collected using a rubber policeman, transferred to microcentrifuge tubes and vortexed. Each sample was then homogenized by passing the lysate at least 5 times through a blunt 20-gauge needle (0.9 mm diameter) fitted to a syringe. One volume of 70 % ethanol was added to each homogenized lysate sample, after which the samples were mixed by pipetting. The samples were then added to RNeasy mini columns (Qiagen) and centrifuged for 15 s at >10,000rpm (>8000 x g), in a benchtop microfuge. The samples were subsequently washed by the addition of 700 μL of Buffer RW1 to each RNeasy column. After the wash, 500 μL of Buffer RPE was pipetted onto each RNeasy column and the tubes were centrifuged for 15 s at >10,000rpm. Then, 500 μL of Buffer RPE was pipetted onto each RNeasy column and the tubes were centrifuged for 2 min at >10,000rpm. Each RNeasy spin column was then placed in a new 2 mL collection tube centrifuged at full speed (14,000 rpm) for 1 min. This step was repeated a second time to ensure complete removal of ethanol. Elution of the RNA was achieved by the addition of 50 μL of RNase-free water directly onto each

RNeasy silica-gel membrane and then centrifuging for 1min at >10,000rpm. To obtain a higher total RNA concentration, the elution step was repeated using the first eluate.

2.19 RT-PCR

Each RT-PCR reaction (Qiagen OneStep RT-PCR method) was prepared by mixing 1X Qiagen OneStep RT-PCR Buffer (20 mM Tris-HCl, 10 mM KCl, 10 mM $(NH_4)_2SO_4$, 2.5 mM $MgCl_2$, 1 mM dithiothreitol; pH 8.7), 0.4 mM each dNTP, 2 μL Qiagen OneStep RT-PCR enzyme mix, 1 μg template RNA extract, and 0.6 μM each primer. The RT-PCR reactions were allowed to proceed through reverse transcription at 50 ^{o}C for 30 min, and then DNA polymerase activation at 95 ^{o}C for 15 min. The reactions were then allowed to proceed for 40 cycles using the following parameters: denaturation was at 94 ^{o}C for 45 s, annealing was at 50 ^{o}C for 45 s, extension was at 72 ^{o}C for 10 min. The tubes then underwent one final extension cycle at 72 ^{o}C for 10 min. After the cycling reactions, the samples were cooled to 4 ^{o}C.

All the RT-PCR primers were designed such that their 5' ends would anneal exon1/exon2 junctions of mRNA, so as to be able to specifically amplify mRNA. The RT-PCR primers were also designed to have GC contents of 40-60 %. To amplify VHL mRNA, sense primer 5'-CAG GCG TCG AAG AGT ACG-3'and antisense primer 5'-CTT TCA GAG TAT ACA CTG GCA GTG-3' were used, and the predicted product size was 411 bp. To amplify HIF-1α mRNA, sense primer 5'-GAA CGT CGA AAA GAA AAG TC-3'and antisense primer 5'-GCT TGG TGC TGA TTT GTG-3' were used, and the predicted product size was 628 bp. To amplify VEGF mRNA, sense primer 5'-CTT TCT GCT GTC TTG GGT GC-3' and antisense primer 5'-CTC GGC TTG TCA CAT

CTG C-3' were used, and the predicted product size was 687 bp. To amplify control β-actin mRNA, sense primer 5'-ACC AGG GCG TGA TGG TG-3' and antisense primer 5'-CTA GAA GCA TTT GCG GTG G-3' were used, and the predicted product size was 1005 bp. RT-PCR reactions were electrophoresed on 1 % agarose gels at 100 V, and then the gels were incubated in 0.01 μg/mL of ethidium bromide to visualize bands.

2.20 Cycloheximide treatment experiments to determine protein half-life

Cells were seeded on 60 mm plates, and subjected to appropriate transfections. 48 h post-transfection, the cells were treated with 100 μM final concentration of cycloheximide (Sigma) for 0 h, 2 h, 4 h, 8 h, 16 h, or 24 h. The cells were then lysed in 1 % NP-40 lysis buffer, and subjected to SDS-PAGE and Western blotting. Quantitation of band intensities was carried out using ImageQuanNT software (Molecular Dynamics).

2.21 ^{35}S metabolic labeling and chase experiments

Cells were starved in methionine (Met)- and cysteine (Cys)- free medium for 2 h, then labeled in Met- and Cys- free DMEM medium (Gibco) containing 100 μCi/mL ^{35}S-Met and ^{35}S-Cys Promix cell-labeling mix (Amersham Biosciences) for 16 h in order to maximize labeled ^{35}S-Met and ^{35}S-Cys incorporation. After labeling, the cells were then washed two times, and chased with complete DMEM containing 10 % fetal bovine serum and unlabelled Met and Cys at 20-fold excess relative to the normal concentration in DMEM for the indicated times. Cell lysates were prepared in 1 % NP-40 lysis buffer, and the cell lysates were immunoprecipitated with anti-VHL polyclonal antibody, as detailed above. The immunocomplexes were then resolved by SDS-PAGE.

Subsequently, the gels were fixed, treated with ENHANCE solution (Dupont NEN) according to the manufacturer's instructions, dried, and subjected to autoradiography.

2.22 Fluorescence microscopy

Cells were seeded on glass coverslips in a 6 well plate. At 80 % confluency the cells were transfected using Lipofectamine™ 2000 (LF2000). At 24 h post-transfection cells were fixed to the cover slips. The cells were washed twice with cold PBS, fixed with 3.7 % paraformaldehyde/PBS for 20 min, washed three more times, and then permeabilized with 0.1 % NP-40 in PBS for 20 min. The cover slips were incubated in blocking buffer (1 % BSA in PBS) for 1 hour at room temperature, and then washed once with PBS for 5 min. Immunostaining for Src was performed for 1 hour in a humidified chamber, using anti-Src 327 monoclonal antibody (1:100 dilution) in 1 % BSA in PBS. Flag-VHL-GFP was detected by GFP epifluorescence. Cells were then washed three times with PBS for 5 min each, and then incubated with Rhodamine Red-X- labeled secondary antibody (Jackson Laboratories) for 30 min at a dilution of 1:500 in PBS containing 1 % BSA room temperature. After immunostaining, the cover slips were washed two times with PBS for 5 min each at room temperature , and counter-stained with DAPI (Sigma) in PBS (1 μg/mL) for 10 min. The cover slips were then washed three times with PBS for 5 min each at room temperature, then rinsed with ddH_2O and mounted on glass slides using Mowiol (Calbiochem). Immunofluorescence was then visualized with a 100x objective using a Zeiss microscope. Photos were taken using a Photometrics CoolSNAP*cl* (Roper Scientific) camera and RS Image software (Roper Scientific).

2.23 siRNA experiments

Unless otherwise stated, siRNAs were synthesized by Dr. Richard Pon (University of Calgary Oligonucleotide Synthesis Facility). GFP siRNA was purchased from Xeragon. All siRNA sequences were empirically tested for optimal conditions to produce knockdown effects. In summary, for each well of a 12-well dish to be transfected, 4 μl of Oligofectamine™ (Invitrogen) reagent was mixed with 11 μl of Opti-MEM® medium (Gibco), and were kept at room temperature for 7-10 min. For each well to be transfected, 5 μl siRNA (from a 20 μM stock concentration) was mixed with 80 μl Opti-MEM® medium. The Oligofectamine™/Opti-MEM® mixture was then combined with the siRNA/Opti-MEM® mixture, and allowed to stand at room temperature for 20-25 min. Prior to transfection, the cells were rinsed with Opti-MEM® medium and replaced with 0.4 mL of Opti-MEM® medium per well. The Oligofectamine™/siRNA combination mixture was then pipetted dropwise into each well, and the cells were incubated at 37 ^{o}C in 5 % CO_2 for 4 h. 4h post-transfection, 250 μl of DMEM medium containing 30 % FBS with no antibiotics was added to each well, and the cells were incubated at 37 ^{o}C in 5 % CO_2. 48 h post-transfection, the cells were lysed in 1 % NP-40 lysis buffer (150 mM NaCl, 50 mM Tris pH 7.5, 1 % Nonidet P-40, 2mM EDTA, 50 μg/mL leupeptin, 10 μg/mL aprotinin, 200 μM sodium orthovanadate, 4 mg/mL p-nitrophenyl phosphate).

siRNA sequences synthesized and used in target knockdown experiments were as follows:

Control non-targetting siRNA sense strand: 5’-UUC UCC GAA CGU GUC ACG UdTdT-3’

Control non-targetting siRNA antisense strand: 5’-ACGUGACACGUUCGGAGAA dTdT-3’

Src siRNA 1 sense strand: 5’-ACG UGA AGC ACU ACA AGA UUU -3’

Src siRNA 1 antisense strand: 5’-AUC UUG UAG UGC UUC ACG UUU-3’

Src siRNA 2 sense strand: 5’-GGC UCA UUG AAG ACA AUG AUU-3’

Src siRNA 2 antisense strand: 5’-UCA UUG UCU UCA AUG AGC CUU-3’

VHL siRNA 1 sense strand: 5’-ACC CAA AUG UGC AGA AAG AUU-3’

VHL siRNA 1 antisense strand: 5’-UCU UUC UGC ACA UUU GGG UUU-3’

VHL siRNA 2 sense strand: 5’-GGU CGC UCU ACG AAG AUC UUU-3’

VHL siRNA 2 antisense strand: 5’-AGA UCU UCG UAG AGC GAC CUU-3’

Hakai siRNA 1 sense strand: 5’- GGG AAU GAG UCC UGG UAU AdTdT-3’

Hakai siRNA 1 antisense stand: 5’-UAU ACC AGG ACU CAU UCC CdTdT-3’

Hakai siRNA 2 sense strand: 5’- GUU CAA GGG UGC AAG AGA AdTdT-3’

Hakai siRNA 2 antisense stand: 5’-UUC UCU UGC ACC CUU GAA CdTdT-3’

c-Cbl siRNA 1 sense strand: 5’-ACA AGA AGA UGG UGG AGA AdTdT -3’

c-Cbl siRNA 1 antisense stand: 5’-UUC UCC ACC AUC UUC UUG UdTdT-3’

c-Cbl siRNA 2 sense strand: 5’- GCU GGA AGC UCA UGG ACA AdTdT -3’

c-Cbl siRNA 2 antisense stand: 5’- UUG UCC AUG AGC UUC CAG CdTdT-3’

2.24 PP2 treatments

NIH 3T3 cells in DMEM/0.5 % fetal bovine serum were grown to 75 % confluence. Subsequently, the cells were treated with 10 μM PP2 (Calbiochem) dissolved in DMSO or DMSO vector for 15 h. Cell lysates were subjected to Western blotting to detect endogenous VHL protein, phosphotyrosine 419 Src levels, total Src protein levels; or VHL was immunoprecipitated and Western blotted for ubiquitin or VHL.

2.25 Luciferase assays

HEK 293T cells were seeded in 12-well plates. Cells were then transiently transfected using Lipofectamine 2000 transfection reagent, with 250 ng/well of indicated plasmids, or empty control vector, plus 250 ng/well of luciferase reporter plasmid (HREx3-Luc), and 100 ng/well β-galactosidase normalization plasmid (LNCX-β-gal). 48 hours post-transfection, media was aspirated off the cells. The cells were then washed with 2 mLs of PBS at room temperature. The PBS was removed and cells lysed by adding 80 μl of 1X Luciferase assay lysis reagent (Promega) equilibrated to room temperature. After 1 min lysis at room temperature, the lysate was pipetted up and down several times to further lyse the cells and then transferred to eppendorf tubes. The eppendorf tubes were then vortexed for 15 seconds and placed at –80 ^{o}C for 30 min or stored for use at a later time. The cells were then thawed rapidly at 37 ^{o}C and spun at high speed in a microfuge for 3 min. The supernatant was transferred to a new tube and placed on ice. The amount of protein in the lysate was then determined by Bradford assay, and the samples were equalized to the same protein concentration.

For the assay, 20 μL of supernatant lysate was added to a 5 mL polystyrene round-bottom tube (BD Biosciences) and 100 μl of reconstituted Luciferase assay substrate reagent (Promega) was then added and the samples mixed gently by shaking. The tube was immediately placed in a Monolight 2000 Luminometer (Analytical Luminescence Laboratory) and luminescence was detected over 30 seconds with a 2 second delay. Luminescence detected from a lysate control in which cells were transfected with empty vector alone without the luciferase reporter was subtracted from all samples.

2.26 Beta-galactosidase normalization assay

To normalize the results from the luciferase assay for variations in transfection efficiency the cells were co-transfected with the LNCX-β-galactosidase expression plasmid (LNCX-β-gal) (Clontech). Subsequent to the luciferase assays 2-5 μL (equivalent protein anounts) of cell lysate was placed in an eppendorf tube and the volume adjusted to 30 μl with ddH_2O. Then 70 μL of a 4 mg/mL solution of the β-galactoside ortho-nitrophenyl-β-D-galactopyranoside (ONPG) was added to the diluted lysate. To this mixture was then added 200 μL of 1X cleavage buffer [60 mM Na_2HPO_4-$7H_2O$, 40 mM NaH_2PO_4-H_20, 10 mM KCl, 1 mM $MgSO_4$-$7H_2O$) (pH 7.0) with 38.6 mM 2-mercaptoethanol]. The solution was mixed by gently flicking and the tubes were then centrifuged for 3 seconds. Samples were then incubated at 37 ^oC for 15 min. The reaction was then stopped by adding 500 μl of Stop buffer (1 M Sodium Carbonate). The samples were then transferred to 10 mm path plastic cuvettes (Sarstedt) and the absorbances were measured at a wavelength of 420 nm in a Beckman DU-65

spectrophotometer against a blank containing only ONPG and cleavage buffer without lysate.

2.27 Endothelial tube formation assays

The permanent human endothelial cell line, EA.hy926, was a gift from Dr. Cora-Jean S. Edgell (University of North Carolina). This cell line is a hybrid resulting from the fusion of primary human umbilical vein endothelial cells with cells derived from the human lung carcinoma cell line A549. This cell line maintains angiogenic behaviour and shows sustained expression of many differentiated functions of endothelium, such as release of Factor VIII, tissue plasminogen activator, plasminogen activator inhibitor, thrombomodulin, prostacyclin, platelet-activating factor, and endothelin-1 (Edgell *et al.*, 1983;Ferri *et al.*, 1995). EA.hy926 cells were maintained in DMEM containing 10 % fetal bovine serum, antibiotics (100 units/mL penicillin, 100 μg/mL streptomycin, and 0.25 μg/mL amphotericin), and HAT supplement (100 μM hypoxanthine, 0.4 μM aminopterin, 16 μM thymidine) at 37 ^{o}C in 5 % CO_2.

Endothelial tube formation assays were conducted as detailed in published protocols (Troyanovsky *et al.*, 2001;Potente *et al.*, 2005). In summary, to conduct the endothelial tube formation assays, HEK 293T cells were transfected with Flag-tagged VHL-GFP (Fl-VHL-GFP) individually, or together with constitutively active Src (Y530F Src), or kinase dead Src (K298M Src). 48 h post-transfection, conditioned media from each condition was collected for endothelial tube formation assays. 100 μL of ECM matrix (extracellular matrix from Engelbreth Holm-Swarm mouse sarcoma, BD

Biosciences) was pipetted into each well of a 96-well tissue culture plate. The tissue culture plate was then incubated for one hour at 37 ^{o}C to allow the ECM matrix to gel. EA.hy926 cells were then seeded at $4x10^3$ per well onto the surface of the polymerized ECM matrix. 100 μL of conditioned media from each transfection condition was then overlaid onto each well of endothelial cells seeded on ECM matrix. After 16 h incubation at 37 ^{o}C, the extent of formation of capillary networks for each condition was photographed under an inverted light microscope at 100X magnification. Quantification of capillary network formation was done by measurement of total tube length per well using ImageJ image data analysis software.

2.28 Chorioallantoic Membrane (CAM) Assays

Fertilized chicken eggs (Ijtsma Farms, Airdrie, Alberta) were incubated at 37 °C under conditions of constant humidity. CAM assays were performed as previously described (Kwon *et al.*, 2001). On embryonic day 4, the fertilized chicken eggs were cracked, and chick embryos with intact yolks were placed into 100 x 20 mm culture dishes and returned to incubation. On embryonic day 6, 3×10^5 HEK 293T cells from each transfection condition were loaded onto 5 mm^3 gelatin sponges (Johnson and Johnson) and implanted onto the surface of the developing CAM eggs. The CAM eggs were then returned to incubation. On embryonic day 8, CAM vasculature was digitally photographed and analyzed for extent of angiogenesis. Quantitation of angiogenesis was done measuring length of vasculature per 707 mm^2 field, using ImageJ image data analysis software. Four fields per CAM were measured for nine CAMs per transfection condition.

CHAPTER THREE: SRC DESTABILIZATION OF VHL TUMOUR SUPPRESSOR PROTEIN

3.1 Breast cancer cells and other cell lines with elevated Src activity show increased endogenous VEGF production

Src has been implicated as an important signaling component in hypoxia-induced upregulation of VEGF, as some studies have shown that Src can upregulate VEGF production under hypoxic conditions (Mukhopadhyay *et al.*, 1995;Ellis *et al.*, 1998;Wiener *et al.*, 1999). This evidence is supportive of an important role for Src in tumour angiogenesis. When I examined several breast carcinoma cell lines previously reported by our lab to exhibit high levels of endogenous Src activity (Egan *et al.*, 1999;Bjorge *et al.*, 2000), I found that they also produced high levels of VEGF, even under normoxic conditions (20 % O_2), as measured by Western blot analysis (Figure 7). The breast carcinoma cell lines BT-483 and Hs 578T secreted particularly abundant amounts of VEGF protein, relative to a nontumourigenic breast epithelial cell line MCF-10A. The MDA-MB-435S cell line also produced a significant amount of VEGF protein.

In further experiments, introduction of either wildtype human Src (WT Src) or a constitutively active form of Src (Y530F Src) led to increased VEGF protein production in several cell lines – most markedly in human breast epithelial cell line (MCF-10A), baby hamster kidney cells (BHK), and human embryonic kidney cells (HEK 293T) (Figure 8). In transient transfections of constitutively active Src in these cell lines, I observed a 2.1- to 2.5-fold increase in VEGF production, as measured by ELISA.

Transfections of wildtype Src resulted in approximately 2-fold increases in VEGF production. Because the cells were transfected and maintained under normoxic conditions, these observations indicate that even under normoxic conditions, elevated levels of wildtype Src and constitutively active Src both have the ability to increase VEGF production from cells.

Thus, although there have been previous reports that of Src can drastically upregulate VEGF production under hypoxic environments (Mukhopadhyay *et al.*, 1995;Ellis *et al.*, 1998;Wiener *et al.*, 1999), my results indicate that introduction of activated Src is also able to upregulate VEGF production even in nonhypoxic environments. Therefore, this evidence supports a model in which elevated levels of Src activity may be a key factor regulating the production of VEGF from cells through a mechanism that is independent of oxygen tension in the cellular environment (Mukhopadhyay *et al.*, 1995;Ellis *et al.*, 1998;Wiener *et al.*, 1999).

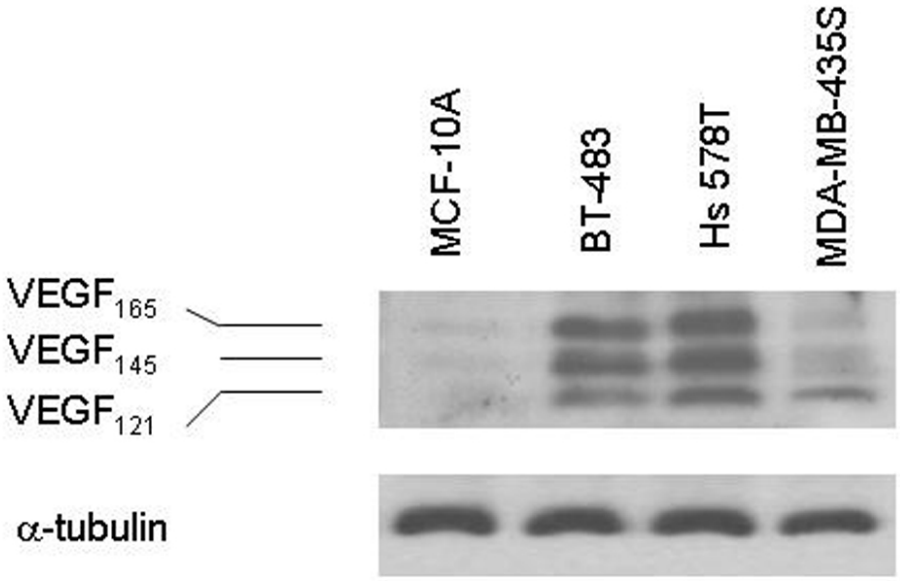
MCF-10A
BT-483
Hs 578T
MDA-MB-435S
VEGF165
VEGF145
VEGF121
α-tubulin

Figure 7. Breast cancer cells that exhibit elevated Src activity also exhibit upregulated VEGF production.

MCF-10A are nontumourigenic breast epithelial cells, BT-483, Hs 578T, and MDA-MB-435S are breast cancer cells. Conditioned media samples were collected from the different cell lines and were analyzed by Western blotting for VEGF protein using anti-VEGF polyclonal antibody. Conditioned media volumes assayed were adjusted for differences in the cell numbers of the cell cultures from which the samples were collected. Cell lysates from these cell lines were also Western blotted for α-tubulin using anti-α-tubulin monoclonal antibody. The results are representative of two independent experiments.

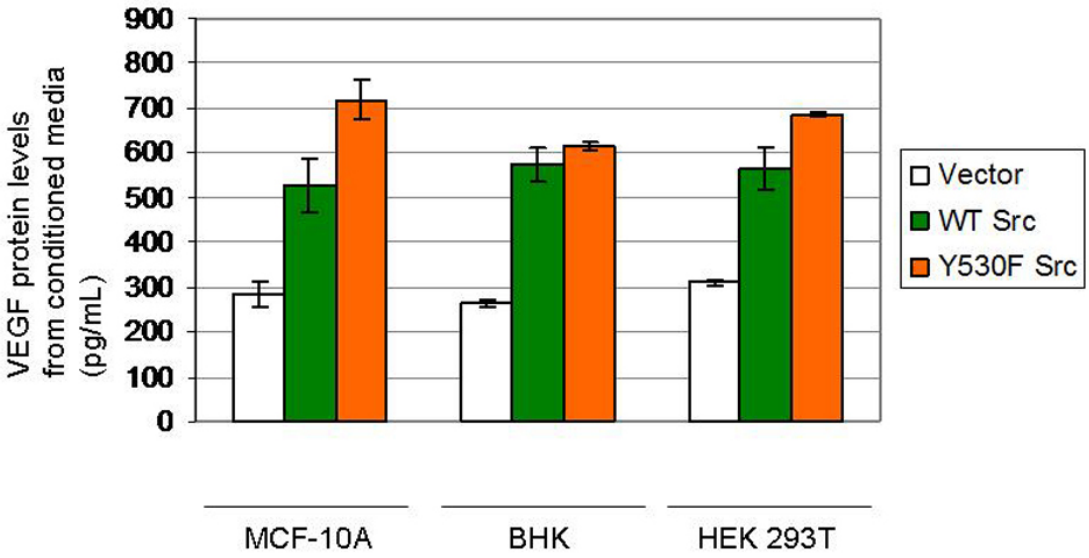

Figure 8. Introduction of Src into cells results in increased VEGF protein in conditioned media.

MCF-10A (normal breast epithelial cells), baby hamster kidney cells (BHK), and HEK 293T cells were transiently transfected with the following constructs: empty vector (pCI), wildtype Src (WT Src), and constitutively active Src (Y530F Src). 48 h after transfection, conditioned media samples were collected from the different cell lines and were assayed for VEGF protein levels by ELISA using anti-VEGF polyclonal antibody. Conditioned media volumes assayed were adjusted for differences in the cell numbers of the cell cultures from which the samples were collected. The graph charts the mean +/- 1 SD of three independent experiments done in triplicate.

3.2 Lower levels of VHL and higher levels of tyrosine phosphorylation in breast cancer cells lines with elevated Src activity

In initial experiments, I observed that some breast carcinoma cells lines such as SK-BR-3 and Hs 578T with elevated levels of endogenous Src activity (Egan *et al.*, 1999), endogenous VHL levels that were lower than in nontumourigenic breast epithelial cells MCF-10A (Figure 9). There was lower VHL protein levels concomitant with higher tyrosine phosphorylated VHL protein levels in the breast cancer cells (SK-BR-3, Hs 578T, and MDA-MB-435S) than in nontumourigenic breast epithelial cells MCF-10A. The higher levels of tyrosine phosphorylated VHL existing in the cancer cell lines suggest that post-translational tyrosine modification of VHL could contribute to the lower levels of VHL in the cancer cell lines. Thus, these results suggest that high Src activity is able to switch off VHL.

Interestingly, in support of my findings, it has been reported by one research group that highly aggressive cancers have little or no VHL protein and low levels of VHL transcript (Zia *et al.*, 2007). They used immunohistochemical analysis and quantitative reverse transcriptase PCR (qRT-PCR) methods to screen primary breast cancer tissues and several breast cancer cell lines. Based on their results, they concluded that VHL acts as a powerful tumour suppressor gene in human breast cancer, and presented data suggesting that VHL exerts inhibitory effects on the *in vitro* invasive migratory ability of breast cancer cells.

3.3 Src does not downregulate VHL transcript levels

In order to study whether Src could affect VHL transcript levels, I assayed VHL mRNA transcript levels by RT-PCR (Figure 10). The cellular RNA tested was from HEK 293T cells transfected with vector, Y530F Src, (activated Src), and K298M Src (kinase dead Src) expression plasmids. I found that Y530F Src did not cause any substantial decrease in VHL mRNA transcript levels. Rather Y530F Src contributed to a slight increase in VHL mRNA transcript levels. Thus, upregulated Src levels did not case any reduction in VHL transcription, based on RT-PCR experiments. In addition, upregulated Src levels caused some increased in VEGF mRNA and HIF-1α mRNA transcript levels.

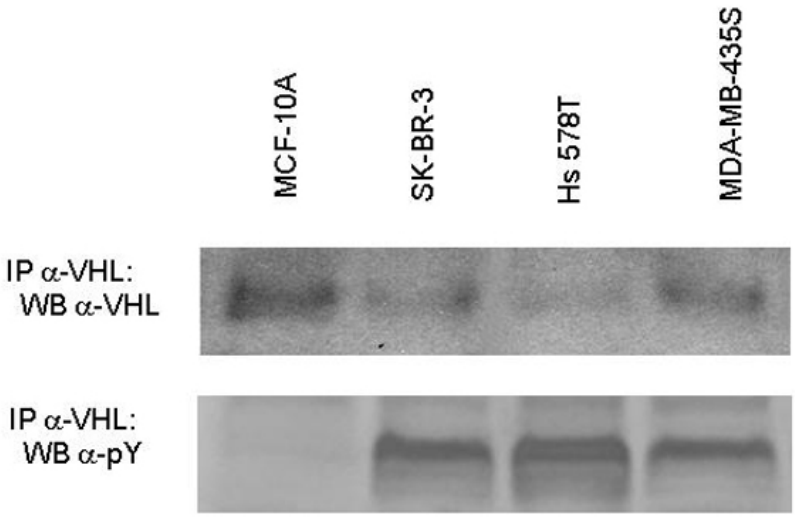

Figure 9. Lower levels of VHL and higher levels of tyrosine phosphorylation in breast cancer cells lines with elevated Src activity compared to nontumourigenic breast epithelial MCF-10A.

Endogenous VHL was isolated by immunoprecipitation using anti-VHL polyclonal antibody followed by immunoblotting using anti-VHL monoclonal antibody or anti-phosphotyrosine monoclonal antibody. The results are representative of two independent experiments.

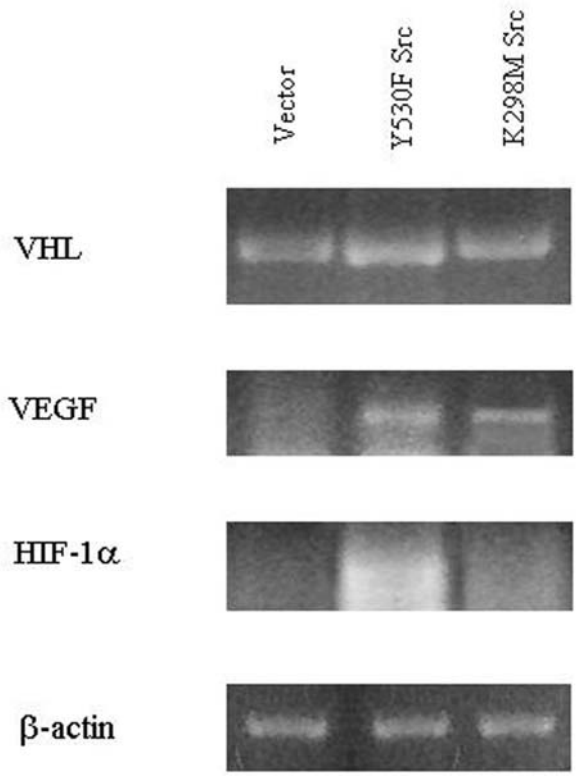

Figure 10. RT-PCR of VHL, VEGF, and HIF-1α transcript levels, in Src-transfected cells.

HEK 293T cells were transfected with vector, activated Src (Y530F Src) or kinase dead Src (K298M Src) constructs. 48 hours post-transfection whole cell RNA was isolated, and RT-PCR was performed using primers to amplify the mRNA of VHL, VEGF, HIF-1α, or β-actin. The results are representative of three independent experiments.

3.4 Elevated Src activity is associated with phosphorylation and ubiquitination and a reduction of VHL protein

In order to study the effect of elevated Src activity on VHL protein levels, I conducted transient transfections in HEK 293T cells. I investigated the effects of Src on endogenous as well as exogenous VHL tumour suppressor protein in HEK 293T cells. In these experiments, I discovered that constitutively active Y530F Src caused a reduction in endogenous VHL protein levels (Figure 11i), as well as a reduction in exogenous VHL levels (Figure 12). The results showed that both elevated wildtype Src levels as well as elevated constitutively active Y530F Src levels caused a marked increase in levels of polyubiquitinated VHL. At the same time, levels of endogenous VHL protein decreased (Figure 11i and Figure 11iii, compare lanes 3-4). Importantly, Src-mediated reductions in VHL levels were correlated with increased tyrosine phosphorylation of VHL by Src (Figure 11ii, lanes 3 and 4), at the same time as increased polyubiquitination of VHL (Figure 11iii, lanes 3 and 4).

Of note, I observed lower levels of Src protein expression in constitutively active Src-transfected cells compared to wildtype or kinase dead Src-transfected cells (Figure 11iv). This is routinely observed, and is consistent with previous reports that high Src activity is able to promote auto-ubiquitination and proteasome-mediated degradation of Src protein (Hakak and Martin, 1999).

Consistent with this, exogenous expression of Fl-VHL-GFP with constitutively active Src also showed that MG-132 could protect exogenous VHL protein from degradation (Figure 12, lane 9). Because MG-132 is an inhibitor of the 26S proteasome, this finding suggests that the Src-mediated reduction in VHL protein levels is likely due

to proteasome-dependent degradation. Also, in breast cancer cells (SK-BR-3), upregulation of Src activity by transfection of Src led to tyrosine phosphorylation and ubiquitination of VHL protein (Figure 13ii and iii). At the same time, exogenous upregulation of Src activity resulted in downregulation of VHL levels (which were better protected under MG-132 proteasome inhibitor treatment). Experiments were also conducted by transiently expressing exogenous HA-ubiquitin in HEK293T cells as an alternative method to study effects of this pathway on ubiquitination *in vivo* (in intact cells) (Figure 14). In these experiments, elevated Src activity also resulted in increased tyrosine phosphorylation and increased ubiquitination of Fl-VHL-GFP (Figure 14ii and iii). Also, consistent with earlier data, these experiments also showed that elevated Src activity resulted in upregulated VEGF protein levels (Figure 14v).

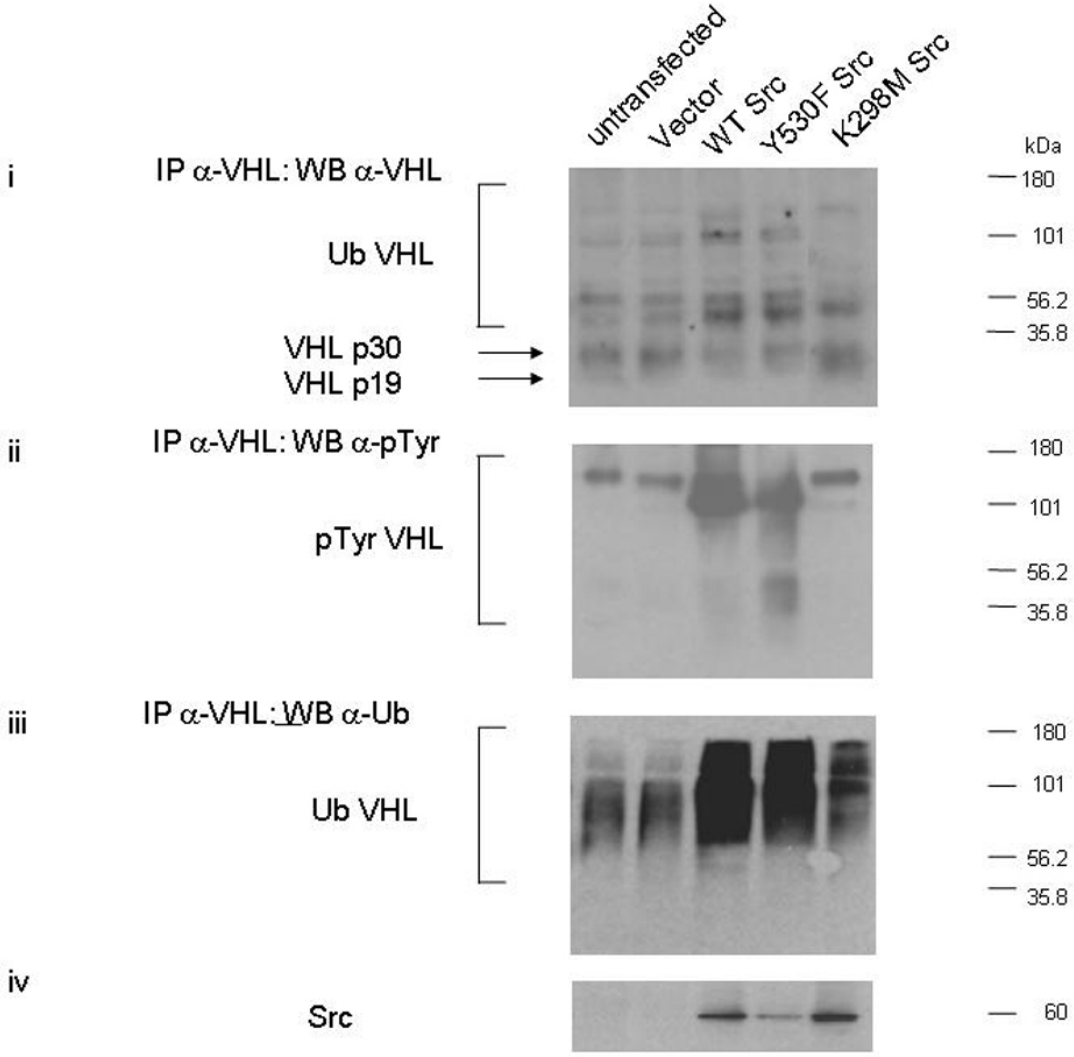
untransfected
Vector
WT Src
Y530F Src
K298M Src
kDa
i
IP α-VHL: WB α-VHL
Ub VHL
VHL p30
VHL p19
180
101
56.2
35.8
ii
IP α-VHL: WB α-pTyr
pTyr VHL
180
101
56.2
35.8
iii
IP α-VHL: WB α-Ub
Ub VHL
180
101
56.2
35.8
iv
Src
60

Figure 11. Elevated Src activity is associated with increased tyrosine phosphorylation, increased ubiquitination, and a reduction of endogenous VHL protein.

HEK 293T cells were transfected with empty vector pCI, Y530F Src, or K298M Src. 48 h post-transfection, the cells were treated with 25 μM MG-132 for 16 h. Cells were lysed in 2 % SDS, 50 mM Tris pH 6.8 lysis buffer, and boiled. Endogenous VHL was then isolated by immunoprecipitation with anti-VHL polyclonal antibody, followed by immunoblotting using (i) anti-VHL monoclonal antibody, (ii) anti-phosphotyrosine monoclonal antibody, or (iii) anti-ubiquitin monoclonal antibody. (iv) Total Src protein levels were detected by Western blotting using anti-Src monoclonal antibody. The results are representative of three independent experiments.

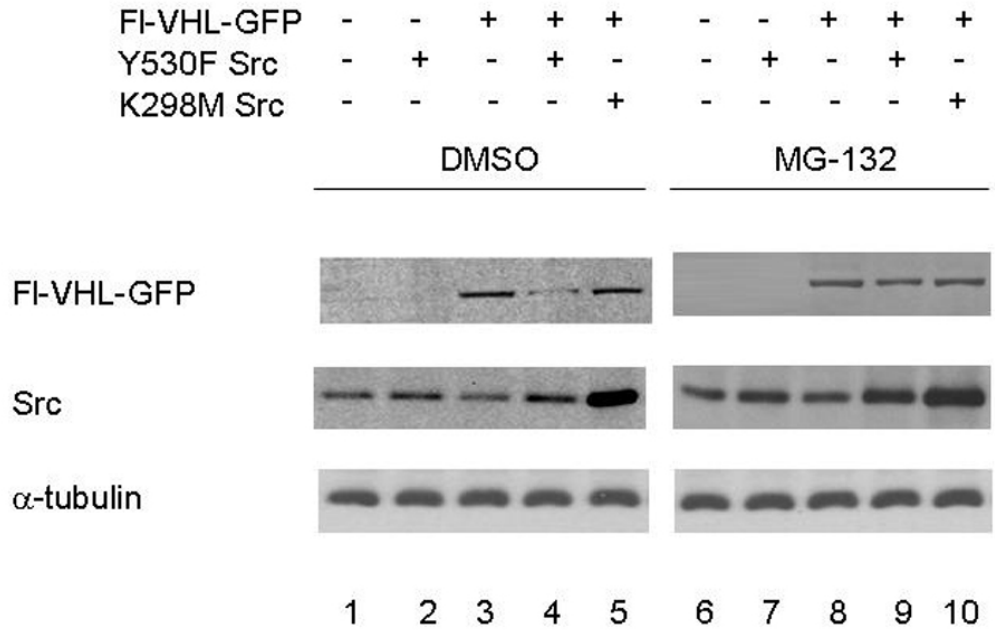
Fl-VHL-GFP - - + + + - - + + +
Y530F Src - + - + - - + - + -
K298M Src - - - - + - - - - +
DMSO
MG-132
Fl-VHL-GFP
Src
α-tubulin
1 2 3 4 5 6 7 8 9 10

Figure 12. MG-132 proteasome inhibitor protects VHL protein stability.

Src HEK 293T cells were transfected with Flag-tagged VHL-GFP expression plasmid (Flag-VHL-GFP) alone or together with constitutively active Src plasmid (Y530F Src) or kinase dead Src plasmid (K298M Src). 48 h post-transfection, the cells were treated with either DMSO (lanes 1-5) or 25 μM MG-132 for 16 h (lanes 6-10). The cells were then lysed, and Western blotting was performed to detect exogenous VHL using anti-Flag M2 monoclonal antibody. Total Src protein levels were detected by Western blotting using anti-Src monoclonal antibody, and total α-tubulin levels were detected by Western blotting using anti-α-tubulin monoclonal antibody. The results are representative of three independent experiments.

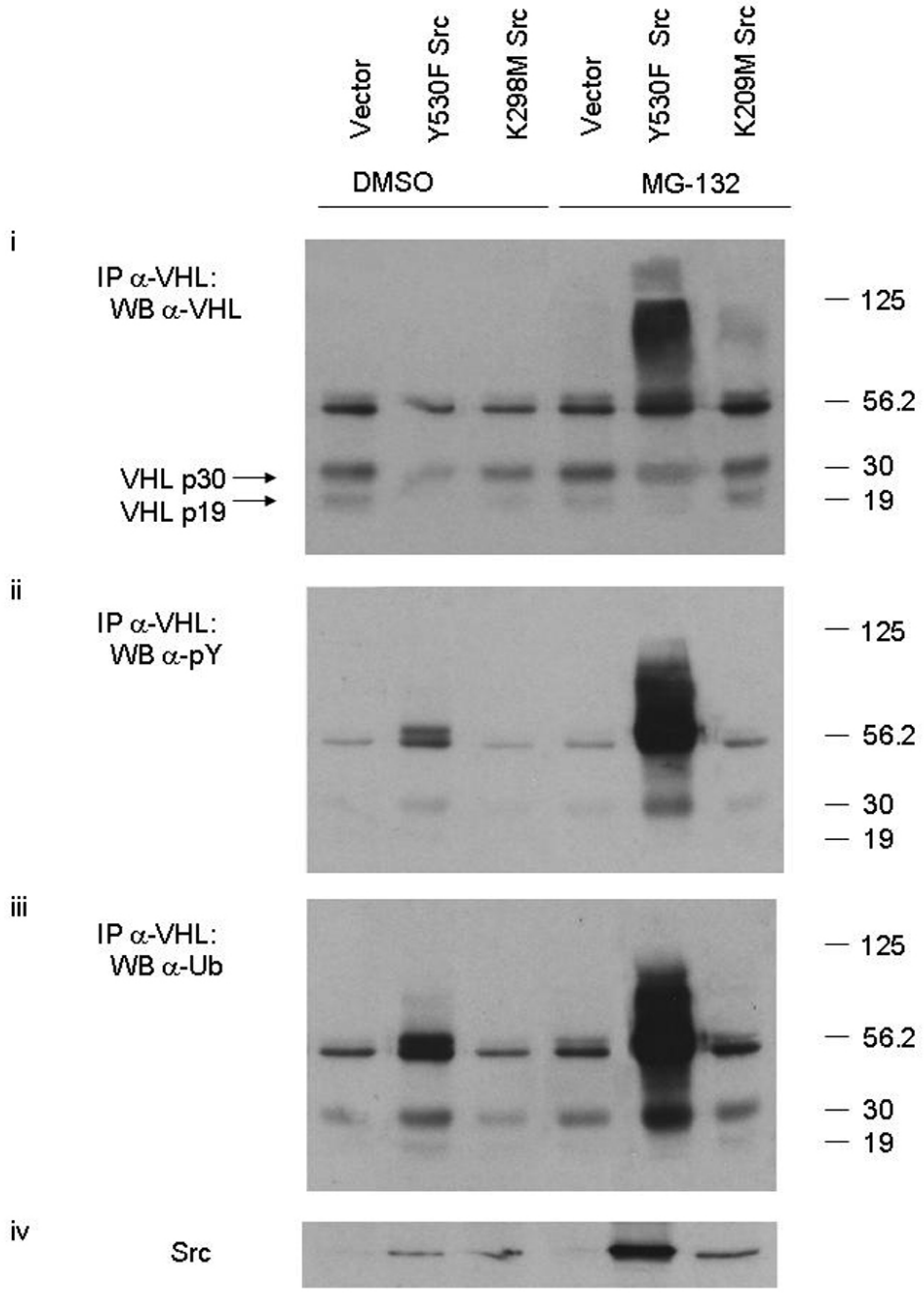
Vector
Y530F Src
K298M Src
Vector
Y530F Src
K209M Src
DMSO
MG-132
i
IP α-VHL:
WB α-VHL
VHL p30
VHL p19
125
56.2
30
19
ii
IP α-VHL:
WB α-pY
125
56.2
30
19
iii
IP α-VHL:
WB α-Ub
125
56.2
30
19
iv
Src

Figure 13. Elevated Src activity leads to phosphorylation and ubiquitination of endogenous VHL protein in SK-BR-3 breast cancer cells.

SK-BR-3 cells were transfected with empty vector pCI, Y530F Src, or K298M Src. 48 h post-transfection, the cells were treated with DMSO or 25 μM MG-132 for 16 h. Cells were lysed in 2 % SDS, 50 mM Tris pH6.8 lysis buffer, and boiled. Endogenous VHL was then isolated by immunoprecipitation with anti-VHL polyclonal antibody, followed by immunoblotting using (i) anti-VHL monoclonal antibody, (ii) anti-phosphotyrosine monoclonal antibody, or (iii) anti-ubiquitin monoclonal antibody. (iv) Total Src protein levels were detected by Western blotting using anti-Src monoclonal antibody. The results are representative of two independent experiments.

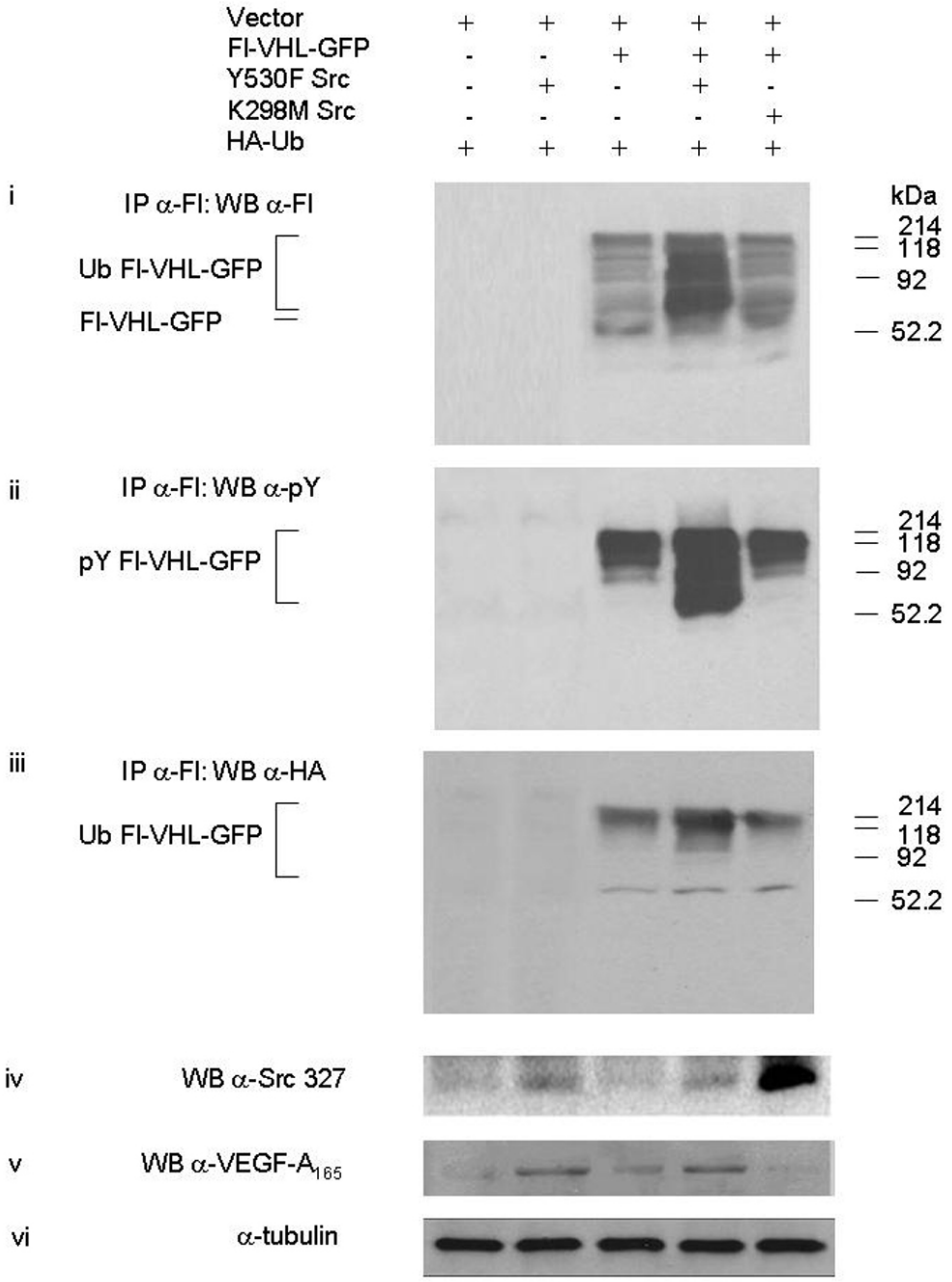
Vector + + + + +
Fl-VHL-GFP - - + + +
Y530F Src - + - + -
K298M Src - - - - +
HA-Ub + + + + +
i
IP α-Fl: WB α-Fl
Ub Fl-VHL-GFP
Fl-VHL-GFP
kDa
214
118
92
52.2
ii
IP α-Fl: WB α-pY
pY Fl-VHL-GFP
214
118
92
52.2
iii
IP α-Fl: WB α-HA
Ub Fl-VHL-GFP
214
118
92
52.2
iv
WB α-Src 327
v
WB α-VEGF-A165
vi
α-tubulin

Figure 14. Elevated Src activity in the presence of exogenous HA-ubiquitin causes increased tyrosine phosphorylation of VHL, increased ubiquitination of VHL, and upregulated VEGF.

HEK 293T cells were transfected with HA-Ub alone or together with Fl-VHL-GFP, and/or Y530F Src, or K298M Src . 48 h post-transfection, the cells were treated with 25 μM MG-132 for 16 h. Cell were lysed in 2 % SDS, 50 mM Tris pH6.8 lysis buffer, and boiled. Exogenous VHL then was isolated by immunoprecipitation with anti-Flag monoclonal antibody covalently conjugated to agarose beads, followed by imunnoblotting using (i) anti-VHL polyclonal antibody, (ii) anti-phosphotyrosine monoclonal antibody, or (iii) anti-HA monoclonal antibody. (iv) Total Src protein levels were detected by Western blotting using anti-Src monoclonal antibody, (v) total VEGF levels were detected by Western blotting using anti-VEGF polyclonal antibody, and (vi) total α-tubulin levels were detected by Western blotting using anti-α-tubulin monoclonal antibody. The results are representative of two independent experiments.

3.5 Elevated Src activity decreases the protein half-life of VHL

In order to study the effect of Src on the stability and half-life of VHL, I transiently transfected of Src and VHL (Flag-VHL-GFP) in HEK 293T cells, followed by cycloheximide treatment at 48 h after transfection. Cycloheximide blocks the translation of messenger RNA on cytosolic 80S ribosomes, thereby allowing a determination of protein half-lives in the absence of new protein synthesis. When the cells were transfected with empty vector (pCI) and VHL expression plasmid (Flag-VHL-GFP), the exogenously expressed VHL was very stable and exhibited a half-life of greater than 16 h (Figure 15A, left panel; and Fig. Figure 15B). However, when HEK 293T cells were transfected with constitutively active Src (Y530F Src) and Flag-VHL-GFP, VHL exhibited a drastically shortened half-life of approximately 5 hours (Figure 15A, middle panel; and Figure 15B). Interestingly, when the cells were transfected with kinase dead Src (K298M Src) and Flag-VHL-GFP, VHL exhibited a half-life of about 12 hours (Figure 15A, right panel; and Figure 15B). The intermediate level of VHL half-life reduction observed in the presence of kinase dead Src suggested that there might also be a kinase-independent function of Src that could play a partial role in VHL downregulation.

^{35}S metabolic labeling-chase experiments also confirmed that elevated Src activity was correlated with a shortened half-life of VHL. Introduction of activated Src into cells promoted a marked decrease in the levels of ^{35}S-labeled VHL within a 6-hour chase period (Figure 16). However, introduction of control pCI vector led to no apparent decrease in VHL levels even after 16 h, whereas introduction of kinase dead Src led to a slight decrease by 16 h (Figure 16). Thus, these results further support a model in which

elevated Src activity results in a decrease in VHL protein half-life through increased protein degradation of VHL.

Similar reductions in VHL protein stability were also observed for endogenous VHL in HEK 293T cells, although a somewhat larger amount of endogenous VHL appeared to be more resistant to Src-mediated degradation (Figure 17). When the cells were transfected with vector alone or kinase dead Src, endogenous VHL exhibited stability for greater than 16 h. However, when HEK 293T cells were transfected with constitutively active Src, levels of endogenous VHL were reduced down to about 50 % within 6 to 8 hours (Figure 17B,C). Notably, decreases in protein stability were observed for both the 30 kDa isoform of endogenous VHL as well as for the 19 kDa isoform of endogenous VHL, in cells transfected with activated Src (Figure 17B,C).

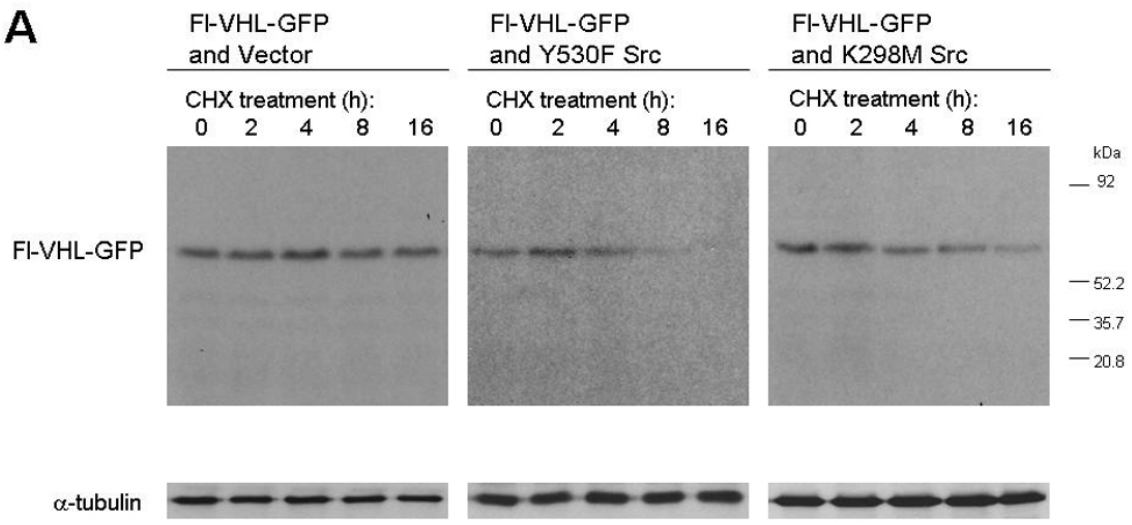
A
Fl-VHL-GFP and Vector
Fl-VHL-GFP and Y530F Src
Fl-VHL-GFP and K298M Src
CHX treatment (h):
0 2 4 8 16
kDa
92
52.2
35.7
20.8
Fl-VHL-GFP
α-tubulin

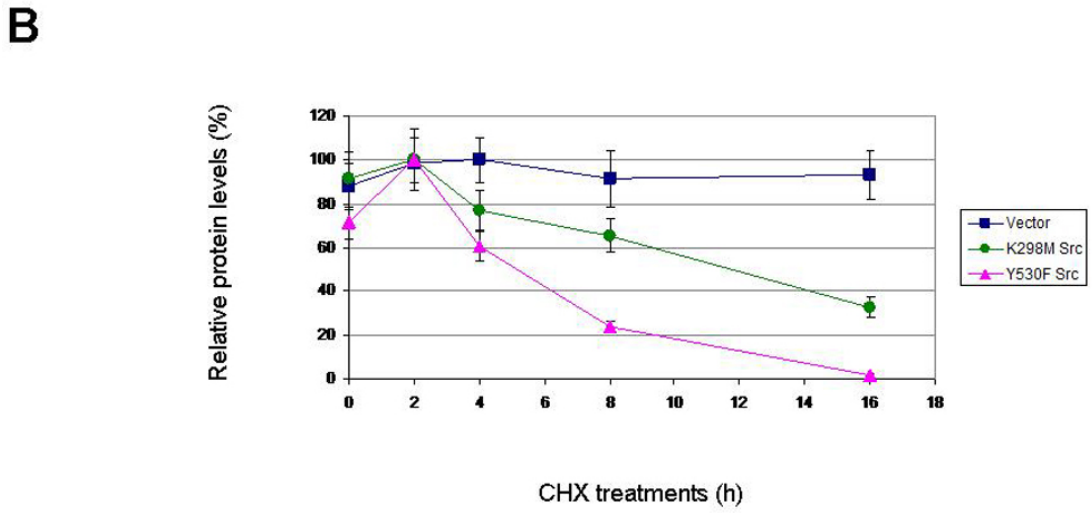
B
Relative protein levels (%)
120
100
80
60
40
20
0
0 2 4 6 8 10 12 14 16 18
CHX treatments (h)
Vector
K298M Src
Y530F Src

Figure 15. Src activity decreases the protein half-life of VHL in cycloheximide treatment experiments.

(A) HEK 293T cells were transfected with Flag-VHL-GFP, in the presence of empty vector, Y530F Src, or K298M Src. 48 h post-transfection, the cells were treated with 100 μM final concentration of cycloheximide for 0 h, 2 h, 4 h, 8 h, or 16 h. The cells were then lysed, and Western blotting was performed for exogenous VHL protein levels using anti-Flag monoclonal antibody, and total α-tubulin levels using anti-α-tubulin monoclonal antibody.

(B) Graphical representation of the effect of cycloheximide on Flag-VHL-GFP protein half-life. VHL protein levels were normalized to α-tubulin. The darkest band density for each trial set was assigned a protein level of 100 %, and the other protein levels were plotted relative to 100 %. The results are the mean of three independent experiments.

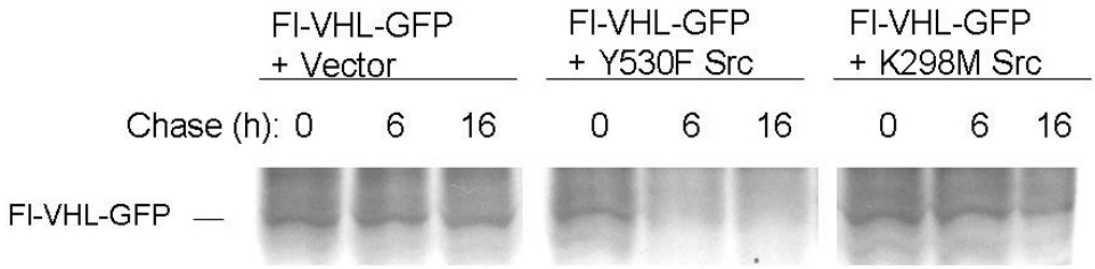

Figure 16. Src activity decreases the protein half-life of VHL in ^{35}S metabolic labeling-chase experiments.

HEK 293T cells were transfected with Flag-VHL-GFP, in the presence of empty vector, Y530F Src, or K298M Src. The cells were then subjected to ^{35}S metabolic labeling and chase *in vivo* (in intact cells). VHL was isolated by immunoprecipitation with anti-VHL polyclonal antibody. The immune complexes were then resolved by SDS-PAGE, the gels were dried, and the labelled proteins were detected by autoradiography. The results are representative of three independent experiments.

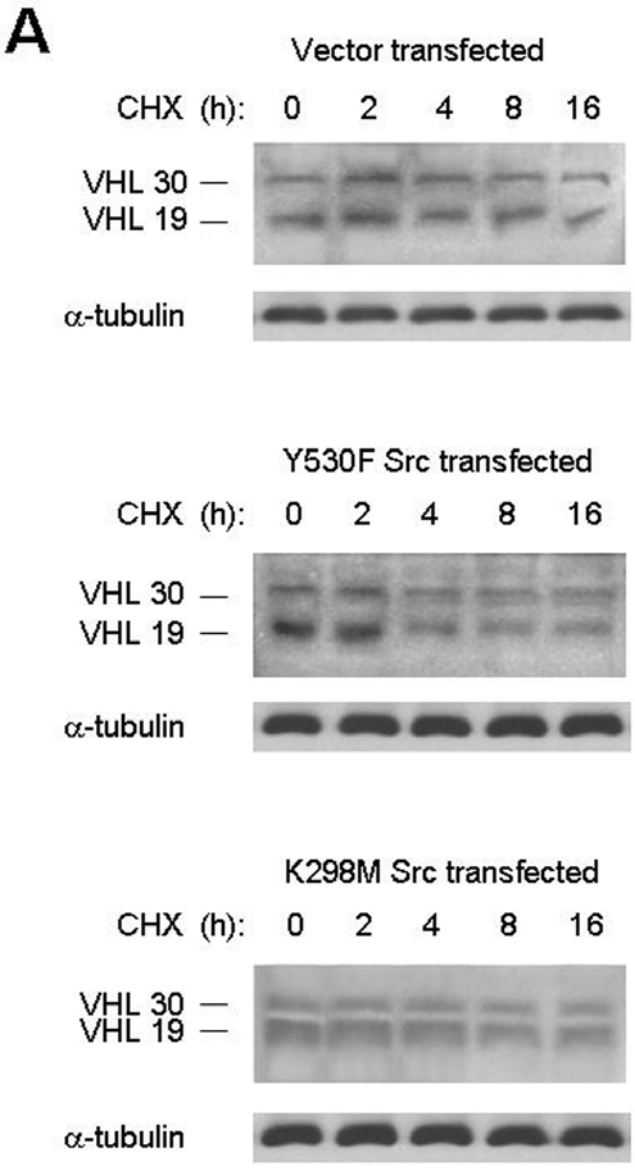
A
Vector transfected
CHX (h): 0 2 4 8 16
VHL 30
VHL 19
α-tubulin
Y530F Src transfected
CHX (h): 0 2 4 8 16
VHL 30
VHL 19
α-tubulin
K298M Src transfected
CHX (h): 0 2 4 8 16
VHL 30
VHL 19
α-tubulin

B

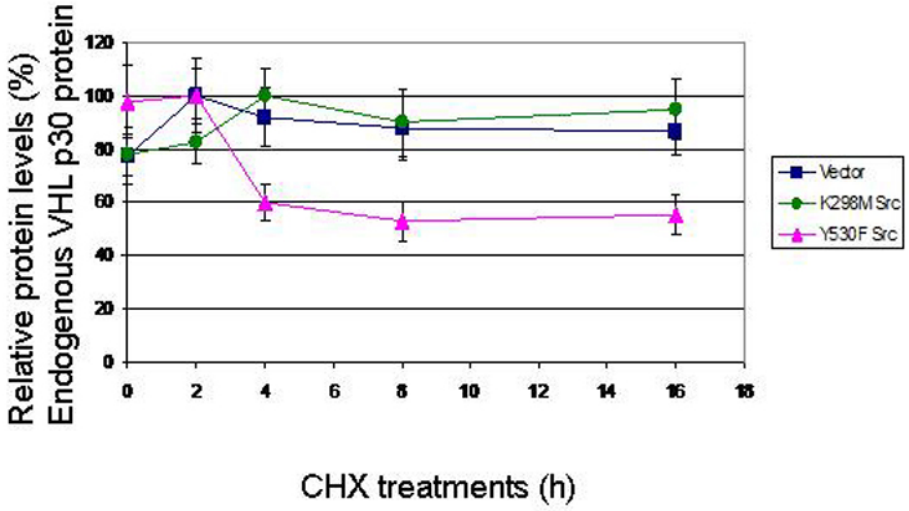
Relative protein levels (%)
Endogenous VHL p30 protein
120
100
80
60
40
20
0
0
2
4
6
8
10
12
14
16
18
Vector
K298M Src
Y530F Src
CHX treatments (h)

C

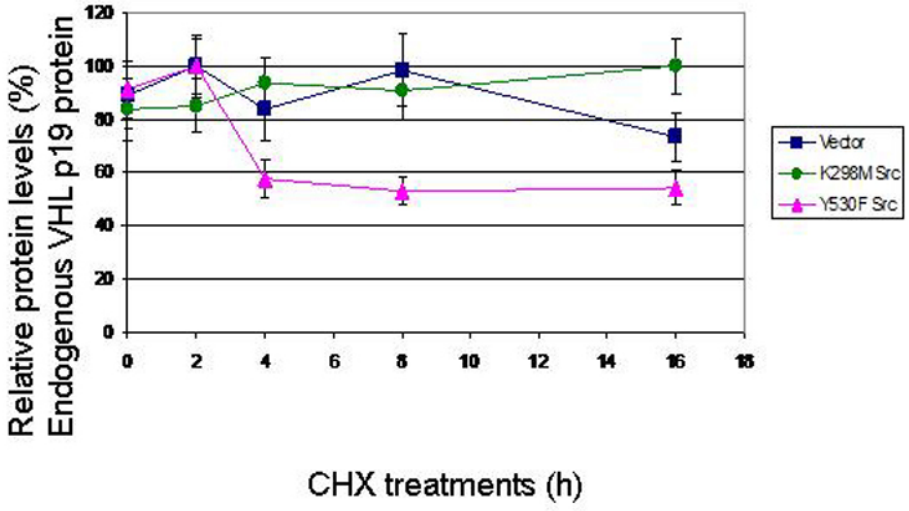
Relative protein levels (%)
Endogenous VHL p19 protein
120
100
80
60
40
20
0
0
2
4
6
8
10
12
14
16
18
Vector
K298M Src
Y530F Src
CHX treatments (h)

Figure 17. Src activity decreases the protein half-life of endogenous VHL in cycloheximide treatment experiments.

(A) HEK 293T cells were transfected with empty vector, Y530F Src, or K298M Src. 48 h post-transfection, the cells were treated with 100 μM final concentration of cycloheximide for 0 h, 2 h, 4 h, 8 h, or 16 h. The cells were then lysed, and Western blotting was performed for endogenous VHL protein levels using anti-VHL polyclonal antibody, and total α-tubulin levels using anti-α-tubulin monoclonal antibody. (B,C) Graphical representation of the effect of cycloheximide on endogenous VHL p30 half-life (B) and p19 half-life (C). VHL protein levels were normalized to α-tubulin. The darkest band density for each trial set was assigned a protein level of 100 %, and the other protein levels were plotted relative to 100 %. The results are the mean of three independent experiments.

3.6 Elevated Src activity downregulates intracellular VHL protein levels analyzed by fluorescence microscopy

I next performed fluorescence microscopy studies to investigate the effects of upregulating Src levels on VHL protein stability *in vivo* (in intact cells). Cellular levels of VHL could be detected by the signal produced by the GFP-tagged VHL construct when introduced into the RCC 786-O cell line [a renal cell carcinoma cell line lacking endogenous wildtype VHL, previously described (Pause *et al.*, 1998)]. Fluorescence microscopy data further supported the results of my biochemical experiments, indicating a mechanism of Src-induced degradation of VHL. RCC 786-0 cells cotransfected with Flag-VHL-GFP and activated Src exhibited a 66 % decrease in intensity of the green fluorescent signal, in comparison to control RCC 786-0 cells cotransfected with Flag-VHL-GFP and empty vector (Figure 18). In contrast, RCC 786-0 cells cotransfected with Flag-VHL-GFP and kinase dead Src exhibited a small 22 % decrease in green fluorescent signal (Figure 18). These results could additionally suggest that the kinase dead form of Src may have a small destabilizing effect on VHL protein. However, the strongest effect was that of activated Src on the decrease on Fl-VHL-GFP levels.

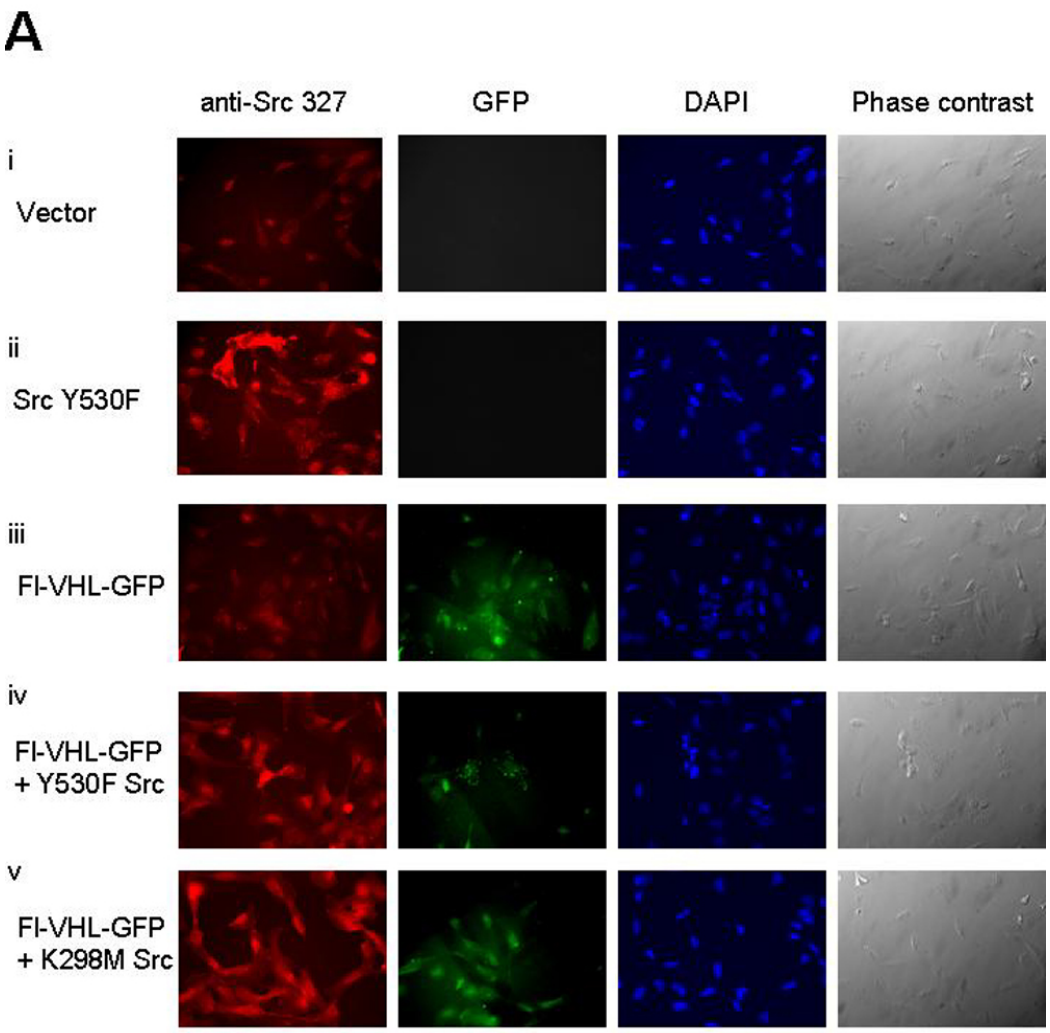
A
anti-Src 327
GFP
DAPI
Phase contrast
i
Vector
ii
Src Y530F
iii
Fl-VHL-GFP
iv
Fl-VHL-GFP
+ Y530F Src
v
Fl-VHL-GFP
+ K298M Src

B

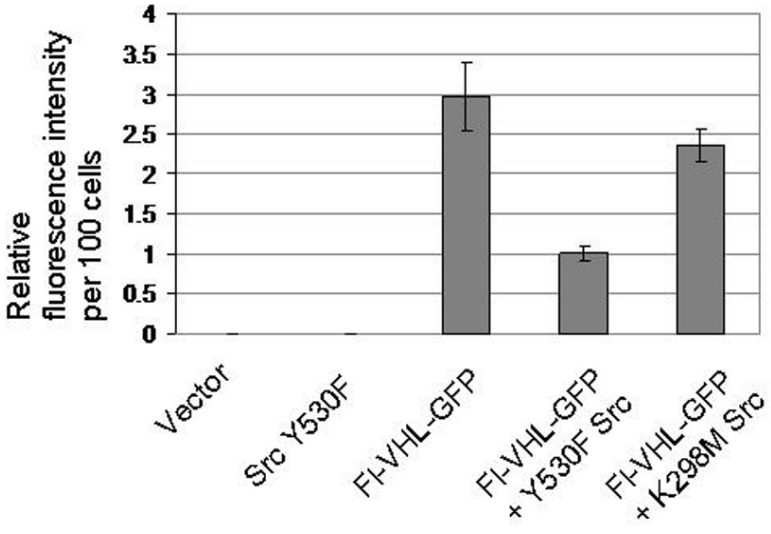
Relative fluorescence intensity per 100 cells
4
3.5
3
2.5
2
1.5
1
0.5
0
Vector
Src Y530F
Fl-VHL-GFP
Fl-VHL-GFP + Y530F Src
Fl-VHL-GFP + K298M Src

Figure 18. Src activity downregulates the intracellular fluorescence of GFP-tagged VHL protein.

(A) RCC 786-O renal carcinoma cells were seeded on glass coverslips in 6-well plates. At 80 % confluency, cells transfected with the indicated plasmids for 24 hours. The cover slips were then processed for fluorescence microscopy. Anti-Src monoclonal antibody was used to probe for Src. Flag-tagged VHL-GFP was visualized by GFP epifluorescence.

(B) Intensities of GFP fluorescence were measured using ImageJ image data analysis software. GFP fluorescence intensities per 300 cells were measured for each transfection, and these raw fluorescence intensity vaules were normalized to intensity values per 100 cells. The fluorescence intensity values per 100 cells were then standardized relative to a value of 1 per 100 cells assigned to the fluorescence intensity for the Flag-VHL-GFP and Y530F Src cotransfection condition. The graph charts the mean +/- 1SD, from three independent experiments done in triplicate.

3.7 **Src destabilization of VHL affects HIF-1α activity**

As a readout for the effects of Src-directed destabilization of VHL tumour suppressor protein, I conducted luciferase reporter assays utilizing a luciferase reporter construct containing a triple hypoxia responsive element repeat (HREx3-Luc) to study downstream HIF activity (Eickelberg *et al.*, 2002). As seen in Figure 19A, activated Src upregulated HRE-luciferase reporter activity by 3.6 fold (Figure 19A, left group). Src kinase activity was required for this upregulation, as it was not observed with the kinase dead Src mutant (Figure 19A, left group). In order to study whether Src was causing an increase in HIF activity through effects on VHL, I performed reciprocal dose-response experiments by introducing graduated amounts of activated Src or Flag-VHL-GFP, respectively, into HEK 293T cells (Figure 19A, middle and right groups). Cotransfection of low equal amounts of Flag-VHL-GFP plasmid (0.25 μg) and activated Src plasmid (0.25 μg) reduced luciferase reporter activity to near control levels. However, introduction of increasing amounts of activated Src was able to override the dampening effects of Flag-VHL-GFP (Figure 19A, middle group). In contrast, when I conducted the reverse dose response experiments by introducing increasing amounts of Flag-VHL-GFP in the presence of constant amounts of activated Src plasmid (Y530F Src), I observed that HRE-luciferase reporter activity decreased to sub-basal levels (Figure 19, right group). Immunoblot analyses of cell lysates further supported this interrelationship between Src and VHL, and demonstrated that degradation of VHL parallels increased levels in HIF-1α protein as well as increased levels of VEGF protein production (Figure 19B). Taken together, these results and my previous results, indicate that Src activation is able to

promote destabilization of VHL, and also causes increased levels of HIF-1α and increased HIF-1α activity.

A

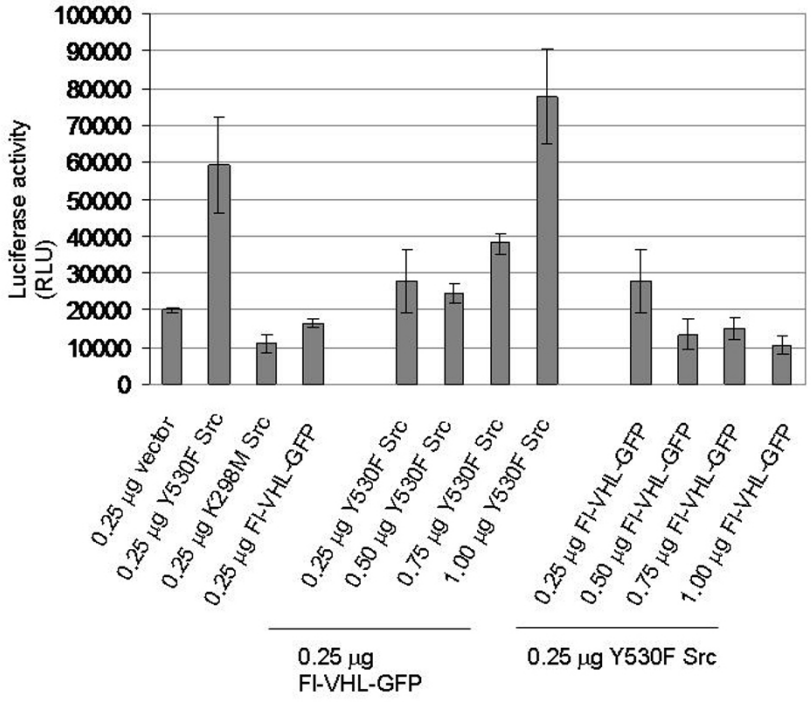
100000
90000
80000
70000
60000
50000
40000
30000
20000
10000
0
Luciferase activity (RLU)
0.25 μg vector
0.25 μg Y530F Src
0.25 μg K298M Src
0.25 μg Fl-VHL-GFP
0.25 μg Y530F Src
0.50 μg Y530F Src
0.75 μg Y530F Src
1.00 μg Y530F Src
0.25 μg Fl-VHL-GFP
0.50 μg Fl-VHL-GFP
0.75 μg Fl-VHL-GFP
1.00 μg Fl-VHL-GFP
0.25 μg Fl-VHL-GFP
0.25 μg Y530F Src

B

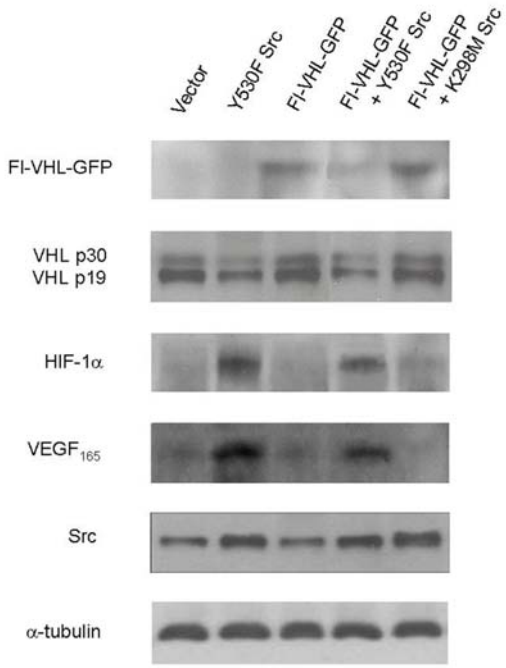
Vector
Y530F Src
Fl-VHL-GFP
Fl-VHL-GFP + Y530F Src
Fl-VHL-GFP + K298M Src
Fl-VHL-GFP
VHL p30
VHL p19
HIF-1α
VEGF165
Src
α-tubulin

Figure 19. Src destabilization of VHL affects HIF-1α activity downstream

(A) HEK 293T cells grown in 12-well plates were transiently transfected with the indicated plasmids and 250 ng/well of luciferase reporter plasmid (HREx3-Luc). In all cases, 100 ng β-galactosidase plasmid were co-transfected to normalize for transfection efficiency. The total DNA used for transfections was equalized to 1.60 μg with empty vector. 48 hours post-transfection, the cells were lysed, and lysates were subjected to luciferase activity assays (Promega). The graph charts the mean +/- 1SD, from three independent experiments.

(B) HEK 293T cells grown in 6-well plates were transfected with 1 μg each of the indicated plasmids. The total DNA used for transfections was equalized to 2 μg with empty vector. 48 h post-transfection, the cells were lysed, and Western blotting was performed using anti-Flag monoclonal antibody to detect exogenous VHL protein, anti-VHL polyclonal antibody to detect endogenous VHL protein, anti-HIF-1α monoclonal antibody, VEGF polyclonal antibody, anti-Src monoclonal antibody, and anti-α-tubulin monoclonal antibody. The results are representative of three independent experiments.

3.8 Src destabilization of VHL affects tubulogenesis *in vitro*

I performed further experiments to study downstream biological effects of Src-directed destabilization of VHL protein, including experiments measuring endothelial tube formation. I conducted endothelial tube formation assays on ECM matrix (Matrigel, extracellular matrix from Engelbreth Holm-Swarm mouse sarcoma, BD Biosciences), following previously published protocols (Troyanovsky *et al.*, 2001;Potente *et al.*, 2005). In this assay, endothelial cells will form capillary networks when seeded on Matrigel in response to angiogenic factors such as VEGF that are present in conditioned media. The extent and lengths of endothelial tube formation are indicators of the angiogenic potential. As seen in Figure 20, significant endothelial tube formation occurred in the presence of conditioned medium from HEK 293T cells that had been transfected with activated Src. In contrast, the least tube formation was observed with conditioned medium from cells transfected with a control vector alone or with Flag-VHL-GFP alone. Importantly, the effect of elevated Src activity on this angiogenesis assay was reduced when VHL was cotransfected with activated Src into the HEK 293T cells.

A

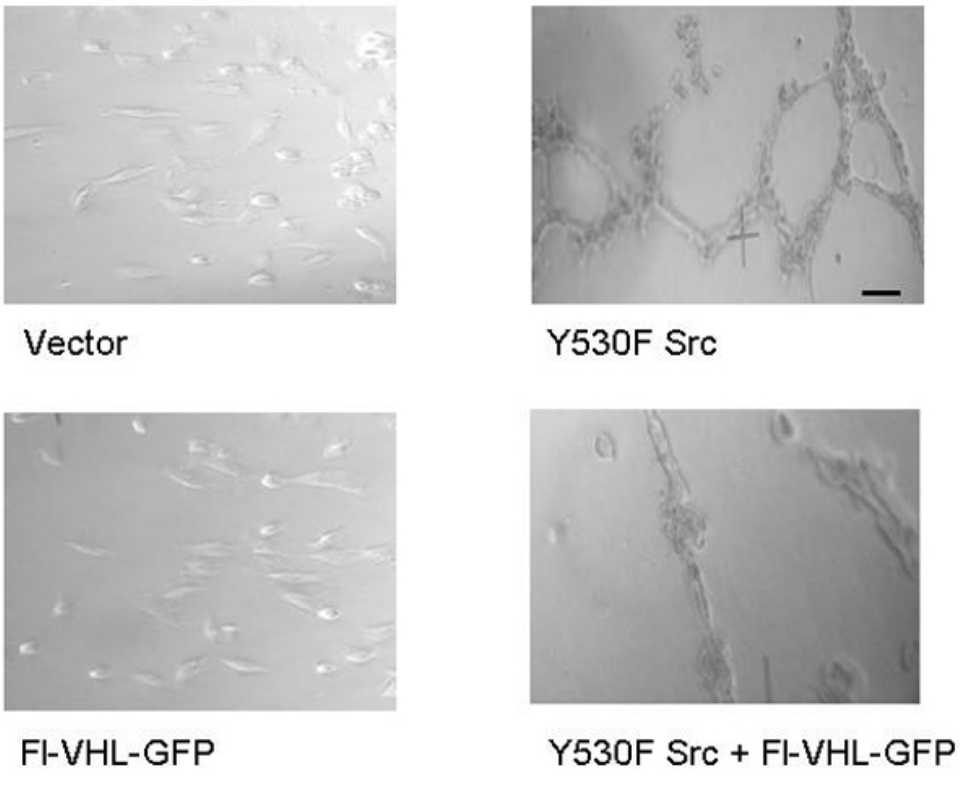
Vector
Y530F Src
Fl-VHL-GFP
Y530F Src + Fl-VHL-GFP

B

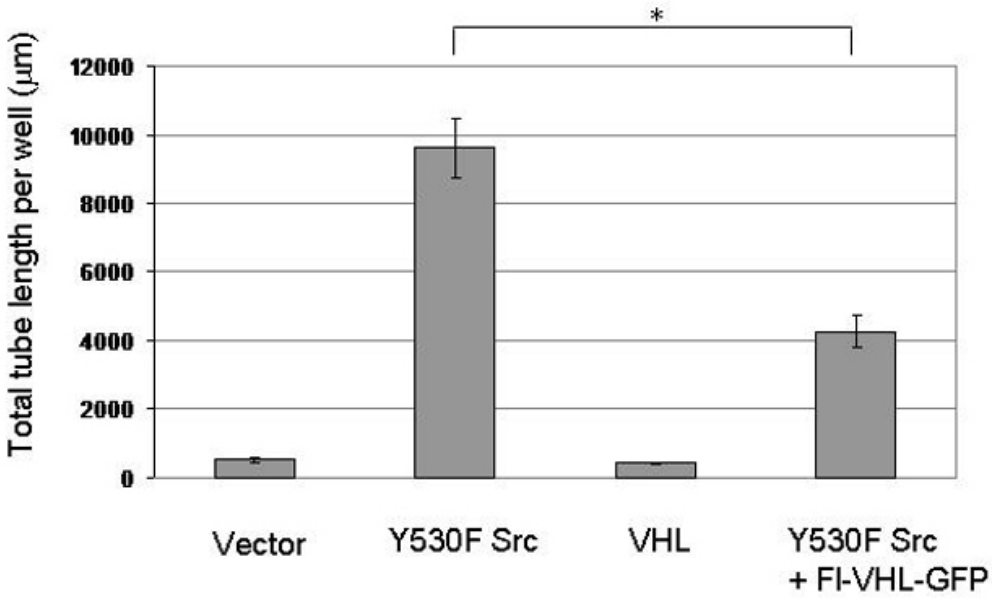
*
Total tube length per well (μm)
12000
10000
8000
6000
4000
2000
0
Vector
Y530F Src
VHL
Y530F Src
+ Fl-VHL-GFP

Figure 20. Src destabilization of VHL affects tubulogenesis *in vitro*.

(A) HEK 293T cells were transfected with vector, Y530F Src, Flag-VHL-GFP, or Flag-VHL-GFP plus Y530F Src. 48 h post-transfection conditioned media from each condition was collected for endothelial tube formation assays. 100 μL of ECM matrix (extracellular matrix from Engelbreth Holm-Swarm mouse sarcoma) was pipetted into each well of a 96-well tissue culture plate. The tissue culture plate was then incubated for one hour at 37 ^{o}C to allow the ECM matrix to gel. EA.hy926 cells (of the permanent human endothelial cell line) were then seeded at $4X10^{3}$ cells per well onto the surface of the polymerized ECM matrix. 100 μL of conditioned media from each transfection condition were then overlaid onto each well of endothelial cells seeded on ECM matrix. After 16 h incubation at 37 ^{o}C, the extent of formation of capillary networks for each condition was photographed under an inverted light microscope at 100X. (B) Quantification of capillary network formation was done by measurement of total tube length per well using ImageJ image data analysis software. Scale bar: 100 μm. The graph charts the averages +/- 1SD, from three separate transfections done in duplicate. Statistical significance was determined by Student's t test; *$P<0.05$.

3.9 Src destabilization of VHL affects chick embryo chorioallantoic membrane blood vessel growth

As a readout for the effects of Src destruction of VHL tumour suppressor protein on angiogenesis *in vivo*, I performed chorioallantoic membrane assays as previously described (Kwon *et al.*, 2001). In this assay, blood vasculature of the chick chorioallantoic membrane (CAM) grows in response to growth signals received from cells loaded onto gelatin sponges placed onto the CAM. The average lengths of vasculature per field are indicators of angiogenic potential. As shown in Figure 21, extensive angiogenesis occurred in the presence of HEK 293T cells that had been transfected with activated Src. In contrast, the least angiogenesis occurred in cells transfected with a control vector alone or with Flag-VHL-GFP alone. Furthermore, the effect of elevated Src activity on this angiogenesis assay was reduced when Flag-VHL-GFP was cotransfected with activated Src into the HEK 293T cells.

C

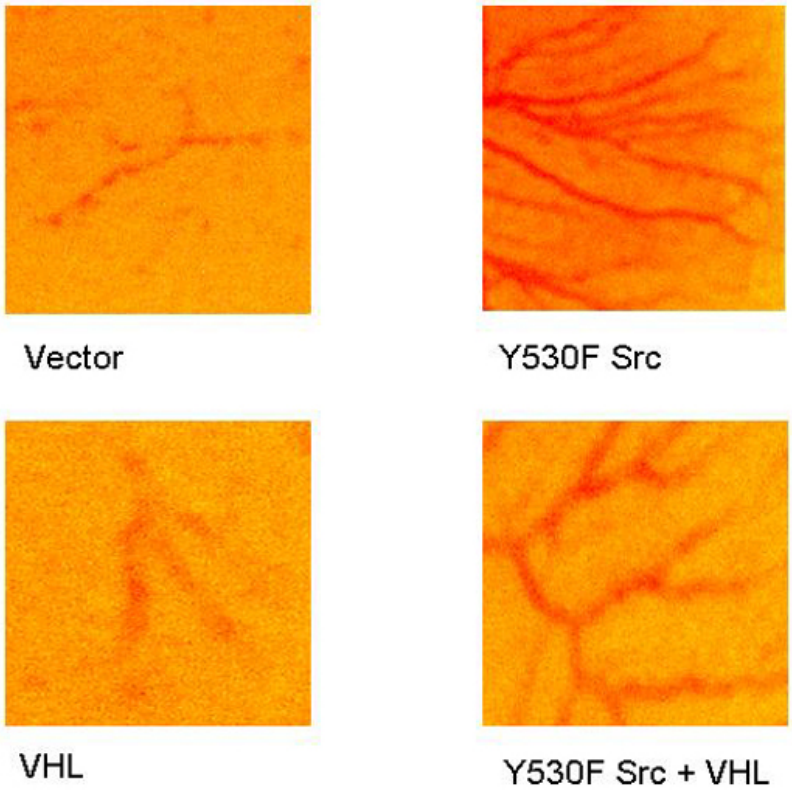
Vector
Y530F Src
VHL
Y530F Src + VHL

D

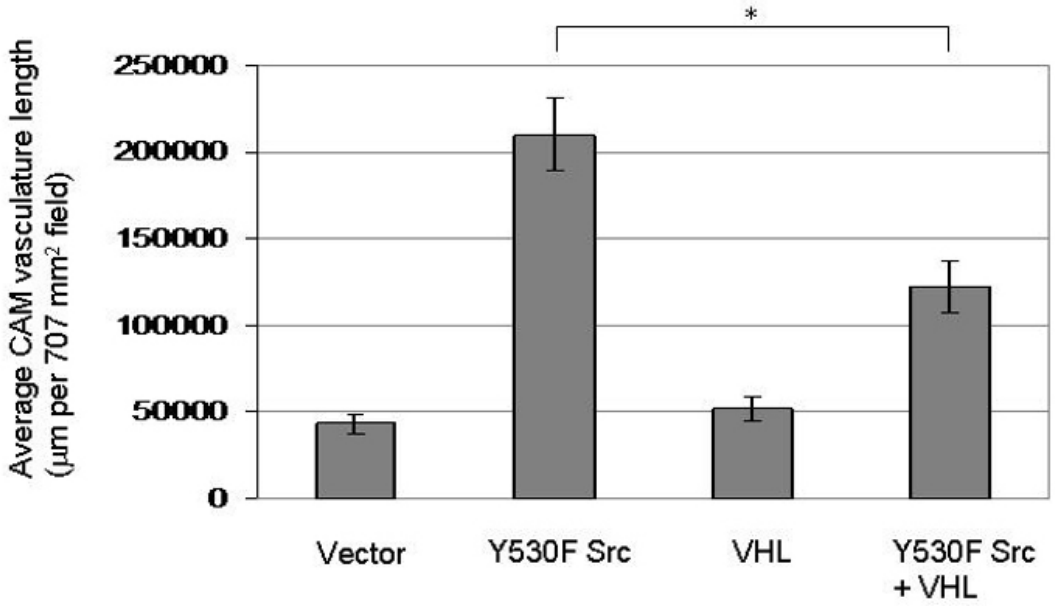
Average CAM vasculature length (μm per 707 mm² field)
250000
200000
150000
100000
50000
0
*
Vector
Y530F Src
VHL
Y530F Src + VHL

Figure 21. Src destabilization of VHL affects chick embryo chorioallantoic membrane blood vessel growth.

(A) Photographs of developing chick chorioallantoic membranes, implanted with gelatin sponges loaded with HEK 293T cells transfected with vector, Y530F Src, Flag-VHL-GFP, or Flag-VHL-GFP plus Y530F Src.

(B) Quantitation of angiogenesis was done by measuring the length of vasculature per 707 mm^2 field, using ImageJ image data analysis software. Four fields per CAM were measured for nine CAMs per transfection condition. The graph charts the averages +/- 1SD. Statistical significance was determined by Student's t test; *$P<0.05$.

3.10 siRNA knockdown of Src increases endogenous VHL protein levels

In order to further study Src's involvement in targeting VHL protein for degradation, I transfected short interfering RNA (siRNA) to reduce Src levels in several cell types. I observed 70 % knockdown in Src protein levels, compared to Src protein levels in cells transfected with control, non-targeting siRNA in HEK 293T, SK-BR-3 breast cancer, and MCF-10A breast epithelial cells (Figure 22, Figure 23, Figure 24). The results also indicated the VHL siRNA was able to specific\ally knockdown endogenous VHL p30 and p19 protein levels by 83 %. Knockdown of Src resulted in increased VHL protein levels of 4.0- fold in HEK 293T, SK-BR-3, and MCF-10A cells (Figure 22, Figure 23, Figure 24). Consistent with this and earlier data, after transfection of Src-specific siRNA into these cells, I also observed a 60 % decrease in VEGF protein production in conditioned media from these cells, compared to VEGF production from cells transfected with control siRNA (Figure 23). Thus, these results support a significant role for Src and Src activity in downregulating VHL protein levels. Also, these experiments add further support for the model that high Src protein levels and high Src activity play a role in the upregulating VEGF protein production.

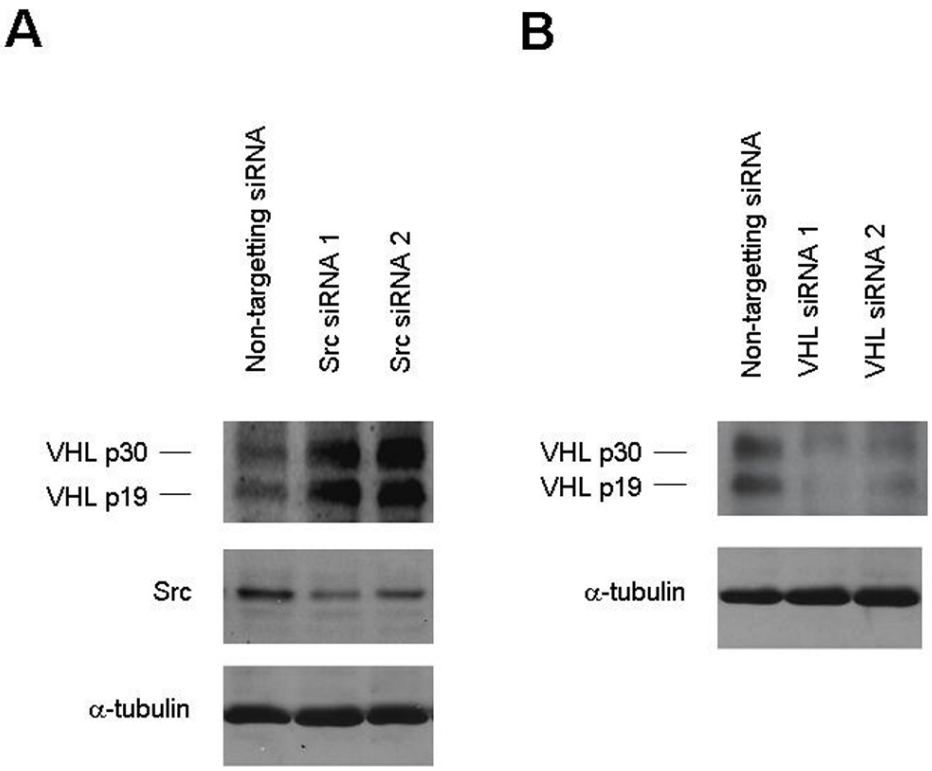
A
Non-targetting siRNA
Src siRNA 1
Src siRNA 2
VHL p30
VHL p19
Src
α-tubulin
B
Non-targetting siRNA
VHL siRNA 1
VHL siRNA 2
VHL p30
VHL p19
α-tubulin

C

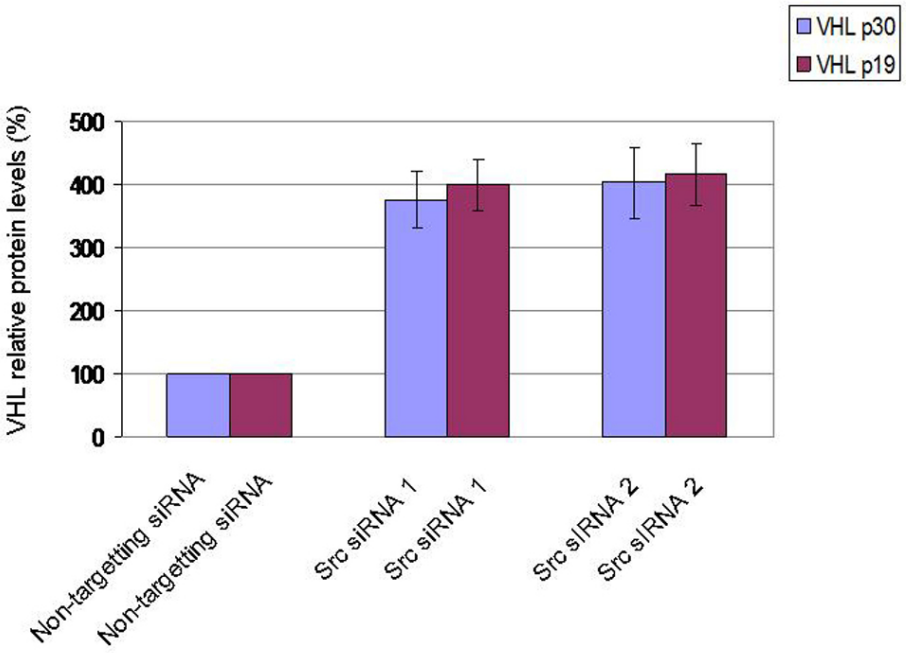
VHL p30
VHL p19
VHL relative protein levels (%)
500
400
300
200
100
0
Non-targetting siRNA
Non-targetting siRNA
Src siRNA 1
Src siRNA 1
Src siRNA 2
Src siRNA 2

D

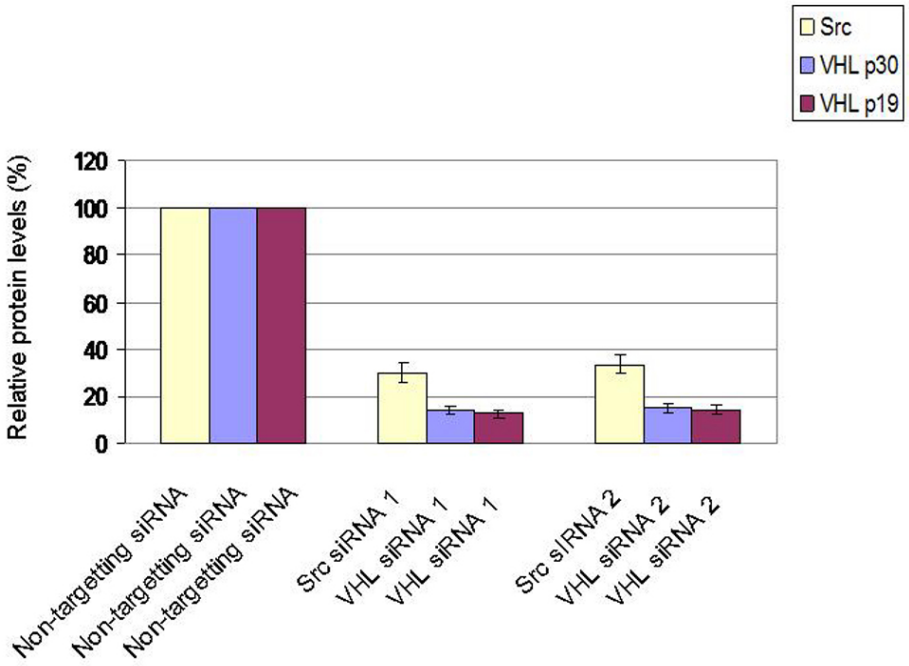
Src
VHL p30
VHL p19
Relative protein levels (%)
120
100
80
60
40
20
0
Non-targetting siRNA
Non-targetting siRNA
Non-targetting siRNA
Src siRNA 1
VHL siRNA 1
VHL siRNA 1
Src siRNA 2
VHL siRNA 2
VHL siRNA 2

Figure 22. siRNA knockdown of Src increases endogenous VHL protein levels.

(A) HEK 293T cells were transfected with non-targeting control siRNA or Src siRNA. 48 h post-transfection, the cells were lysed, and Western blotting was performed to detect endogenous VHL using anti-VHL polyclonal antibody, Src, using anti-Src monoclonal antibody and total α-tubulin protein levels using anti-α-tubulin monoclonal antibody.
(B) HEK 293T cells were transfected with non-targeting control siRNA or VHL siRNA for 48 hours. Cell lysates were then subjected to Western blotting to detect endogenous VHL and total α-tubulin protein levels.
(C) Src siRNA Upregulation of VHL protein levels. Quantitation of the VHL protein levels of the immunoblot results from part A. Densitometry was performed using ImageQuant TL software from Amersham Biosciences. Results are representative of n = 3.
(D) Effective siRNA knockdown of Src and VHL protein. Quantitation of the VHL and Src protein levels of the immunoblot results from part B. Densitometry was performed using ImageQuant TL software from Amersham Biosciences. Values in C and D were normalized relative to the values for α-tubulin protein levels. Results are representative of n = 3.

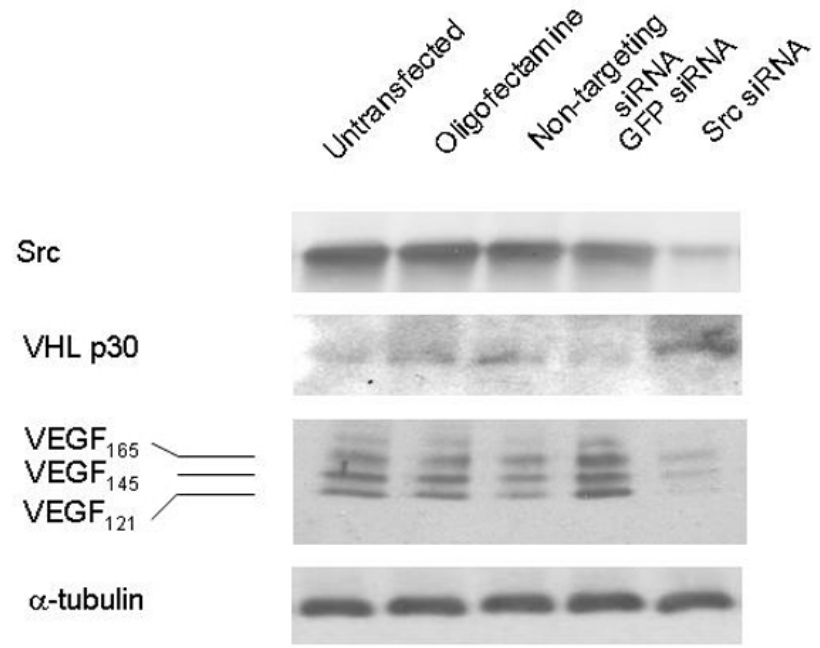

Figure 23. siRNA Knockdown of Src increases VHL protein levels in SK-BR-3 breast cancer cells.

SK-BR-3 breast cancer cells were transfected with Oligofectamine alone (no siRNA), non-targeting control siRNA, GFP siRNA, or Src siRNA 1. Conditioned media samples were collected 48 h after transfection and were analyzed by Western blotting for VEGF protein. The conditioned media volumes assayed were corrected for differences in the cell numbers of the cell cultures from which the samples were collected. Cell lysates were subjected to Western blotting to detect endogenous Src protein, VHL protein levels, and α-tubulin protein levels. The results are representative of two independent experiments.

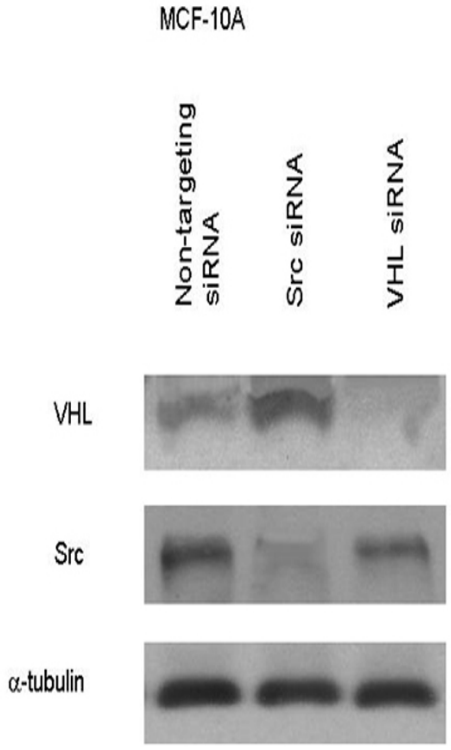

Figure 24. Knockdown of Src increased VHL protein levels in MCF-10A breast epithelial cells.

MCF-10A breast epithelial cells were transfected with non-targeting control siRNA, Src siRNA, or VHL siRNA, for 48 hours. Cell lysates were subjected to Western blotting to detect endogenous VHL protein, Src protein, and total α-tubulin protein levels. The results are representative of two independent experiments.

3.11 Inhibition of Src by PP2 increases VHL protein levels

Experiments designed to investigate the effects of knockdown of endogenous cellular Src levels are important approaches for the study of its function. However, in addition, these experiments can be complimented by experiments inhibiting Src directly by chemical inhibition. Therefore, I tested the effect of inhibiting Src activity using the Src family inhibitor PP2. Src activity decreased upon PP2 treatment, as detected by blotting for phosphorylated Src with anti-phosphotyrosine 419 Src antibody. At the same time, PP2 treatment resulted in increased levels of endogenous stable (unmodified and unubiquitinated) VHL levels and this was correlated with lower levels of ubiquitinated VHL. Indeed, the results indicated that PP2 treatment of NIH 3T3 effectively decreased phosphotyrosine 419 Src activity, and led to increased stability of VHL protein (Figure 25).

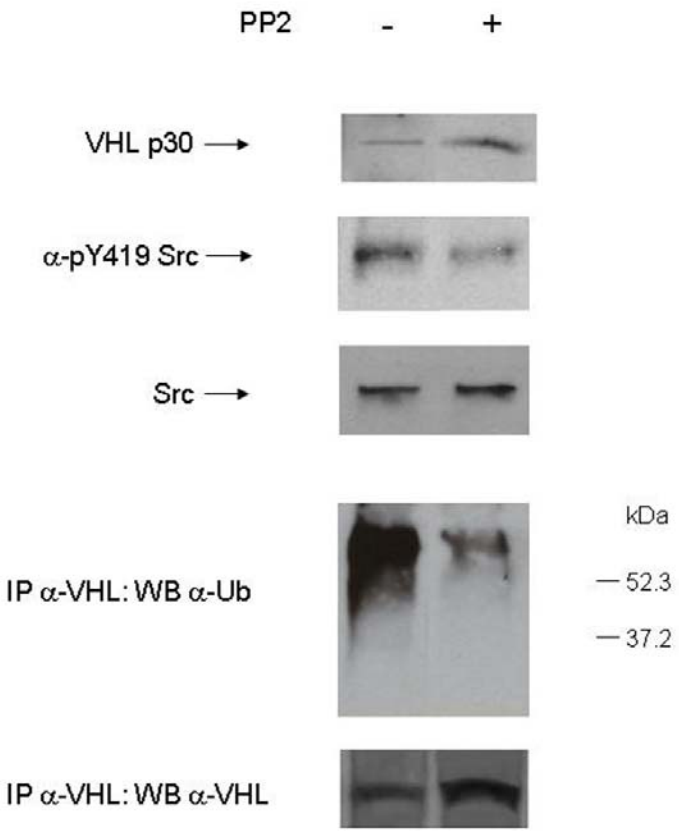
PP2
-
+
VHL p30
α-pY419 Src
Src
IP α-VHL: WB α-Ub
IP α-VHL: WB α-VHL
kDa
52.3
37.2

Figure 25. Inhibition of Src by PP2 treatment increased VHL protein levels.

NIH 3T3 cells at 75 % confluence were treated with DMSO or 10 μM PP2 dissolved in DMSO for 15 h. Cell lysates were subjected to Western blotting to detect endogenous VHL protein levels using anti-VHL polyclonal antibody, phosphotyrosine 419 Src levels using anti- phosphotyrosine 419 Src monoclonal antibody, and total Src protein levels using anti-Src monoclonal antibody. Also, endogenous VHL was isolated by immunoprecipitation with anti-VHL polyclonal antibody, followed by immunoblotting using anti-ubiquitin monoclonal antibody or anti-VHL monoclonal antibody. The results are representative of two independent experiments.

CHAPTER FOUR: MAPPING THE SRC TYROSINE PHOSPHORYLATION SITE ON THE VHL TUMOUR SUPPRESSOR PROTEIN

4.1 Y185 is a major phosphorylation site on VHL and Y185F mutation confers increased protein stability to VHL protein

I conducted further experiments to study whether Src was able to directly phosphorylate VHL. Furthermore, mass spectrometry analysis was also performed to identify the target Src phosphorylation site on VHL. When *in vitro* kinase reactions were performed with purified baculovirus expressed human Src kinase and GST or GST-VHL wildtype (GST-VHL WT) (Figure 26), I found that GST-VHL phosphorylation occurred only in the presence of Src. Control GST alone was not phosphorylated by baculovirus Src kinase. These results indicated that Src is able to directly phosphorylate VHL.

Phospho-GST-VHL produced by baculovirus Src kinase reaction on GST-VHL was isolated by SDS-PAGE. The tyrosine phosphorylation on Src phosphorylated GST-VHL was subsequently mapped through mass spectrometric analysis performed by the proteomics centre at the University of Victoria. In summary, this analysis involved MALDI TOF in positive and negative ion mode, and electrospray ionization scanning both for the neutral loss of the phosphotyrosine precursor, and ms/ms for fragmentation/sequence determination. This process revealed that tyrosine 185 of VHL was a site phosphorylated by Src *in vitro* (Figure 27). Interestingly, analysis of the candidate Src tyrosine targets on VHL through the ExPASy (**Ex**pert **P**rotein **A**nalysis **S**ystem of the proteomics server of the Swiss Institute of Bioinformatics (SIB)) Swiss-

Prot program revealed that the sequences surrounding VHL tyrosines 23, 98, 112, 156, 175, 185 exhibited similarity indices of 89, 89, 86, 76, 90, and 95, respectively, to the Src target tyrosine consensus sequence [N/D]XYEEIϕ, where ϕ represents a hydrophobic residue (Songyang *et al.*, 1995) (Table 1). Thus, VHL tyrosine 185 had high likelihood of being able to be phosphorylated by Src.

These results mapping the tyrosine target for Src phosphorylation on VHL are intriguing in light of reported studies of PDGFR in the literature. For PDGFRα, Src family kinases (SFKs) seem to enhance Cbl-mediated degradation of the receptor (Rosenkranz *et al.*, 2000). In SYF cells, or in cells expressing a mutant PDGFRα that cannot bind SFKs, the half-life of the receptor is prolonged. Furthermore, overexpression of Cbl is able to promote the degradation of receptors containing SFK-binding sites (Rosenkranz *et al.*, 2000)

When I coexpressed constitutively active Src (Y530F Src) with wildtype VHL (WT VHL), or with a phosphotyrosine site mutant of VHL (Y185F VHL), I found that Y185F VHL protein was more stable than WT VHL in the presenceof Src (Figure 28). These results also showed that there was tyrosine phosphorylation and ubiquitination when WT VHL was coexpressed with activated Src *in vivo* (in intact cells) (Figure 28A). On the other hand, *in vivo* tyrosine phosphorylation and ubiquitination when Y185F VHL was coexpressed with activated Src was markedly decreased, in contrast to when WT VHL was coexpressed with activated Src (Figure 28A).

Cycloheximide treatment experiments further showed that Y185F VHL protein had higher protein stability than compared to WT VHL protein levels in the presence of activated Src (Figure 29A). As shown in Figure 29B-C, WT VHL, in the presence of

activated Src, exhibited a markedly decreased half-life of 6 h on average, compared to Y185F VHL, which even in the presence of activated Src exhibited stability for greater than 16 h. Together, the data indicated that the Y185F VHL protein levels were better maintained in the presence of activated Src, compared to WT VHL protein levels in the presence of activated Src.

During the course of this project, the results also suggested that an interesting effect of reciprocal VHL control over Src protein stability could exist. It appears that as Src is responsible for destabilizing VHL, there may exist a negative feedback role for VHL destabilization of Src (Figure 28B and Figure 29A). The data suggest that VHL might be able to cause negative feedback destabilization of Src protein. In contrast Y185F VHL does not seem to be as effective in destabilizing Src protein, and in fact Y185F VHL expression may promote Src protein stability. To date, Src kinase stability regulation by VHL tumour suppressor has not been reported. This could be an important finding to additionally explain the reasons for greater destabilization of active Src protein in contrast to the greater stabilization of inactive Src protein. Thus, further studies on this reciprocal VHL effect on Src oncoprotein stability could help elucidate their complex roles in their protein degradation mechanisms.

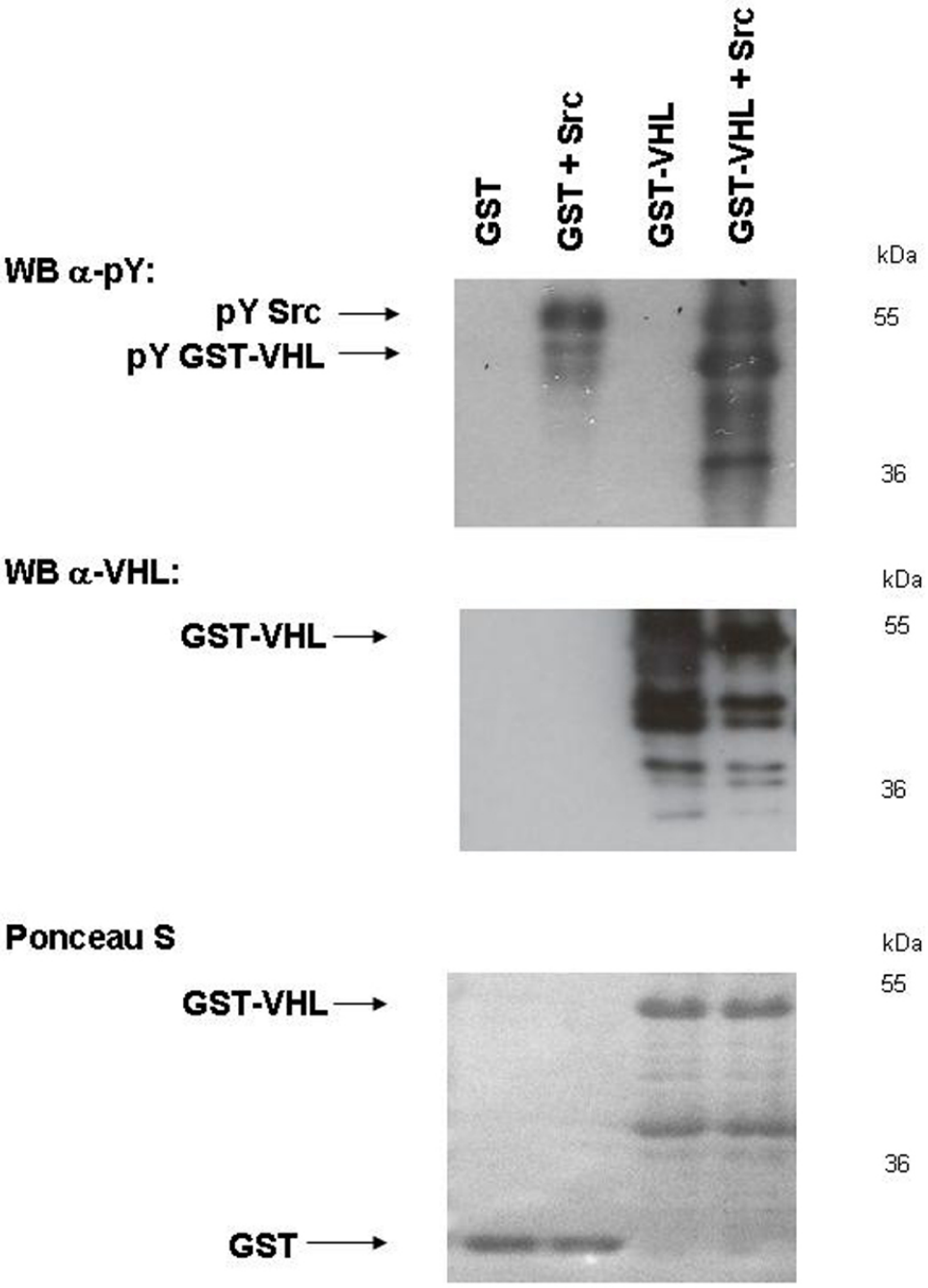
GST
GST + Src
GST-VHL
GST-VHL + Src
WB α-pY:
pY Src
pY GST-VHL
kDa
55
36
WB α-VHL:
GST-VHL
kDa
55
36
Ponceau S
GST-VHL
GST
kDa
55
36

Figure 26. Src phophorylates GST-VHL.

GST and GST-VHL wildtype full-length 213 aa proteins were produced, bound to glutathione-agarose beads, and purified. *In vitro* kinase phosphorylation reactions were conducted on GST and GST-VHL wildtype (500 pmol each), in the absence and presence of baculovirus Src. The reactions were stopped by boiling, resolved on 10 % acrylamide SDS-PAGE gel, and transferred to nitrocellulose. Immunoblotting was then performed using anti-phosphotyrosine monoclonal antibody and anti-VHL polyclonal antibody. Ponceau S staining of the nitrocellulose was also performed. The results are representative of three independent experiments.

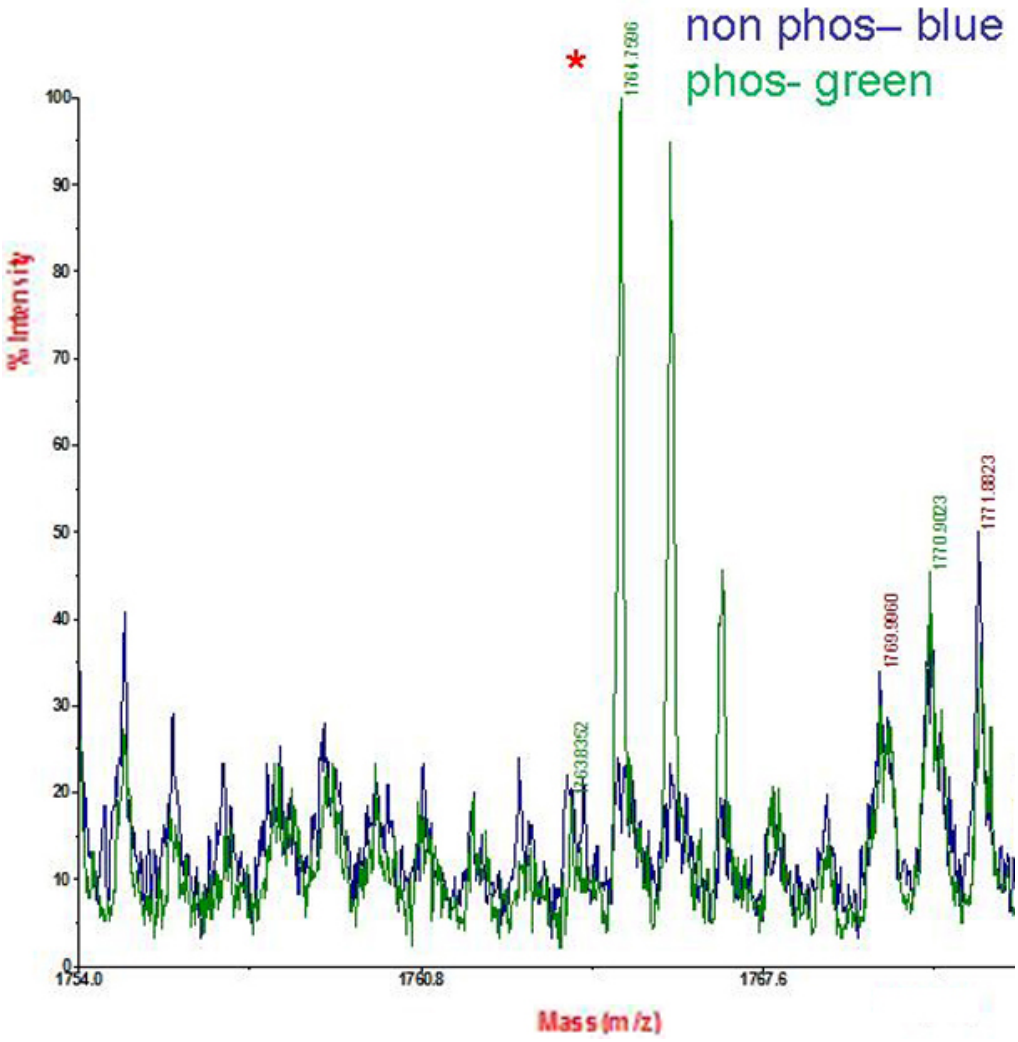
non phos– blue
phos- green
*
1764.7596
1769.9060
1770.9023
1771.8823
% Intensity
Mass (m/z)
1754.0
1760.8
1767.6

Figure 27. Mass spectrometric assays of baculovirus Src phosphorylated GST-VHL indicates that Y185 is phosphorylated.

Tyrosine phosphorylation on Src phosphorylated GST-VHL was mapped through mass spectrometric analysis performed by the proteomics centre at the University of Victoria. In summary, this analysis involved MALDI TOF in positive and negative ion mode, and electrospray ionization scanning both for the neutral loss of the phosphotyrosine precursor, and ms/ms for fragmentation/sequence determination. The phosphorylation peak is indicated with a red asterisk.

Table 1. Results of Swiss-Prot analysis of target tyrosine consensus sequences for Src phosphorylation on VHL.

VHL Tyrosine Site	Similarity Index	Sequence
Site Tyrosine 23	89	vgaeeagvee_YGPE_edggeesgae
Site Tyrosine 98	89	wlnfdgepqp_YPTL_ppgtgrrihs
Site Tyrosine 112	86	ppgtgrrihs_YRGH_lwlfrdagth
Site Tyrosine 156	76	pifanitlpv_YTLK_erclqvvrsl
Site Tyrosine 175	90	vvrslvkpen_YRRL_divrslyedl
Site Tyrosine 185	**95**	**yrrldivrsl_YEDL_edhpnvqkdl**

Src target tyrosine consensus sequence is [N/D]XYEEIϕ, where ϕ represents a hydrophobic residue (Songyang *et al.*, 1995).

Candidate target VHL tyrosine residues are capitalized in the sequences.

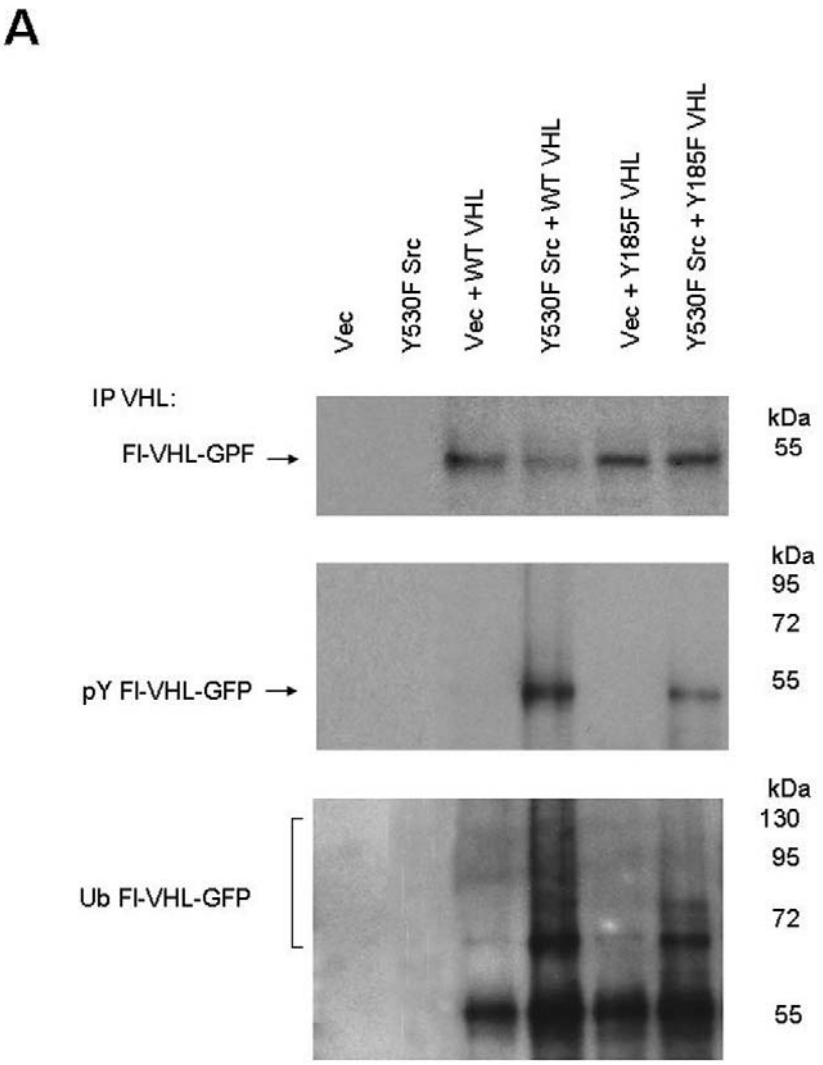
A
Vec
Y530F Src
Vec + WT VHL
Y530F Src + WT VHL
Vec + Y185F VHL
Y530F Src + Y185F VHL
IP VHL:
Fl-VHL-GPF
kDa
55
pY Fl-VHL-GFP
kDa
95
72
55
Ub Fl-VHL-GFP
kDa
130
95
72
55

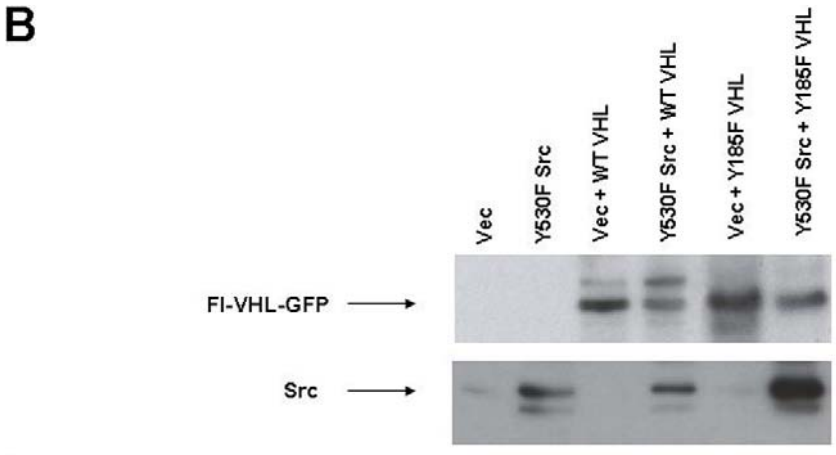
B
Vec
Y530F Src
Vec + WT VHL
Y530F Src + WT VHL
Vec + Y185F VHL
Y530F Src + Y185F VHL
Fl-VHL-GFP
Src

Figure 28. Y185F mutation reduces tyrosine phosphorylation and ubiquitination of VHL.

(A) HEK 293T cells were transfected with vector or constitutively active Src (Y530F Src) alone or together with Flag-tagged VHL-GFP (WT VHL) or Flag-tagged Y185F VHL-GFP (Y185F VHL). 48 h post-transfection, cell lysates were prepared in 2 % SDS, 50 mM Tris pH6.8 lysis buffer, and boiled. Exogenous VHL was isolated by immunoprecipitation with anti-VHL polyclonal antibody, followed by immunoblotting using anti-VHL monoclonal antibody, anti-phosphotyrosine monoclonal antibody, or monoclonal anti-ubiquitin antibody.

(B) Total cell lysate Fl-VHL-GFP protein levels were detected by Western blotting using anti-VHL polyclonal antibody, and Src protein levels were detected by Western blotting using anti-Src monoclonal antibody. The results are representative of three independent experiments.

A

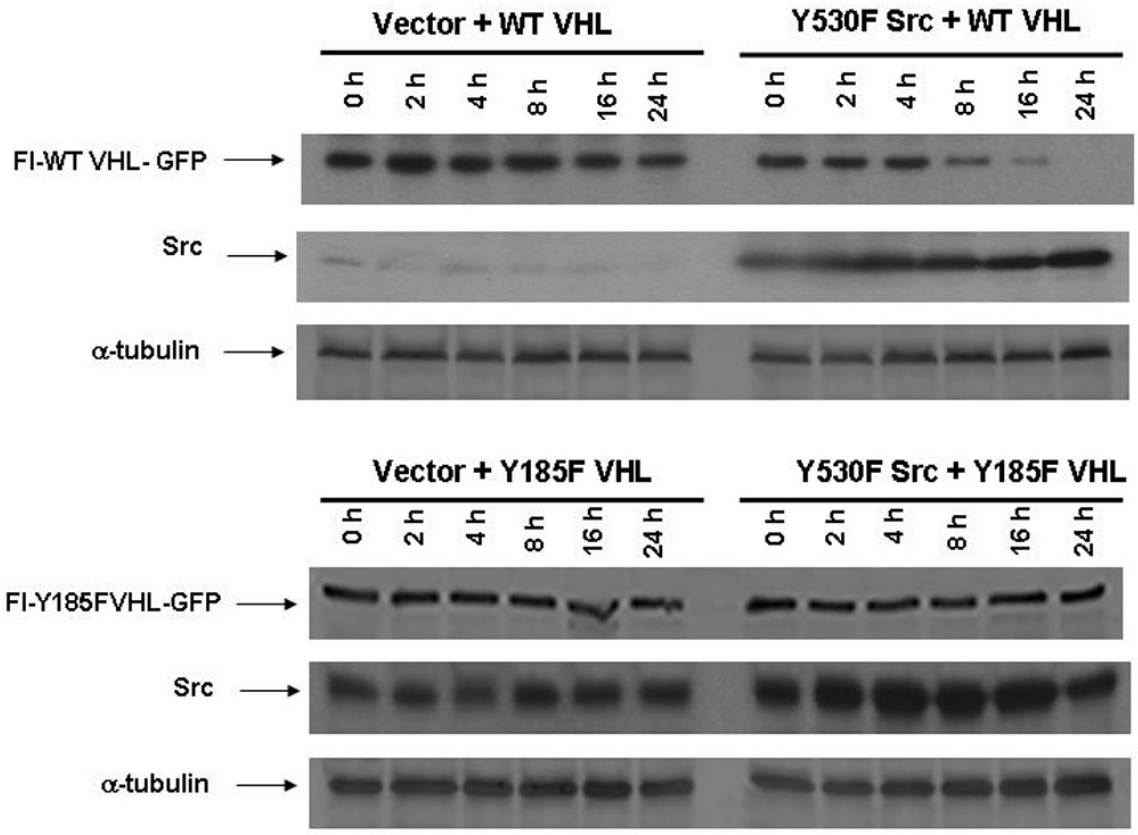
Vector + WT VHL
Y530F Src + WT VHL
0 h
2 h
4 h
8 h
16 h
24 h
Fl-WT VHL- GFP
Src
α-tubulin
Vector + Y185F VHL
Y530F Src + Y185F VHL
Fl-Y185FVHL-GFP
Src
α-tubulin

B

Effect of Src on wildtype VHL half-life.

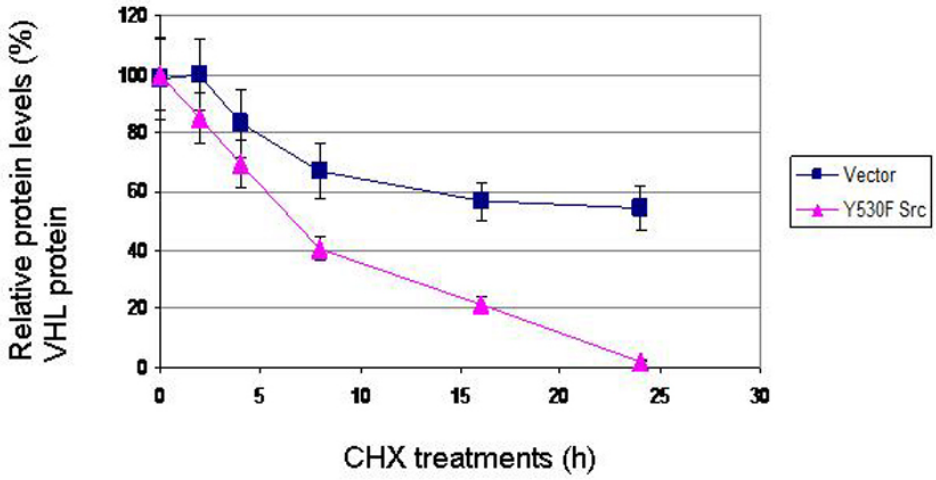

C

Effect of Src on Y185F VHL half-life.

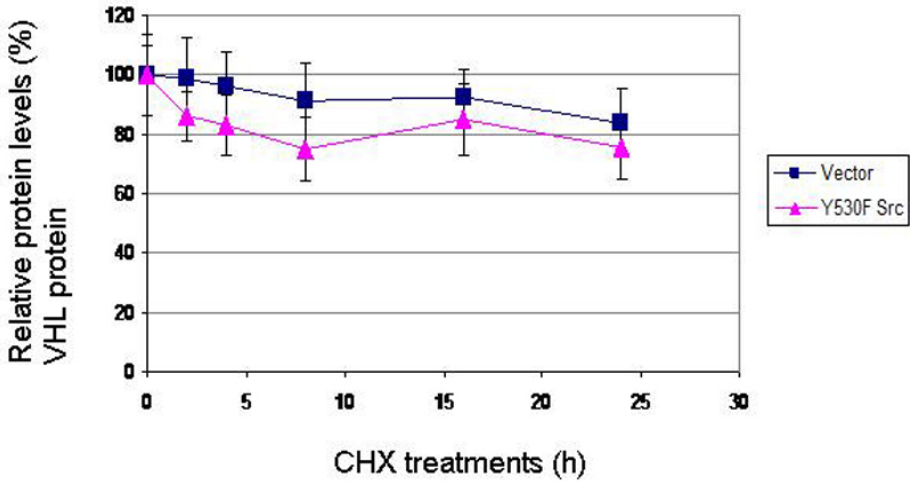

Figure 29. Y185F mutation confers increased VHL protein stability.

(A) HEK 293T cells were transfected with Flag-VHL-GFP (WT VHL) or Flag-Y185F VHL-GFP (Y185F VHL), in the presence of vector or activated Src (Y530F Src). 48 h post-transfection, the cells were treated with 100 μM final concentration of cycloheximide for 0 h, 2 h, 4 h, 8 h, 16 h, or 24 h. Cell lysates were then subjected to Western blotting for exogenous VHL protein levels using anti-VHL polyclonal antibody, Src protein levels using anti-Src monoclonal antibody, and total α-tubulin protein levels using anti-α-tubulin monoclonal antibody.

(B, C) Graphical representations of the effect of activated Src on wildtype Flag-VHL-GFP protein half-life (B) and the effect of activated Src on Y185F Flag-VHL-GFP protein half-life (C). VHL protein levels were normalized to α-tubulin. The darkest band density for each trial set was assigned a protein level of 100 %, and the other protein levels were plotted relative to 100 %. The results are the mean of three independent experiments.

4.2 Coimmunoprecipitation of Src and VHL

I conducted experiments to determine if Src was able to coimmunoprecipitate with VHL, and *vice versa*. Moreover, in order to study if a difference in Src interaction with wildtype VHL compared to mutant Y185F VHL existed, and in order to gain insight into whether a difference in Src-VHL interaction could contribute to regulating VHL protein stability, I conducted coimmunoprecipitation experiments comparing wildtype VHL and mutant Y185F VHL coimmunoprecipitation with Src. I found that exogenous Src coimmunoprecipitates with exogenous wildtype VHL (Figure 30A, lane 10). In contrast, there was less coimmunoprecipitation of exogenous Src with exogenous mutant Y185F VHL (Figure 30A, lane 12). Thus, mutant Y185F VHL appears not to coimmunoprecipitate as well as wildtype VHL with Src. Consistent with my previous data, Y185F VHL continued to exhibit higher steady state levels in lysates, and also exhibited better resistance to targeted degradation by Src (Figure 30B, lanes 5 and 6). In light of the findings in Chapter Five, it is possible that Src (targeting VHL for destruction) could compete for VHL-stabilizing proteins for binding to VHL. It can be hypothesized that decreased ability of Src binding to mutant Y185F VHL *in vivo* might favour preferred VHL binding to VHL-stabilizing proteins such as elongin C.

Interestingly, the most efficient coimmunoprecipitation between Src and VHL occurred in coimmunoprecipitates of exogenous Src and endogenous VHL (Figure 30A, IP VHL:WB Src, lane 8). The next most efficient coimmunoprecipitation occurred between exogenous Src and exogenous WT VHL (Figure 30A, IP VHL:WB Src, lane 10). Although the difference was quite dramatic, it could be expected, in light of the fact that Src does promote degradation of VHL. Whole cell lysate levels of VHL supported

my previous findings that Src activation promoted VHL protein degradation (Figure 30B). These experiments suggest that Src and WT VHL coimmunoprecipitation interaction correlated inversely with levels of stabilized wildtype VHL.

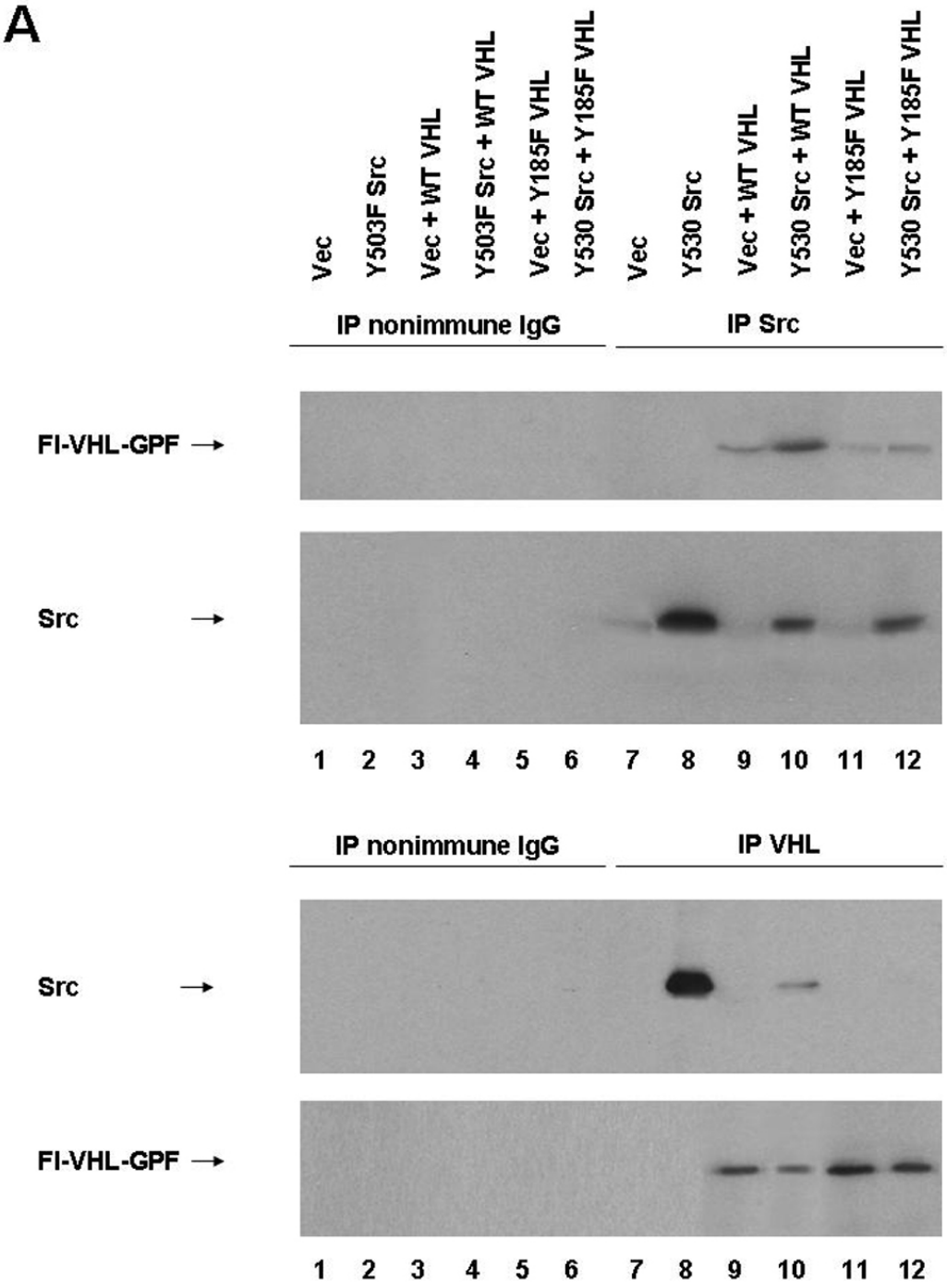
A
Vec
Y503F Src
Vec + WT VHL
Y503F Src + WT VHL
Vec + Y185F VHL
Y530 Src + Y185F VHL
Vec
Y530 Src
Vec + WT VHL
Y530 Src + WT VHL
Vec + Y185F VHL
Y530 Src + Y185F VHL
IP nonimmune IgG
IP Src
Fl-VHL-GPF
Src
1 2 3 4 5 6 7 8 9 10 11 12
IP nonimmune IgG
IP VHL
Src
Fl-VHL-GPF
1 2 3 4 5 6 7 8 9 10 11 12

B

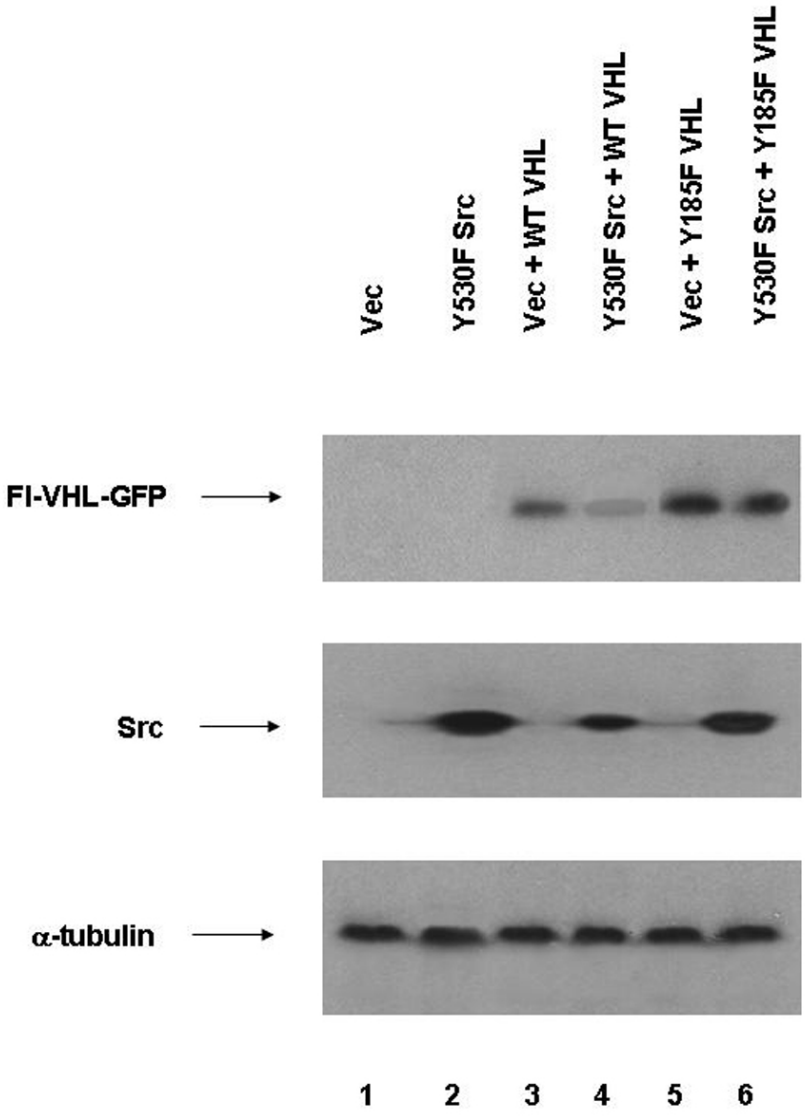
Vec
Y530F Src
Vec + WT VHL
Y530F Src + WT VHL
Vec + Y185F VHL
Y530F Src + Y185F VHL
Fl-VHL-GFP
Src
α-tubulin
1
2
3
4
5
6

Figure 30. Coimmunoprecipitation of Src and VHL.

(A) HEK 293T cells were transfected with vector or constitutively active Src (Y530F Src) alone or together with Flag-tagged VHL-GFP (WT VHL) or Flag-tagged Y185F VHL-GFP (Y185F VHL). 48 h post-transfection, the cells were lysed. Exogenous Src was isolated by immunoprecipitation with anti-Src monoclonal antibody covalently conjugated to protein A agarose beads, followed by Western blotting using anti-VHL polyclonal antibody, or anti-Src monoclonal antibody. Exogenous VHL was isolated by immunoprecipitation with anti-VHL polyclonal antibody covalently conjugated to protein A agarose beads, followed by Western blotting using anti-Src monoclonal antibody, or anti-VHL polyclonal antibody. Control immunoprecipitations using nonimmune IgGs covalently conjugated to protein A agarose beads were also performed in parallel. The results are representative of two independent experiments.

(B) Whole cell lysates were Western blotted for total Fl-VHL-GFP protein levels using anti-VHL polyclonal antibody, total Src protein levels using anti-Src monoclonal antibody, and total α-tubulin protein levels using anti-α-tubulin monoclonal antibody. The results are representative of two independent experiments.

4.3 Mapping the region of GST-VHL that binds Src

To study the interaction between VHL and Src, I conducted pull-downs with GST-VHL beads in HEK 293T cell lysates (following the methodology as diagrammed in Figure 6). These experiments additionally allowed me to map the region of VHL with the most affinity for binding Src. GST-VHL constructs containing wildtype or C-terminal truncated VHL (containing the N-terminal 184 amino acids of VHL), were generated. GST proteins were harvested and purified by binding to glutathione sepharose 4B beads. I found that GST-VHL wildtype bound the most to Src (Figure 31). In contrast, GST-VHL 184 aa bound less to Src. This suggests that the truncation GST-VHL 184 aa lacks part of the region for Src binding. In contrast, GST alone bead pull-down assays did not result in binding to Src.

A

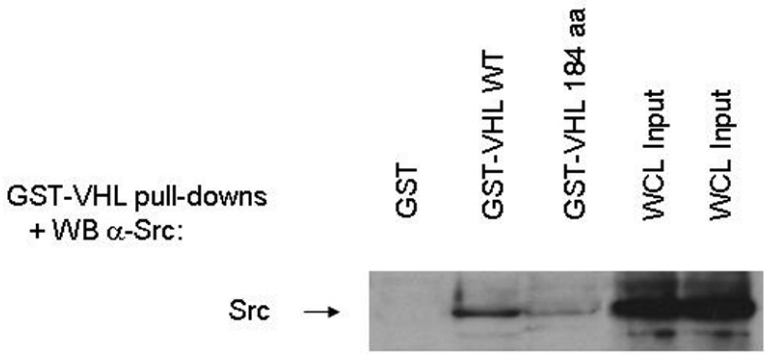
GST-VHL pull-downs
+ WB α-Src:
GST
GST-VHL WT
GST-VHL 184 aa
WCL Input
WCL Input
Src

B

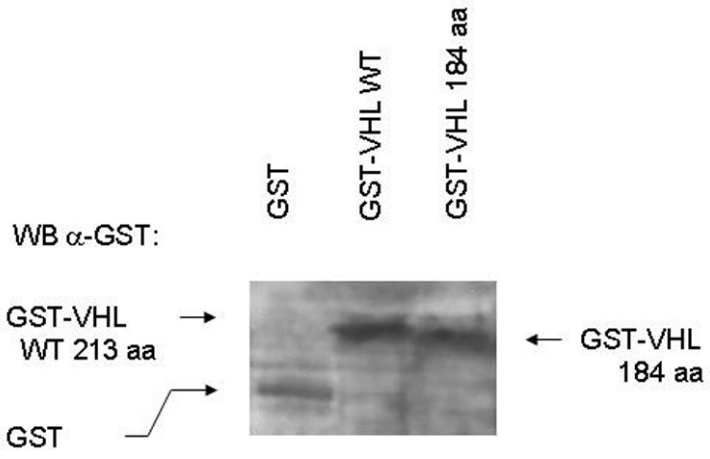
GST
GST-VHL WT
GST-VHL 184 aa
WB α-GST:
GST-VHL
WT 213 aa
GST
GST-VHL
184 aa

Figure 31. GST-VHL pull-down of Src.

GST, GST-VHL full-length 213 aa, or GST-VHL 184 aa N-terminal proteins were produced, bound to glutathione-agarose beads, and purified. The GST-VHL fusion protein beads were then phosphorylated in the presence of baculovirus Src. The GST-VHL fusion protein beads were subsequently used in pull-down incubations (500 pmol equimolar amounts each fusion protein) with equal amounts of protein lysate (500 μg protein lysate each, from HEK 293T cells expressing activated Src). The pull-down complexes were resolved on 10 % acrylamide SDS-PAGE gels and transferred to nitrocellulose. Immunoblotting was then performed using (A) anti-Src monoclonal antibody or (B) anti-GST monoclonal antibody. Pre-pull-down samples of HEK 293T (50 μg each) were also immunoblotted using anti-Src monoclonal antibody. The results are representative of two independent experiments.

4.4 Mapping the region of GST-Src that binds VHL

To further study the interaction between Src and VHL, I conducted pull-downs with GST-Src domain beads in HEK 293T cell lysate (following the methodology as diagrammed in Figure 6). These experiments also allowed me to map the region of VHL with the most affinity for binding Src. Through the experiments decribed earlier in this thesis, I have identified one mechanism by which VEGF induction occurs, and demonstrated the ability of Src to reduce VHL protein half-life by targeting VHL for proteasome-mediated destruction, through a mechanism that appears to have both kinase-dependent and kinase-independent components. Supporting this idea, my findings indicated that kinase dead Src (K298M Src) has some effect on reducing VHL protein stability, although this effect is not as dramatic as the kinase active Src-mediated effect. Interestingly, in binding assays using a panel of GST-Src domain fusion proteins in pull-down experiments from cell extracts ectopically expressing Fl-VHL-GFP, I observed binding of VHL to GST-Src SH2 and SH3 domains (Figure 32A). The data suggest that VHL has preference for binding to the Src SH2 domain, and that the Src SH2 domain is able to interact and bind to VHL. Control experiments showed that vector Fl-GFP-GFP transfected lysate did not bind significantly to the GST-Src fusion proteins (Figure 32D). Also, control GST alone bead pull-down assays did not result in binding. Interestingly, the Src-VHL pull-down complexes appeared to be tyrosine phosphorylated (Figure 32C). Since these experiments are from pull-downs from *in vivo* HEK293T lysates, it cannot be ruled out that other tyrosine phosphorylated Src-VHL-interacting proteins are also being pulled downdetected in the pull-downs. However, the data do support the earlier *in vitro* phosphorylation experiments with VHL.

The Src-SH3 domain pull-down assays bound what appeared to be shorter VHL fragments (Figure 32A). It is known that Src family SH3 domains preferentially bind proline-rich motifs with the sequence RPLPXXPX (Alexandropoulos *et al.*, 1995). It is possible that in the Src-SH3 domain pull-downs, the shorter molecular weight species are dregraded fragments of VHL. The shorter fragments could be polyproline sequence containing protein fragments of VHL made more accessible to Src-SH3 binding due to their shorter fragment size, and/or having better steric accessibility to Src-SH3 binding in VHL-Src complexes.

A

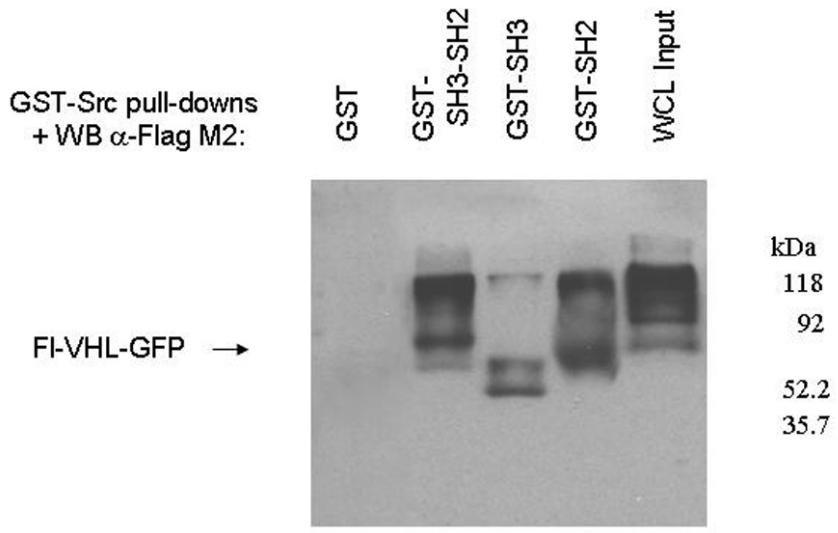
GST-Src pull-downs
+ WB α-Flag M2:
GST
GST-SH3-SH2
GST-SH3
GST-SH2
WCL Input
Fl-VHL-GFP
kDa
118
92
52.2
35.7

B

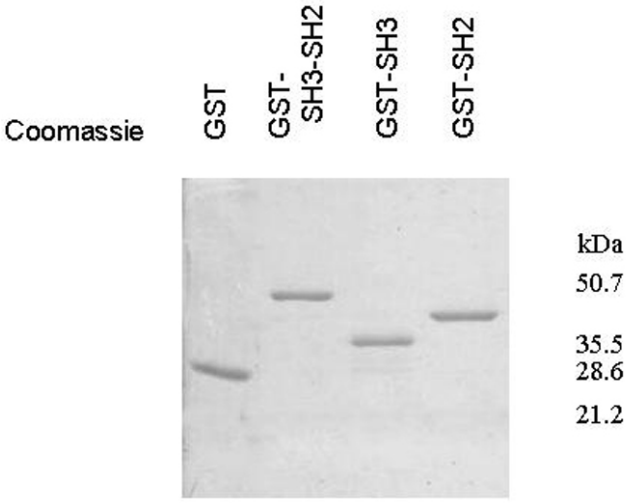
Coomassie
GST
GST-SH3-SH2
GST-SH3
GST-SH2
kDa
50.7
35.5
28.6
21.2

C

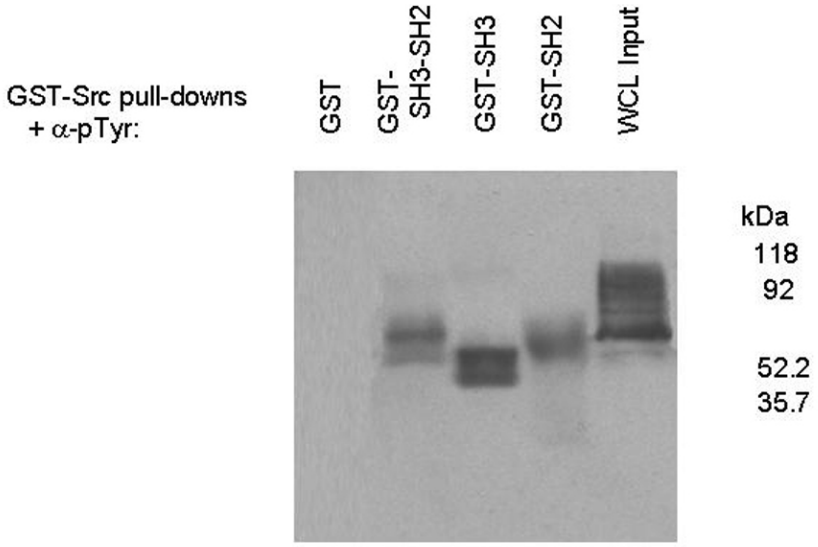
GST-Src pull-downs
+ α-pTyr:
GST
GST-SH3-SH2
GST-SH3
GST-SH2
WCL Input
kDa
118
92
52.2
35.7

D

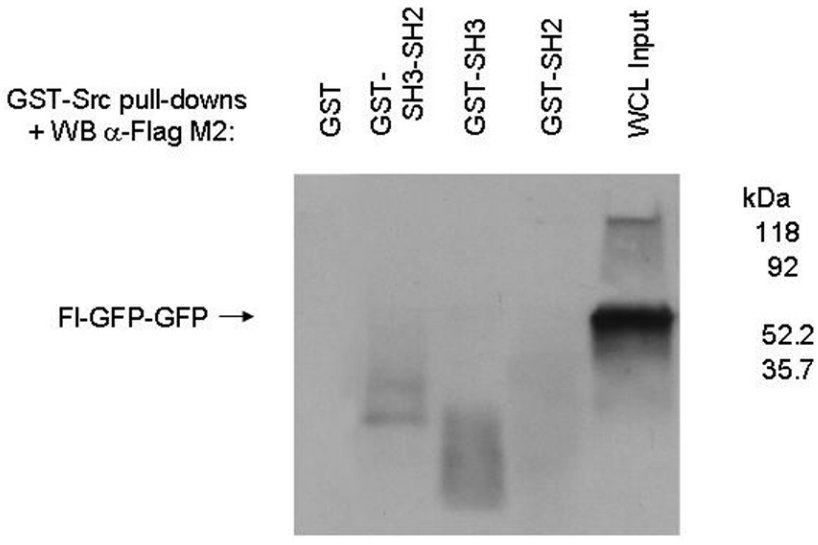
GST-Src pull-downs
+ WB α-Flag M2:
GST
GST-SH3-SH2
GST-SH3
GST-SH2
WCL Input
Fl-GFP-GFP →
kDa
118
92
52.2
35.7

Figure 32. GST-Src pull-down of VHL.

(A,C,D) GST, GST-Src SH3-SH2, GST-Src SH3, or GST-Src SH2 fusion proteins were produced, bound to glutathione-agarose beads, and purified. The GST-Src domain fusion protein beads were subsequently used in pull-down incubations (500 pmol equimolar amounts each fusion protein) with equal amounts of protein lysate (500 μg protein lysate). The lysates used were HEK 293T lysates expressing Fl-VHL-GFP (in A and C) or HEK 293T lysates expressing Fl-GFP -GFP control lysate (in D). The pull-down complexes were resolved on 10 % acrylamide SDS-PAGE gels and transferred to nitrocellulose. Immunoblotting was then performed using anti-Flag monoclonal antibody (in A and D), or anti-phosphotyrosine monoclonal antibody (in C). WCL lanes indicate pre-pull-down whole cell lysate samples of 50 μg each.

(B) Coomassie blue staining of the GST-Src domain fusion proteins was also performed. The results are representative of three independent experiments.

CHAPTER FIVE: INTERACTION OF SRC AND OTHER CANDIDATE VHL COMPLEX PROTEINS WITH VHL

5.1 Role of Hakai and c-Cbl in regulating VHL protein level

There have been some studies on E3 ubiquitin ligase,s such as Hakai and c-Cbl, suggesting their Src-dependency for degradation of target proteins (Fujita *et al.*, 2002;Bao *et al.*, 2003) . Thus, I conducted experiments to study the effects of the candidate E3 ubiquitin ligases, Hakai and c-Cbl, on VHL protein stability. First, I conducted experiments to determine whether siRNA targeted knockdown of Hakai and c-Cbl would have any effects on VHL protein steady state (Figure 33). Two distinct siRNA sequences were designed for each protein targetted in the knockdown experiments. After transfection of Hakai and c-Cbl siRNA into HEK 293T cells, Hakai protein level was knocked down 41.9 % to 50.2 %; c-Cbl protein level was knocked down 54.4 % to 57.6 %. Interestingly upregulation of VHL p30 protein steady state levels was observed. The upregulations obtained in VHL were 2.7–fold to 2.8–fold in VHL p30 by Hakai siRNA, and 1.4–fold to 1.6–fold in VHL p19 by Hakai siRNA. Similarly, upregulations obtained in VHL were 1.9–fold to 2.2–fold in VHL p30 by c-Cbl siRNA, and 2.2–fold to 2.4–fold in VHL p19 by c-Cbl siRNA.

As shown in Figure 34, VHL protein levels were most markedly increased by siRNA knockdown of Src, Hakai, and c-Cbl together. After siRNA knockdown of Src alone, VHL protein levels increased 1.8 fold (VHL p19) to 3.0-fold (VHL p30). However, siRNA knockdown of Src, Hakai, and c-Cbl together caused VHL protein

levels to increase the most by 6.0-fold (VHL p30) to 7.9-fold (VHL p19). Intermediate levels of VHL protein level upregulation occurred after siRNA knockdown of both Src and c-Cbl (upregulation of VHL protein levels by 3.3 –fold for p30 and 3.5–fold for p19), and after siRNA knockdown of both Src and Hakai (upregulation of VHL protein levels by 5.0–fold for p30 and 6.3–fold for p19).

I next studied the separate effect of Hakai and c-Cbl on VHL protein stability. I expressed either wildtype Hakai, RING finger domain mutant C309A Hakai, wildtype c-Cbl, or RING finger domain mutant C381A c-Cbl in HEK 293T cells, in the absence or presence of activated Src. Wildtype Hakai expression was able to reduce VHL protein levels (Figure 35A, lane 7). In contrast, the RING finger domain mutant C309A Hakai did not dramatically reduce VHL protein levels in the presence of activated Src (Figure 35A, lane 8). This indicated that the RING finger domain is needed for promoting VHL protein degradation. Interestingly, Y185F VHL was not able to be degraded efficiently in the presence of wildtype Hakai (Figure 35A, lane 9). This indicated that Y185F VHL may promote VHL protein stability even in the presence of Hakai.

Wildtype c-Cbl expression was also able to reduce VHL protein levels (Figure 35B, lane 7). In contrast, RING finger domain mutant C381A c-Cbl did not dramatically reduce VHL protein levels in the presence of activated Src (Figure 35B, lane 8). This indicated that RING finger domain is needed for promoting VHL protein degradation. Interestingly, Y185F VHL was not able to be degraded efficiently in the presence of wildtype c-Cbl (Figure 35B, lane 9). This indicated that Y185F VHL promotes VHL protein stability even in the presence of c-Cbl. Furthermore, VHL degradation did not occur as efficiently in the absence of Src, even in the presence of Hakai E3 ligase (Figure

35A, lane 10) or c-Cbl E3 ligase Figure 35B, lane 10). Thus, E3 ligases Hakai and c-Cbl are not able to efficiently promote degradation of VHL without Src. This supports my previous findings that Src expression promotes VHL degradation, and further emphasizesa requirement for Src in the degradation of VHL protein.

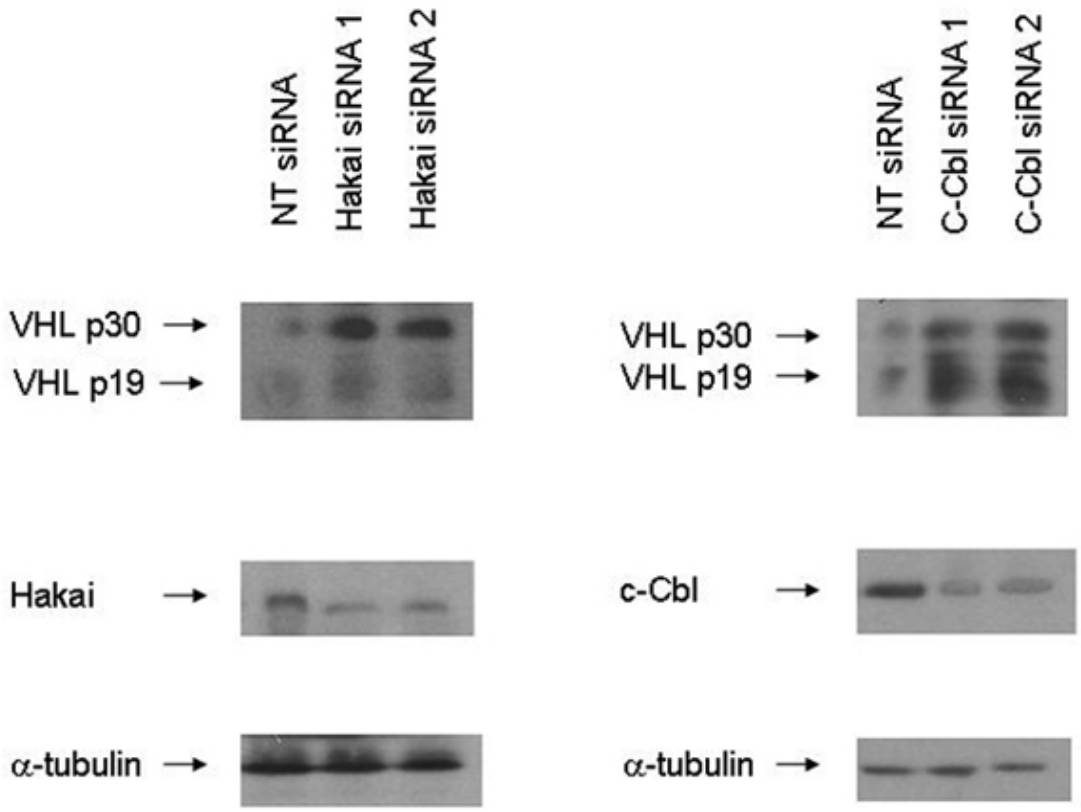
NT siRNA
Hakai siRNA 1
Hakai siRNA 2
VHL p30
VHL p19
Hakai
α-tubulin
NT siRNA
C-Cbl siRNA 1
C-Cbl siRNA 2
VHL p30
VHL p19
c-Cbl
α-tubulin

C

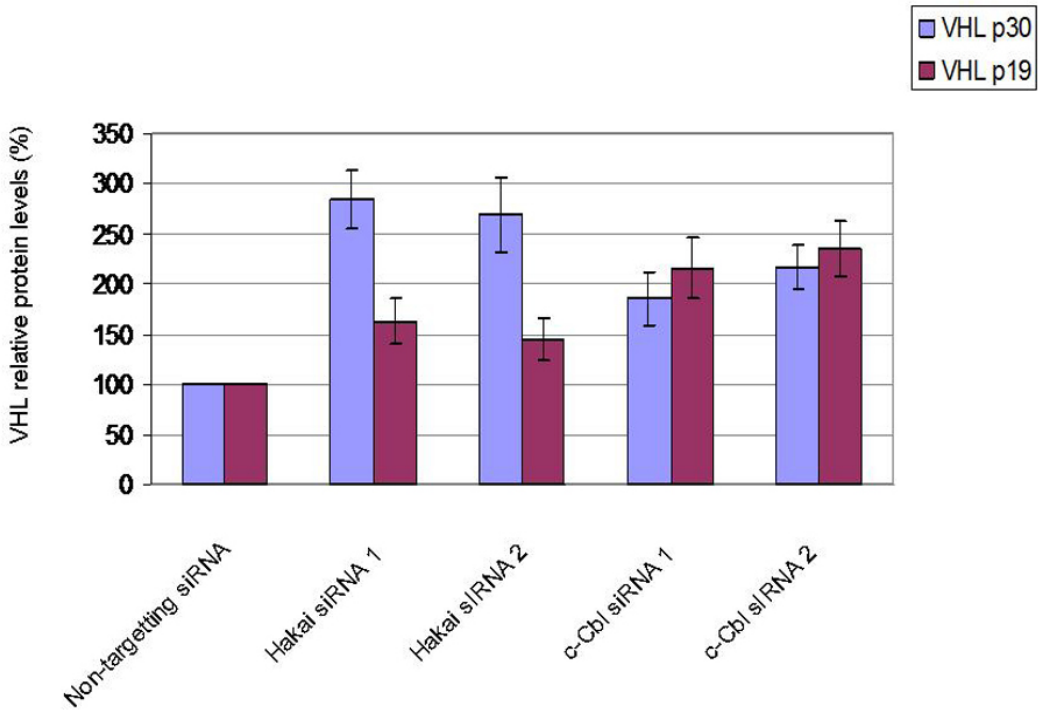
VHL p30
VHL p19
VHL relative protein levels (%)
350
300
250
200
150
100
50
0
Non-targetting siRNA
Hakai siRNA 1
Hakai siRNA 2
c-Cbl siRNA 1
c-Cbl siRNA 2

D

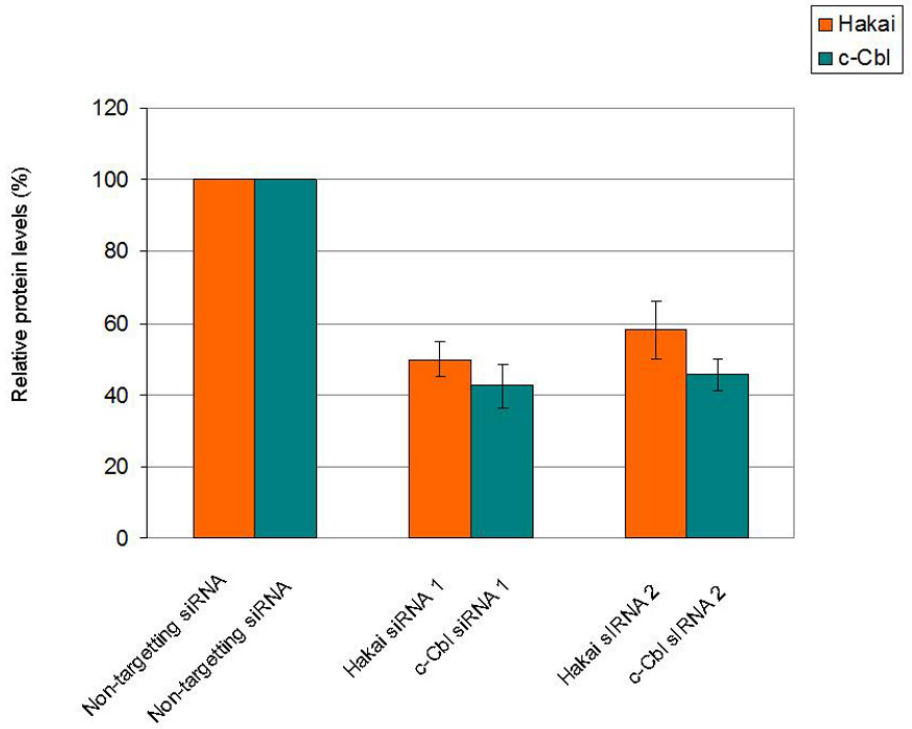
Hakai
c-Cbl
Relative protein levels (%)
120
100
80
60
40
20
0
Non-targetting siRNA
Non-targetting siRNA
Hakai siRNA 1
c-Cbl siRNA 1
Hakai siRNA 2
c-Cbl siRNA 2

Figure 33. siRNA knockdown and Hakai and c-Cbl upregulates VHL.

(A,B) HEK 293T cells were transfected with non-targeting control siRNA, Hakai siRNA 1, Hakai siRNA 2, c-Cbl siRNA 1, or c-Cbl siRNA, 2. 48 h post-transfection, the cells were lysed, and Western blotting was performed to detect endogenous VHL using anti-VHL polyclonal antibody. Hakai using anti- Hakai polyclonal antibody, c-Cbl using anti-c-Cbl monoclonal antibody, and total α-tubulin protein levels using anti-α-tubulin monoclonal antibody. Results are representative of n = 3.

(C) Effect of Hakai siRNA and c-Cbl siRNA on VHL Protein Levels. Quantitation of the VHL protein levels of the immunoblot results from part A. Densitometry was performed using ImageQuant TL software from Amersham Biosciences. Values were normalized relative to the values for α-tubulin protein levels. The graph charts the mean +/- 1 SD of three independent experiments.

(D) Quantitation of the knockdown of Hakai and c-Cbl protein levels by the Hakai siRNAs and c-Cbl siRNAs, of the immunoblot results from part A. Densitometry was performed using ImageQuant TL software from Amersham Biosciences. Values were normalized relative to the values for α-tubulin protein levels. The graph charts the mean +/- 1 SD of three independent experiments.

A

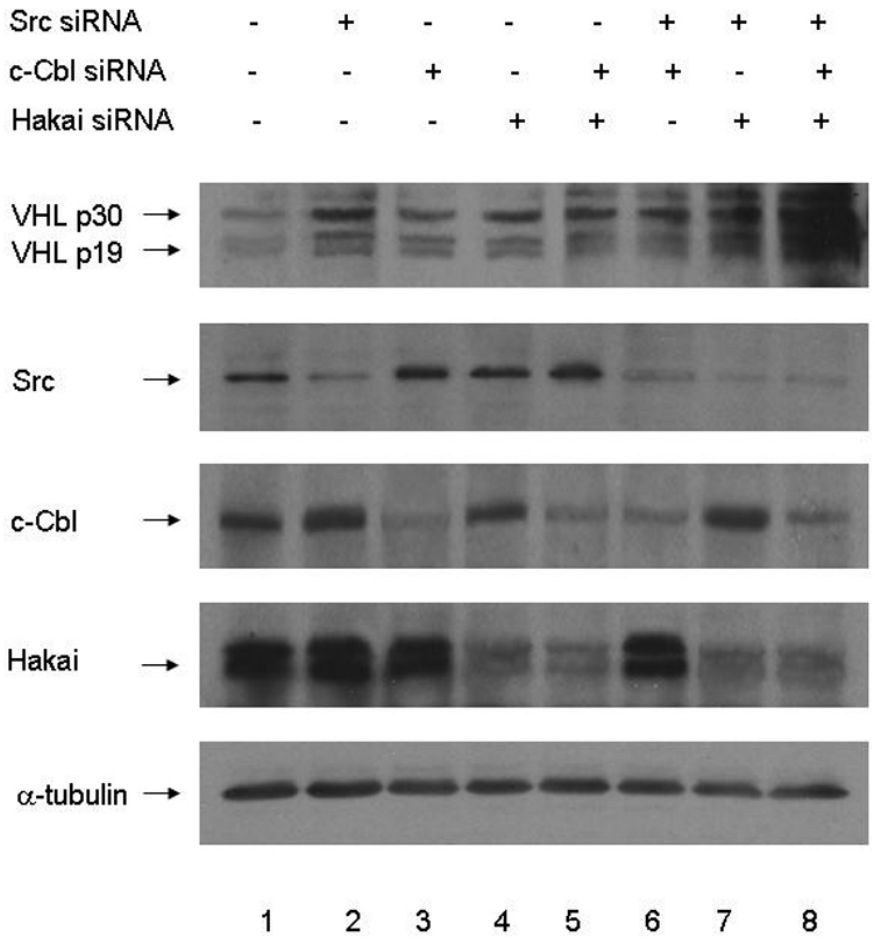
Src siRNA - + - - - + + +
c-Cbl siRNA - - + - + + - +
Hakai siRNA - - - + + - + +
VHL p30
VHL p19
Src
c-Cbl
Hakai
α-tubulin
1 2 3 4 5 6 7 8

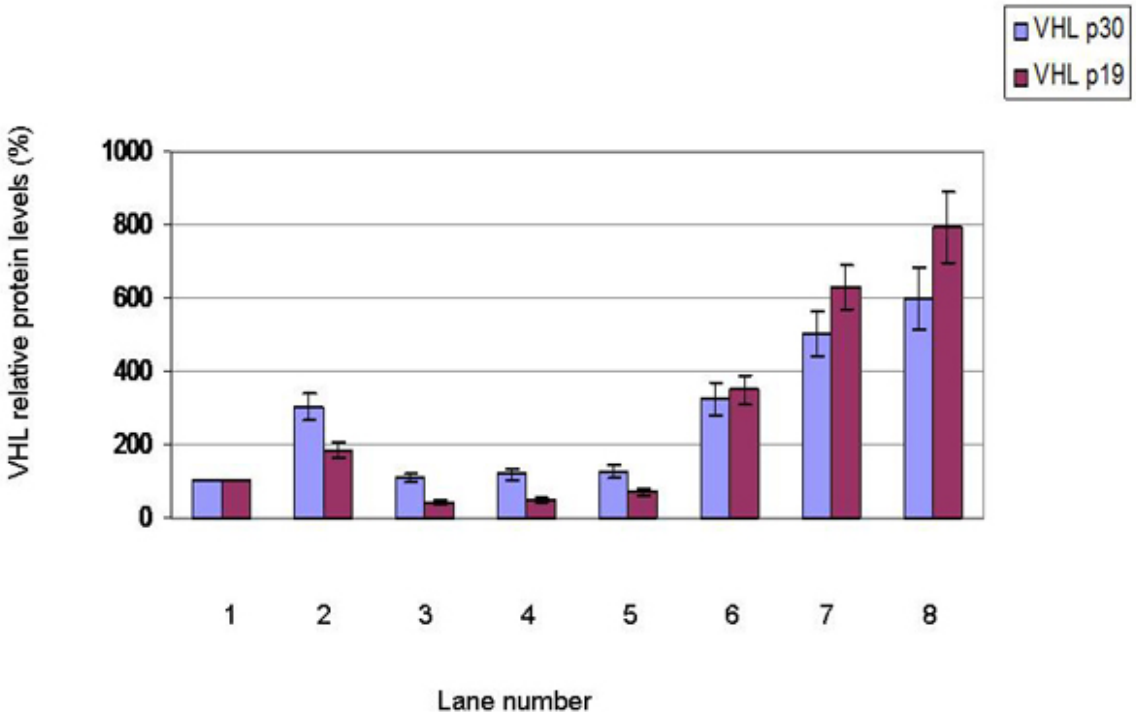
VHL p30
VHL p19
VHL relative protein levels (%)
1000
800
600
400
200
0
1
2
3
4
5
6
7
8
Lane number

Figure 34. siRNA knockdown of Src, c-Cbl, and Hakai together markedly upregulate VHL.

(A) HEK 293T cells were transfected with non-targeting control siRNA, Src siRNA 1, c-Cbl siRNA 2, or Hakai siRNA 1, alone or in the indicated combinations. 48 h post-transfection, the cells were lysed, and Western blotting was performed to detect endogenous VHL, Src, c-Cbl, Hakai, and total α-tubulin protein levels. Results are representative of n = 3.

(B) Effect of c-Cbl, Hakai, and Src siRNA combinations on VHL Protein Levels. Quantitation of the VHL protein levels of the immunoblot results from part A. Densitometry was performed using ImageQuant TL software from Amersham Biosciences. Values were normalized relative to the values for α-tubulin protein levels. The graph charts the mean +/- 1 SD of three independent experiments.

A

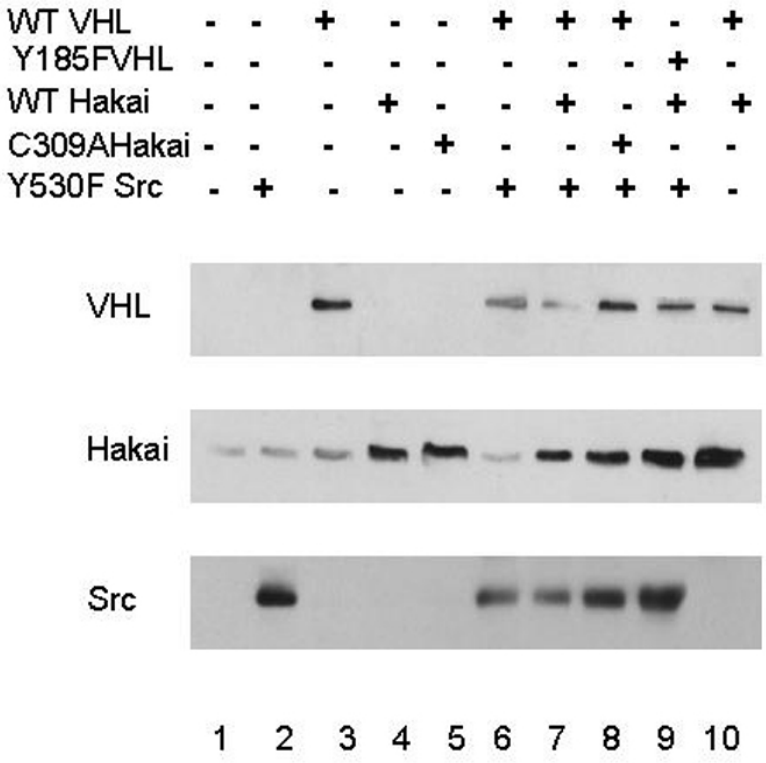
WT VHL - - + - - + + + - +
Y185FVHL - - - - - - - - + -
WT Hakai - - - + - - + - + +
C309AHakai - - - - + - - + - -
Y530F Src - + - - - + + + + -
VHL
Hakai
Src
1 2 3 4 5 6 7 8 9 10

B

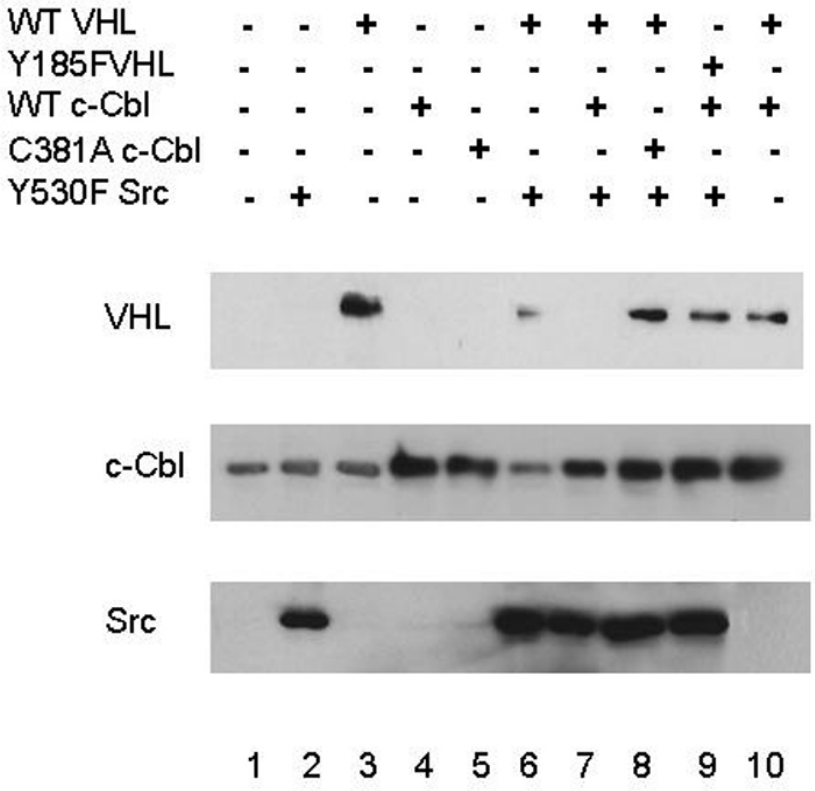
WT VHL - - + - - + + + - +
Y185FVHL - - - - - - - - + -
WT c-Cbl - - - + - - + - + +
C381A c-Cbl - - - - + - - + - -
Y530F Src - + - - - + + + + -
VHL
c-Cbl
Src
1 2 3 4 5 6 7 8 9 10

Figure 35. Hakai or c-Cbl expression downregulates VHL levels.

(A) HEK 293T cells were transfected with active Src plasmid (Y530F Src) alone or together with wildtype Fl-VHL-GFP (WT VHL), Y185F VHL, WT Hakai, and/or RING finger domain mutant C309A Hakai. 48 h post-transfection, the cells were lysed, and Western blotting was performed using anti-VHL polyclonal antibody, anti-Hakai polyclonal antibody, or anti-Src monoclonal antibody. The results are representative of two independent experiments.

(B) HEK 293T cells were transfected with active Src plasmid (Y530F Src) alone or together with wildtype Fl-VHL-GFP (WT VHL), Y185F VHL, WT c-Cbl, and/or RING finger domain mutant C381A c-Cbl. 48 h post-transfection, the cells were lysed, and Western blotting was performed using anti-VHL polyclonal antibody, anti c-Cbl monoclonal antibody, or anti-Src monoclonal antibody. The results are representative of two independent experiments.

5.2 Interaction of Hakai and c-Cbl with VHL

To further study the involvement of potential E3 ubiquitin ligases in Src-directed degradation, I generated GST-VHL fusion constructs containing either wildtype or different N-terminal lengths of VHL (C-terminal truncated VHL constructs). GST proteins were harvested and purified by binding to glutathione sepharose 4B beads. I then phosphorylated the glutathione bead-bound GST proteins in kinase reactions in the presence or absence of baculovirus Src. The two groups of glutathione bead-bound GST proteins (phosphorylated or not phosphorylated) were tested for their ability to bind candidate E3 ubiquitin ligases in GST-pull-down experiments, by pulling down from lysates expressing Y530F Src or K298M Src respectively (following the methodology as diagrammed in Figure 6).

The results indicated that GST-VHL 184 N-terminal amino acids and GST-VHL 111 N-terminal amino acids were able to bind Hakai E3 ligase more efficiently after baculovirus Src phosphorylation than without baculovirus Src phosphorylation (Figure 36). In contrast, GST-VHL wild type and GST-VHL N-terminal proteins were able to bind c-Cbl E3 ligase regarcless of whether or not they were phosphorylated by Src. Control GST alone bead pull-down assays did not result in binding to any E3 ligase. GST VHL WT underwent the most tyrosine phosphorylation as compared to GST-VHL 184 aa and GST-VHL 111 aa tyrosine phosphorylation. Cell lysates (before pull-down) were also immunoblotted for the corresponding E3 ligases studied (lanes labeled WCL Y530F Src and WCL K298M Src). These controls helped verify that the E3 ligase proteins were present and detectable in the cell lysates used in the pull-down assays.

The data suggest that the truncated mutant forms of VHL, especially 184 aa and 111 aa, may allow for more directly accessible interaction with VHL and/or have fewer domains conferring negative regulatory effects on VHL protein interactions. The results indicate that Hakai interaction with VHL may occur within VHL amino acid residues 98 t o 184. The data also indicate that c-Cbl interaction with VHL may occur within VHL amino acid residues 98 t o 111. Therefore, it is also possible that there is less steric and/or negative regulatory inhibition provided by the truncation mutants of VHL, and this may allow for increased preferred binding interaction of some VHL truncation mutants with Hakai and c-Cbl.

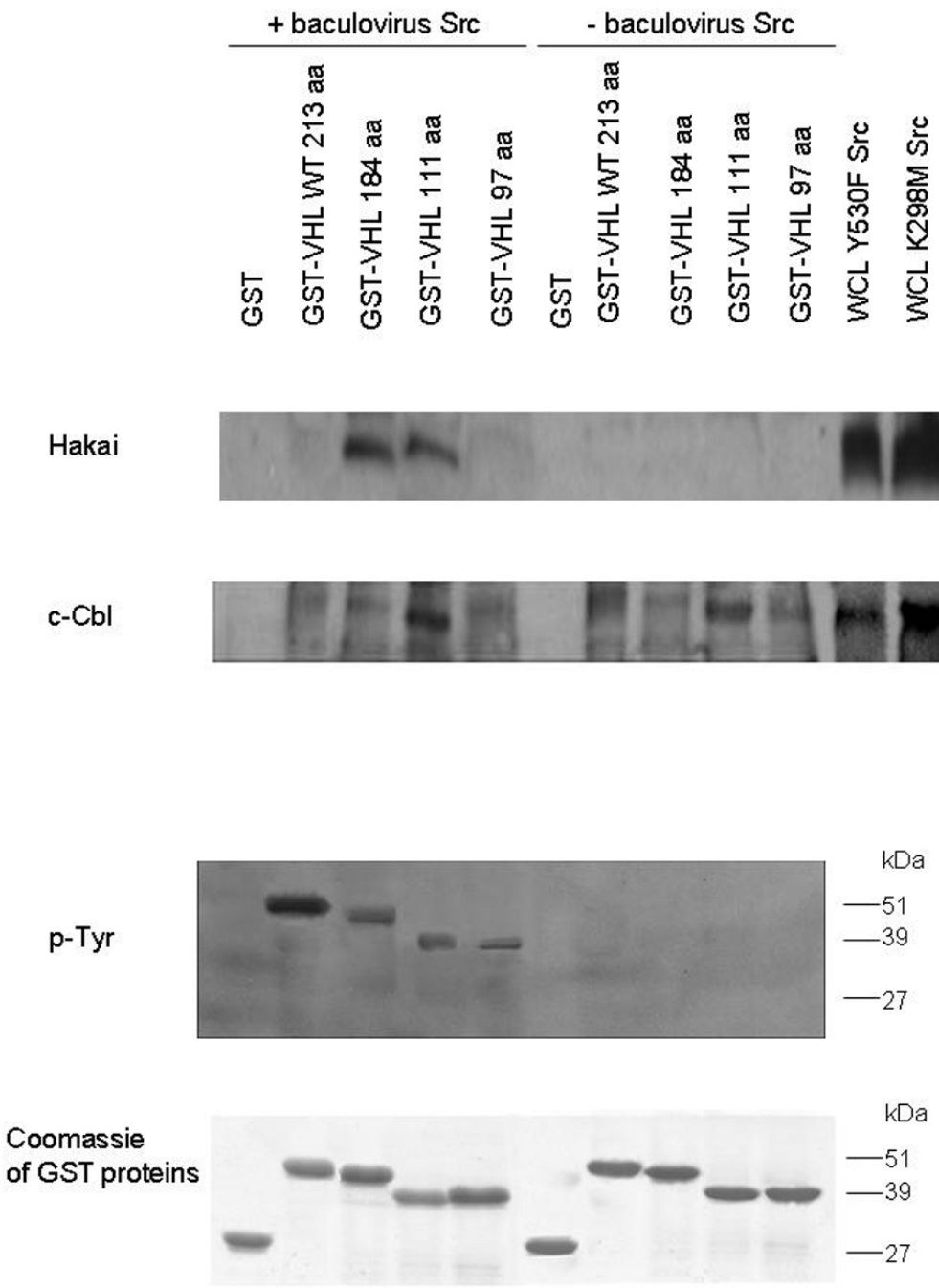
+ baculovirus Src
- baculovirus Src
GST
GST-VHL WT 213 aa
GST-VHL 184 aa
GST-VHL 111 aa
GST-VHL 97 aa
GST
GST-VHL WT 213 aa
GST-VHL 184 aa
GST-VHL 111 aa
GST-VHL 97 aa
WCL Y530F Src
WCL K298M Src
Hakai
c-Cbl
p-Tyr
kDa
51
39
27
Coomassie
of GST proteins
kDa
51
39
27

Figure 36. GST-VHL pull-downs indicate binding of VHL to Hakai and c-Cbl.

GST, GST-VHL wildtype full-length 213 aa, and GST-VHL N-terminal proteins were produced, bound to glutathione sepharose beads, and purified. The GST-VHL fusion protein beads were then phosphorylated in the presence or absence of baculovirus Src. The GST-VHL fusion protein beads were subsequently used in pull-down incubations (500 pmol equimolar amounts each) with equal amounts of protein lysate (500 μg protein lysate each, from HEK 293T cells expressing activated Src or kinase dead Src, for pull-downs using baculovirus Src phosphorylated (+) GST-VHL beads or non-baculovirus Src phosphorylated (-) GST-VHL beads respectively). The pull-down complexes were resolved on 10 % acrylamide SDS-PAGE gels and transferred to nitrocellulose. Immunoblotting was then performed using anti-Hakai antibody or anti-c-Cbl antibody. Pre-pull-down samples of HEK 293T lysate (50 μg each) were also immunoblotted using anti-Hakai antibody or anti-c-Cbl antibody (lanes labeled WCL Y530F Src and WCL K298M Src). Immunoblotting to detect tyrosine phosphorylation of the GST-VHL proteins after kinase reaction, and Coomassie blue staining of the GST-VHL wildtype and GST-VHL truncated proteins were also performed. The results are representative of three independent experiments.

5.3 Interaction of elongin C, Rbx1, and Cul2 with VHL

It had been reported that VHL stability is maintained in the VHL-elongin complex (Schoenfeld *et al.*, 2000a). Thus, I conducted experiments to examine the interaction between VHL and elongin C, under the effect of Src phosphorylation of VHL. Src kinase-treated GST-VHL wildtype interacted less strongly with elongin C. than non-Src kinase-treated GST-VHL wildtype (Figure 37). Control GST alone bead pull-down assays did not result in binding to elongin C. Next, I carried out pull-down experimetns with lysates from HEK 293T cells expressing activated Src compared with lysates expressing kinase dead Src, or neither (vector alone). GST-VHL wildtype interacted less efficiently with elongin C in the presence of activated Src, compared to kinase dead Src or vector alone (Figure 38).

It is important to note thar Y185 is within the previously mapped elongin C binding region of VHL (Ohh *et al.*, 1999;Stebbins *et al.*, 1999) (Figure 39). In light of my data, it is possible that elongin C may compete with Src for similar binding regions on VHL. If elongin C competes with Src for binding to similar VHL regions, this could be a reason for effects on the eventual VHL protein stability. Another possibility is that Src phosphorylation may alter VHL conformation, making it less favourable or optimal for elongin C binding. Regardless, it appears that elongin C binding may alter VHL (and the VHL VEC complex), causing stabilization of VHL protein. In contrast, Src phosphorylation and binding promotes post-translational modification of VHL, altering the VHL (and the VHL VEC complex), ultimately resulting in destabilization of VHL protein.

Rbx1 and Cul2 both are able to act as assembly proteins in the VHL ligase complex, and they enhance recruitment of E2 ubiquitin-conjugating enzyme into the VHL complex (Kaelin, Jr., 2008). In the context of the VHL VEC complex, elongin C binds to VHL, structurally nucleates VHL, and recruits Cul2. In turn, Cul2 recruits Rbx1 (Kaelin, Jr., 2008). Interestingly, my GST-VHL pull-down experiments indicate that Cul2 preferentially binds to non-Src phosphorylated VHL (Figure 40). The experiments also indicate that Rbx1 and Cul2 have different steric requirements for binding to VHL. Nevertheless, the data suggest that elongin C and Cul2 binding to nonphosphorylated VHL may alter VHL (and the VHL VEC complex), causing stabilization of VHL protein. In contrast, Src phosphorylation and binding promotes post-translational modification of VHL, altering the VHL (and the VHL VEC complex), ultimately resulting in destabilization of VHL protein. It is possible that Rbx1 binding occurs temporally later than elongin C and Cul2. The more efficient binding of Rbx1 to the VHL complex, may indicate that Rbx1 binds more efficiently with Src (tyrosine) phosphorylated VHL. Additionally, Rbx1 binding may indeed be a later event more apt to help trigger destabilization of VHL (and the VHL VEC complex), along with targeting by Src and E3 ligase. Furthermore, Src binding to and tyrosine phosphorylation of VHL may also contribute to displacement of VHL from the VHL E3 ligase complex (such as displacement from binding to proteins such as elongin C and Cul2) and further facilitate VHL destabilization.

Indeed, the findings in Chapter Four, support a model where Src (targeting VHL for destruction) competes with VHL-stabilizing proteins for binding to VHL. Interestingly Y185, the Src tyrosine on VHL found in this thesis project, is within the

elongin C binding site on VHL (Richards, 2001) (Figure 39). In light of this information, it is attractive to hypothesize that increased Src binding to VHL and Src tyrosine phosphorylation of VHL Y185 alters the VHL (and the VHL VEC complex), and ultimately results in destabilization of VHL protein. Conversely, competing stabilizing proteins (such as elongin C and Cul 2) promote stabilization of VHL (and the VHL VEC complex).

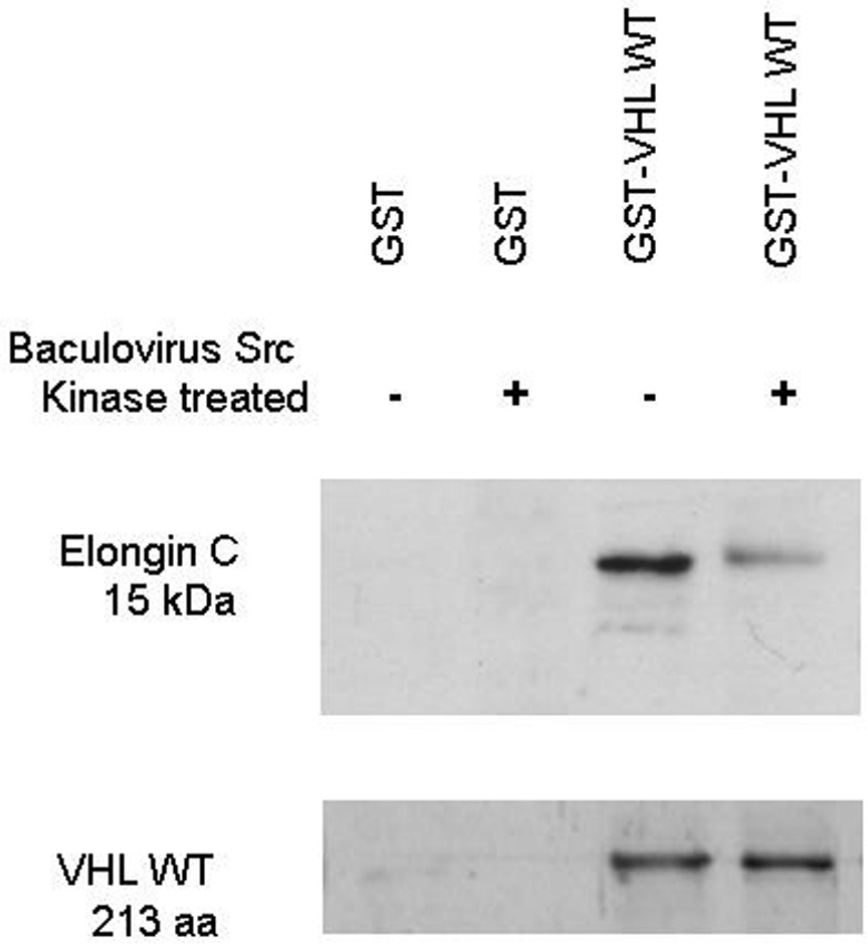
GST
GST
GST-VHL WT
GST-VHL WT
Baculovirus Src
Kinase treated
-
+
-
+
Elongin C
15 kDa
VHL WT
213 aa

Figure 37. GST-VHL pull-downs indicate binding of VHL to elongin C.

GST and GST-VHL wildtype full-length 213 aa protein were produced, bound to glutathione-agarose beads, and purified. The GST-VHL fusion protein beads were then phosphorylated in the presence or absence of baculovirus Src. The GST-VHL fusion protein beads were subsequently used in pull-down incubations (500 pmol equimolar amounts each) with equal amounts of protein lysate (500 μg protein lysate each, from HEK 293T cells expressing activated Src or kinase dead Src, for pull-downs using baculovirus Src phosphorylated (+) GST-VHL beads or non-baculovirus Src phosphorylated (-) GST-VHL beads respectively). The pull-down complexes were resolved on 10 % acrylamide SDS-PAGE gels and transferred to nitrocellulose. Immunoblotting was then performed using anti-elongin C polyclonal antibody, or anti-VHL polyclonal antibody. The results are representative of three independent experiments.

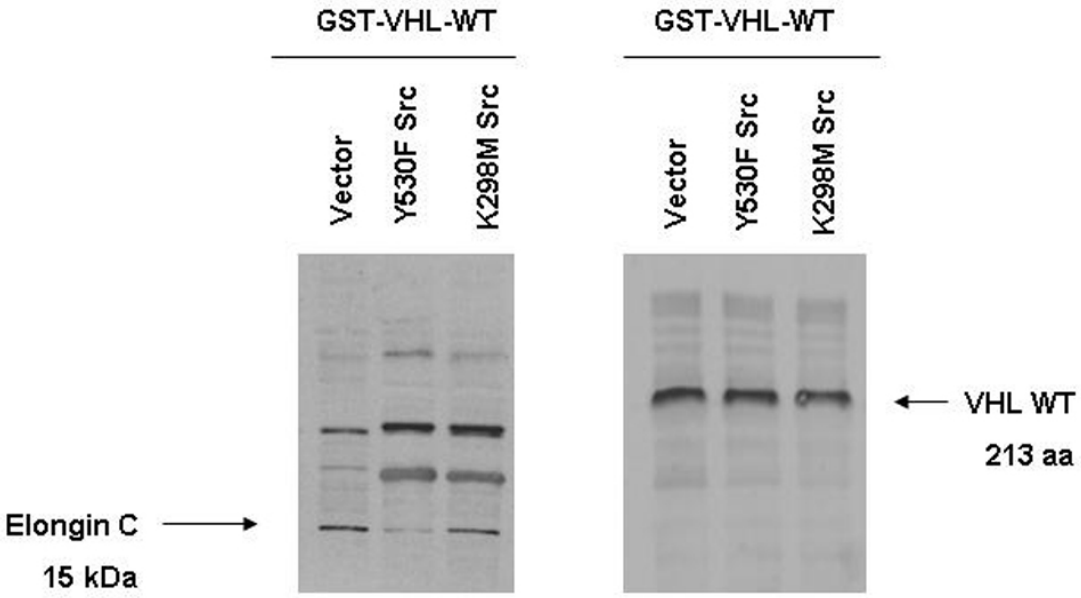
GST-VHL-WT
GST-VHL-WT
Vector
Y530F Src
K298M Src
Vector
Y530F Src
K298M Src
Elongin C
15 kDa
VHL WT
213 aa

Figure 38. Difference in GST-VHL pull-downs of elongin C from lysate expressing activated Src compared to kinase dead Src.

GST-VHL wildtype full-length 213 aa protein was produced, bound to glutathione sepharose beads, and purified. The GST-VHL fusion protein beads were then phosphorylated in the presence or absence of baculovirus Src. The GST-VHL fusion protein beads were subsequently used in pull-down incubations (500 pmol equimolar amounts each) with equal amounts of protein lysate [500 μg protein lysate each, from HEK 293T cells expressing vector, activated Src, or kinase dead Src - for pull-downs using baculovirus Src phosphorylated GST-VHL beads (for pull-downs from vector-expressing and activated Src-expressing lysate) or non-baculovirus Src phosphorylated GST-VHL beads (for pull-downs from kinase dead Src-expressing lysate)]. The pull-down complexes were resolved on 10 % acrylamide SDS-PAGE gels and transferred to nitrocellulose. Immunoblotting was then performed using anti-elongin C polyclonal antibody, or anti-VHL polyclonal antibody. The results are representative of three independent experiments.

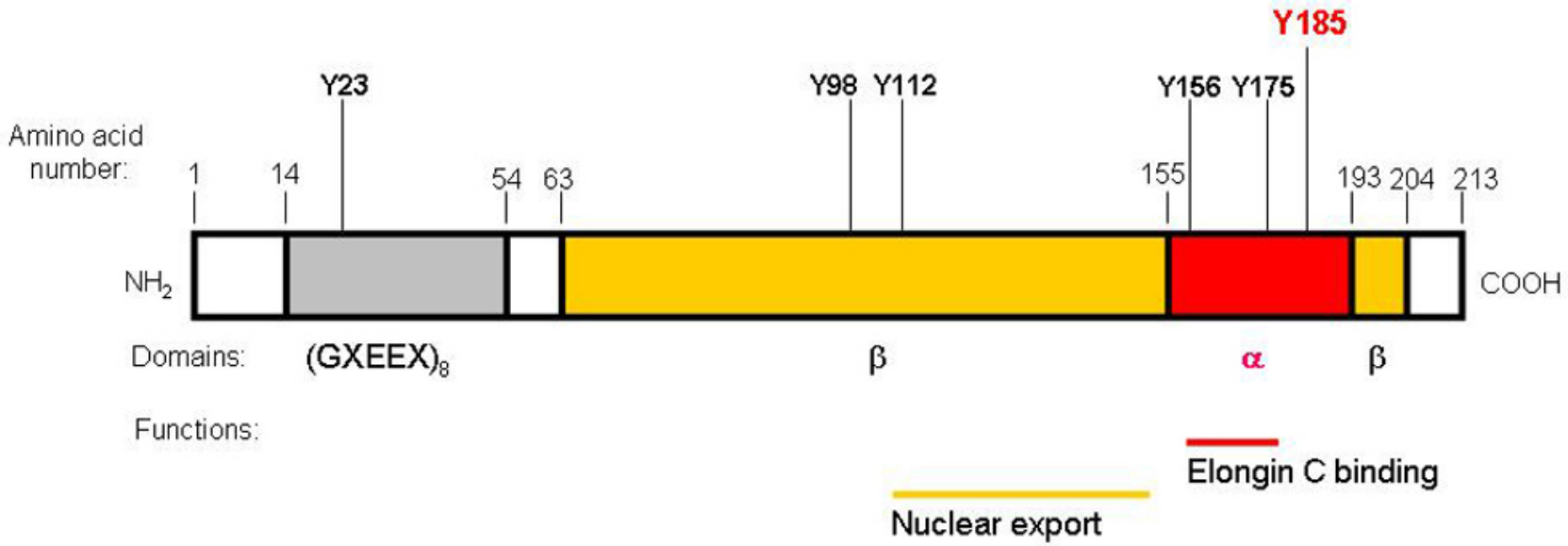

Src target consensus: [N/D]X**Y**EEIΦ

Φ=hydrophobic residue

VHL sites:

Y23	EE**Y**GPEE
Y98	QP**Y**PTLP
Y112	HS**Y**RGHL
Y185	SL**Y**EDLE

Figure 39. Schematic of the distribution of VHL phosphotyrosine residues of special interest.

The locations of candidate VHL tyrosine sites for phosphorylation by Src are indicated. The VHL α region is able to bind proteins that are able to act as assembly proteins in the VHL ligase complex, such as elongin C that enhances recruitment of E2 ubiquitin-conjugating enzyme in to the VHL complex. The VHL β region is able to bind the target for protein degradation.

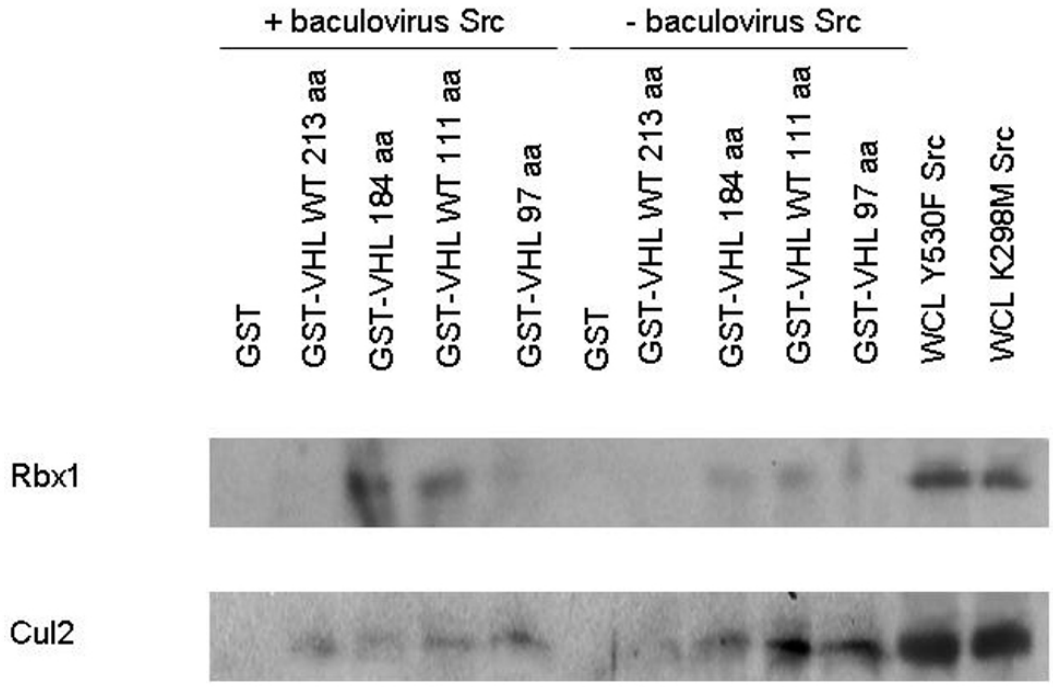
+ baculovirus Src
- baculovirus Src
GST
GST-VHL WT 213 aa
GST-VHL 184 aa
GST-VHL WT 111 aa
GST-VHL 97 aa
GST
GST-VHL WT 213 aa
GST-VHL 184 aa
GST-VHL WT 111 aa
GST-VHL 97 aa
WCL Y530F Src
WCL K298M Src
Rbx1
Cul2

Figure 40. GST-VHL pull-downs indicate binding of VHL to Rbx1 and Cul2.

GST, GST-VHL wildtype full-length 213 aa, and GST-VHL N-terminal proteins were produced, bound to glutathione sepharose beads, and purified. The GST-VHL fusion protein beads were then phosphorylated in the presence or absence of baculovirus Src. The GST-VHL fusion protein beads were subsequently used in pull-down incubations (500 pmol equimolar amounts each) with equal amounts of protein lysate (500 μg protein lysate each, from HEK 293T cells expressing activated Src or kinase dead Src, for pull-downs using baculovirus Src phosphorylated (+) GST-VHL beads or non-baculovirus Src phosphorylated (-) GST-VHL beads respectively). The pull-down complexes were resolved on 10 % acrylamide SDS-PAGE gels and transferred to nitrocellulose. Immunoblotting was then performed using anti-Rbx1 polyclonal antibody or anti-Cul2 monoclonal antibody. Pre-pull-down samples of HEK 293T lysate (50 μg each) were also immunoblotted using anti-Rbx1 polyclonal antibody or anti-Cul2 monoclonal antibody (lanes labeled WCL Y530F Src and WCL K298M Src). The results are representative of three independent experiments.

CHAPTER SIX: SUMMARY AND DISCUSSION

As tumours grow, the diffusional capacity of oxygen from the nearest blood vessel is inevitably surpassed, creating pockets of hypoxia within the tumour. The hypoxic microenvironment triggers the stabilization, as well as the increased translation of HIF-α [through the mammalian target of rapamycin (mTOR)] (Kaelin, Jr., 2008). HIF-α binds to the constitutively expressed and stable ARNT to form an active HIF transcription factor that initiates the transcription of genes containing HREs within the promoter/enhancer regions. HIF-driven gene transcripts responsible for, but not limited to, the promotion of neovascularization, anaerobic metabolism, and cell survival are expressed in adaptation to the reduced and often compromised oxygen availability, underscoring the importance of HIF in the survival, growth, and metastasis of tumours. Not surprisingly, the degree of tumour hypoxia correlates with poor prognosis, as well as with resistance to conventional anticancer therapies. VHL or VEC (elongins/Cul2/VHL) is the major regulator of HIF by determining the stability of the catalytic HIF-α subunit. VEC selectively targets HIF-α that has undergone prolyl hydroxylation by PHDs (prolyl hydroxylases) in the presence of oxygen (Kaelin, Jr., 2008). Thus, ubiquitin-mediated destruction of HIF-α occurs only under normoxic conditions. Interestingly, the engagement of HIF-α to VHL is temporally coordinated with the neddylation of Cul2 through UbcH12 and Rbx1. Neddylated Cul2 enhances its ability to bind UbcH5a (E2 ubiquitin-conjugating enzyme), that then polyubiquitinates HIF-α. Tumour hypoxia or

inactivating mutation in VHL results in the stabilization of HIF-α and in the consequential activation of HIF, triggering the expression of genes that ultimately drive neoplastic transformation - from loss of cell-cell contact inhibition, to dedifferentiation, to tipping of the balance toward survival over death. Elucidation of VHL/VEC functions in the literature has revealed an unprecedented wealth of knowledge on the oxygen-sensing pathway and the pathophysiology of solid tumour development. Such information can afford novel and more targeted avenues of anticancer strategies, directed against important molecular targets revealed along the VHL pathway. A large amount of insight can be gained from deciphering yet to be defined mechanisms and tumour suppressor functions of VHL.

The results of the experiments outlined within this thesis led me to propose the model depicted in Figure 41. In this study, I found that Src can target and phosphorylate the VHL tumour suppressor protein. This is accompanied by increased ubiquitination of VHL, and consequent proteasomal degradation of VHL (summarized in the model in Figure 41). As a result, HIF-1α activity is increased and VEGF production is upregulated.

Malignant growth results from changes in cellular phenotype that provide a selective growth advantage and an ability to grow in an unregulated fashion. As described in this thesis, one key characteristic that stimulates both solid tumour growth and metastasis is the ability to stimulate endothelial cell proliferation and blood vessel formation. VEGF is an important extracellular growth factor involved in this process of angiogenesis, and the VHL tumour suppressor protein is a major negative intracellular regulator of the VEGF pathway due to its ability to bind to and target the VEGF

transcription factor HIF-1α for destruction. Various cellular signalling pathways can potentially affect VEGF production and angiogenesis by targeting upstream regulators of VEGF, and both normal and abnormal angiogenesis can result from changes in VHL and HIF-1α activity.

Src has been implicated as an important signalling component in hypoxia-induced upregulation of VEGF (Mukhopadhyay *et al.*, 1995). Elevated Src activity in breast cancer cells can increase VEGF production to levels far above that of normal epithelial cells and could contribute to their oncogenic properties. In addition, Src activation appears to play a role in VEGF production and vascularization by some colon and ovarian cancer cells (Fleming *et al.*, 1997;Ellis *et al.*, 1998;Wiener *et al.*, 1999). I observed that breast cancer cells, that exhibit high Src activity, also have markedly lower levels of VHL compared to nontumourigenic breast epithelial cells under normoxic conditions. Introduction of active Src in normal breast epithelial cells and several other cells lines reduced VHL protein levels. In contrast, siRNA knockdown of Src resulted in increased VHL protein levels. Thus, I found that VEGF production correlated with Src activity in both breast cancer cells and normal nontmorigenic cells, and identified a mechanism whereby Src may upregulate VEGF production in breast cancer cells, and a variety of neoplastic cells. The effects in breast cancer and other cells that I observed were under conditions independent of hypoxia. In support of my findings, another report has shown Src upregulation of VEGF secretion by vascular endothelial cells independent of hypoxia (Kanda *et al.*, 2007).

One previous report communicated that Src can also regulate VEGF production by promoting elevated HIF-1α expression in NIH3T3 cells, the colon cancer line HT29,

and the osteosarcoma cell line Saos-2 through increased cap-dependent translation of HIF-1α (Karni *et al.*, 2002). Another report showed Src involvement in both constitutive and EGF-induced upregulation of VEGF through activation of phosphatidylinositol 3'-kinase (PI3K) – AKT and p38 mitogen-activated protein kinase (MAPK) pathways in pancreatic cancer cell lines (Summy *et al.*, 2005). Thus, it is possible that several mechanisms may mediate Src-induced upregulation of VEGF from tumour cells, and it is likely that these mechanisms are not mutually exclusive.

In this thesis, I describe the ability of Src to reduce VHL protein half-life by targetting VHL for proteasome-mediated destruction, through a mechanism that could have both kinase-dependent and kinase-independent components. I have further identified a mechanism by which activated Src induction of VEGF occurs under normoxia. My data also indicate that kinase dead Src (K298M Src) has a small effect on reducing VHL protein stability, although this effect is not as dramatic as the kinase active Src-mediated effect. This suggests that there may be a kinase-independent function of Src that could play a partial role in VHL downregulation. In binding assays using GST-Src domain fusion proteins in pull-down experiments, I was able to detect binding of VHL to Src SH2 domain, which offers additional support for this model. It is possible that this effect results from some binding interactions of the kinase dead Src with VHL. This is interesting, in that the possibility of kinase-independent Src functions have also been reported independently by others (Kaplan *et al.*, 1995;Schwartzberg *et al.*, 1997).

Protein ubiquitination stimulated by tyrosine phosphorylation is a well-studied mechanism for downregulating signalling events. In fact, the tyrosine kinase activity of

Src has been reported to induce ubiquitination and proteosomal degradation of Src (Hakak and Martin, 1999;Harris *et al.*, 1999). Harris et al. (1999) showed that an active mutant of Src in which the regulatory tyrosine in the carboxy-terminus was mutated to phenylalanine was an effective target for ubiquitination and was rapidly degraded. In contrast, though, a kinase inactive mutant of Src having an open conformation was not an effective substrate for ubiquitination and was more stable than the active Src mutant. Furthermore, they demonstrated that phosphorylation of tyrosine 419 within the activation loop of Src acts as a signal, targetting it for ubiquitination (Harris *et al.*, 1999). In another study, Src tyrosine phosphorylation of a separate protein target, the proto-oncogene c-Cbl, was shown to be required for c-Cbl ubiquitination and degradation (Yokouchi *et al.*, 2001).

Jung et al. reported that E2-EPF UCP, a gene associated with liver and gastric cancers, is capable of increasing the expression of the HRE-driven luciferase reporter gene, forms a complex with VHL, catalyzes ubiquitination of VHL, and promotes the destruction of VHL via the 26S proteasome (Jung *et al.*, 2006). Under a normal physiologic state, the expression of UCP and HIF-1α was undetectable in the mouse liver, while VHL levels were detecable. However, upon transduction with an adenovirus-encoded UCP, the level of VHL decreased with the concomitant accumulation of HIF-1α. In numerous transformed cell lines, as well as primary and metastatic liver, colon, and breast tumours, an inverse relationship between UCP and VHL was observed where detectable UCP expression correlated with decreased VHL and increased HIF-1α expression. In addition, UCP depletion attenuated the growth rate and invasiveness of tumour cells, while UCP overexpression promoted tumour progression and lung

metastasis of melanoma cells in a mouse xenograft model. This report identifies an E2 ubiquitin-conjugating enzyme that is able to promote VHL degradation. It is interesting to note that their report independently describes degradation of VHL that can promote cancer, and important connections can be made form both of our studies.

Although it is not known how UCP is upregulated in transformed cells, its expression in cancer cells is predicted to result in the induction of HIF-α via VHL degradation in a wide range of tissue types, since *VHL* is ubiquitously expressed. Curiously, however, it has been reported that germline inheritance of a mutated *VHL* allele causes tumour development in some select organs. This would suggest that a loss or functional inactivation of the remaining wildtype VHL alone, in certain tissues, might be insufficient for cellular transformation.

Moreover, VHL has other binding partners, some of which are subjected to VEC-dependent degradation while others are not subjected to the ubiquitin pathway. Jung *et al*. (2006) also noted that UCP may catalyze E3-dependent or -independent ubiquitin-mediated degradation of additional substrates, besides VHL, whose loss might ultimately promote cancer development. For example, atypical protein kinase C (Okuda *et al.*, 1999), VHL-interacting deubiquitinating enzyme (VDU) (Li *et al.*, 2002), and the seventh (Rpb7) and the large (Rbp1) subunits of RNA polymerase II (Na *et al.*, 2003), are ubiquitinated by VEC. In contrast, SP1 transcription factor (Cohen *et al.*, 1979), VHL-associated KRAB-A domain-containing protein (VHLaK) transcription repressor (Li *et al.*, 2003), microtubules (Hergovich *et al.*, 2003), and fibronectin (Ohh *et al.*, 1998;Hoffman *et al.*, 2001), bind to VHL without being targeted for the ubiquitin-mediated destruction. In addition, VHL was unexpectedly shown to directly bind and

stabilize p53 by suppressing Mdm2-mediated ubiquitination, and to induce the acetylation of p53 upon genotoxic stress by promoting p53-p300 interaction, resulting in increased p53 transcriptional activity and p53-mediated cell cycle arrest and apoptosis (Roe *et al.,* 2006). Therefore, it is possible that UCP-mediated degradation of VHL will influence the biological activities associated with one or more of these other VHL binding proteins, which will consequently aid in the process of tumourigenesis.

Other VHL-interacting proteins have also been reported. All tumour-derived VHL mutants examined to date are defective with respect to fibronectin binding, and VHL-defective cells exhibit a profound defect in fibronectin extracellular matrix assembly (Kurban *et al.,* 2006;Tang *et al.,* 2006). Still unclear, however, are how VHL, an intracellular protein, interacts with fibronectin, which is a secreted protein, and how this putative physical interaction affects fibronectin matrix assembly. Furthermore, other consequences of VHL inactivation, such as deregulation of atypical protein kinase C (aPKC**)** activity, altered integrin expression, and increased expression of HIF-responsive matrix metalloproteinases, may also contribute to the fibronectin phenotype (Esteban-Barragan *et al.*, 2002;Petrella *et al.*, 2005). Binding of VHL to PKCδ, PKCλ, and PKCξ inhibits their catalytic activity (Okuda *et al.*, 2001). In addition, VHL has been reported to polyubiquitinate activated, hyperphosphorylated PKCλ and PKCξ (Okuda *et al.*, 2001).

The data presented in this thesis are consistent with a model indicating that Src phosphorylation can target proteins for destruction through a ubiquitin-mediated process. For example, in response to Src activation and phosphorylation of c-Cbl, c-Cbl (a RING finger domain E3 ligase) undergoes tyrosine phosphorylation that facilitates Cbl self-ubiquitination and proteasome-mediated destruction (Bao *et al.,* 2003). As a result, there

is reduced ubiquitination of EGFR by c-Cbl in Src-transformed cells, and impaired EGF-dependent receptor downregulation. Thus, upregulated EGFR levels are maintained. In this manner, Src-mediated destruction of c-Cbl enables Src-EGFR collaboration in oncogenesis.

Another study found that Src activation promotes ubiquitination and endocytosis of E-cadherin complexes in epithelial cells (Fujita *et al.*, 2002). The report also identified involvement of the novel E3 ligase Hakai in binding and mediating ubiquitination of the E-cadherin complex. The authors proposed that Src activity and phosphorylation by Src creates phosphotyrosine binding sites on Hakai, and enhances Hakai-mediated endocytosis of E-cadherin, which would eventually cause disruption of cell–cell adhesions.

In this thesis I describe data that Hakai and c-Cbl E3 ligases may be involved in Src-directed degradation of VHL. This is intriguing, in light of the other studies mentioned above that add support for the ability of Src to phosphorylate and target proteins for ubiquitin-mediated degradation, involving E-cadherin, Hakai, and c-Cbl. I focused my study on two most likely candidate E3 ligases, based on previous literature description of their linked involvement with Src. However, possibilities that other E3 ligase proteins and E3 complex proteins could be involved in Src control of VHL protein stability are not precluded.

In, Chapter Four, I report that VHL becomes phosphorylated on tyrosine 185 in the presence of activated Src. Tyrosine phosphorylation on VHL is likely to occur as a result of direct phosphorylation by Src. Consequently, phosphorylation on tyrosine 185 of VHL could promote VHL stability by targeting VHL for proteolysis by other E3 ligase

complexes or for VHL self-ubiquitination. Chapter Five further suggests that it is also possible, as part of the mechanism, that Src binding to VHL might also contribute to displacement of VHL from the VHL E3 ligase complex (such as displacement from binding to proteins such as elongin C and Cul 2) and further promote VHL destabilization.

These observations are complemented by VHL structural information in the literature. Mutational analysis, in conjunction with X-ray crystallographic and biochemical data, determined that VHL contains two functional subdomains termed the beta domain and the alpha domain, which are frequently compromised by disease-associated VHL mutations (Stebbins *et al.*, 1999) (Figure 39). The beta domain of VHL consists of a seven-stranded beta sandwich (residues 63–154) and an alpha helix (residues 193–204) (Stebbins *et al.*, 1999). This region is largely hydrophobic and has the properties of a substrate docking site (Stebbins *et al.*, 1999). In contrast, the alpha domain of VHL, corresponding to residues 155–192, consists of three alpha helices and nucleates a multiprotein complex that contains elongin C, elongin B, Cul2, and Rbx1 (also known as Roc1) (Kamura *et al.*, 1999). Indeed, the VEC complex possesses ubiquitin ligase activity and is therefore capable of targeting proteins for proteasomal degradation (Iwai *et al.*, 1999;Lisztwan *et al.*, 1999). But, in addition, binding to the elongins promotes the proper folding and stability of VHL (Schoenfeld *et al.*, 2000a;Kamura *et al.*, 2002), probably owing, at least in part, to the fact that elongin C provides an alpha helix that fits together with the three VHL alpha domain helices, in a folded leaf-like, four-helix cluster (Stebbins *et al.*, 1999).

6.1 Significance

Investigations into VEGF signalling and Src's role in VEGF-induced tumour angiogenesis and VEGF upregulation in tumour cells will contribute to better understanding of the mechanisms underlying tumourigenesis and angiogenic support of cancer progression. A much more precise understanding of details of tumour angiogenesis and tumourigenesis will greatly facilitate the future development of tools for detection of hypervascular cancers, and will greatly facilitate the development of anti-angiogenic-based drugs and molecules for tumour therapy.

To date, inhibitors of the VEGF or its receptor KDR have been used to induce symptomatic improvement in retinal and central nervous system hemangioblastomas and perhaps in disease stabilization (Aiello *et al.*, 2002;Girmens *et al.*, 2003;Madhusudan *et al.*, 2004). However, some reports have described worsening effects on treatment, possibly reflecting an increase in intratumoural hypoxia (Richard *et al.*, 2002). Neutralizing antibodies against VEGF, as well as a number of small-molecule KDR inhibitors (many of which also, fortuitously, inhibit the PDGF receptor), have demonstrated significant activity against clear cell renal carcinoma in terms of objective tumour shrinkage and disease stabilization (Kaelin, Jr., 2004). Two of these agents, BAY43-9006 and SU11248, have now been approved by the Food and Drug Administration for this indication. Understanding mechanisms and players involved in angiogenic tumour formation is needed to provide new opportunities for therapeutic intervention, which might complement or supplant the use of existing HIF and VEGF antagonists.

The findings of this thesis project demonstrate the importance of a new mechanism of reciprocal downregulation between the Src oncoprotein and VHL tumour suppressor. My research reveals a key Src-VHL pathway that is likely to be involved in tumour angiogenesis and tumour progression. I found that Src promotes the destabilization of the VHL tumour suppressor protein, which ultimately facilitates Src induction of VEGF production from cells. This mechanism of Src-dependent destruction of VHL provides novel insights into our understanding of interplay between an oncogenic protein and tumour suppressor; and reveals a new mechanism of Src kinase function in targeting a tumour suppressor protein. Determining the relative contributions, of the components of the Src oncoprotein-VHL tumour suppressor mechanism will be undoubtedly important in adding to our understanding of the molecular bases of cancer.

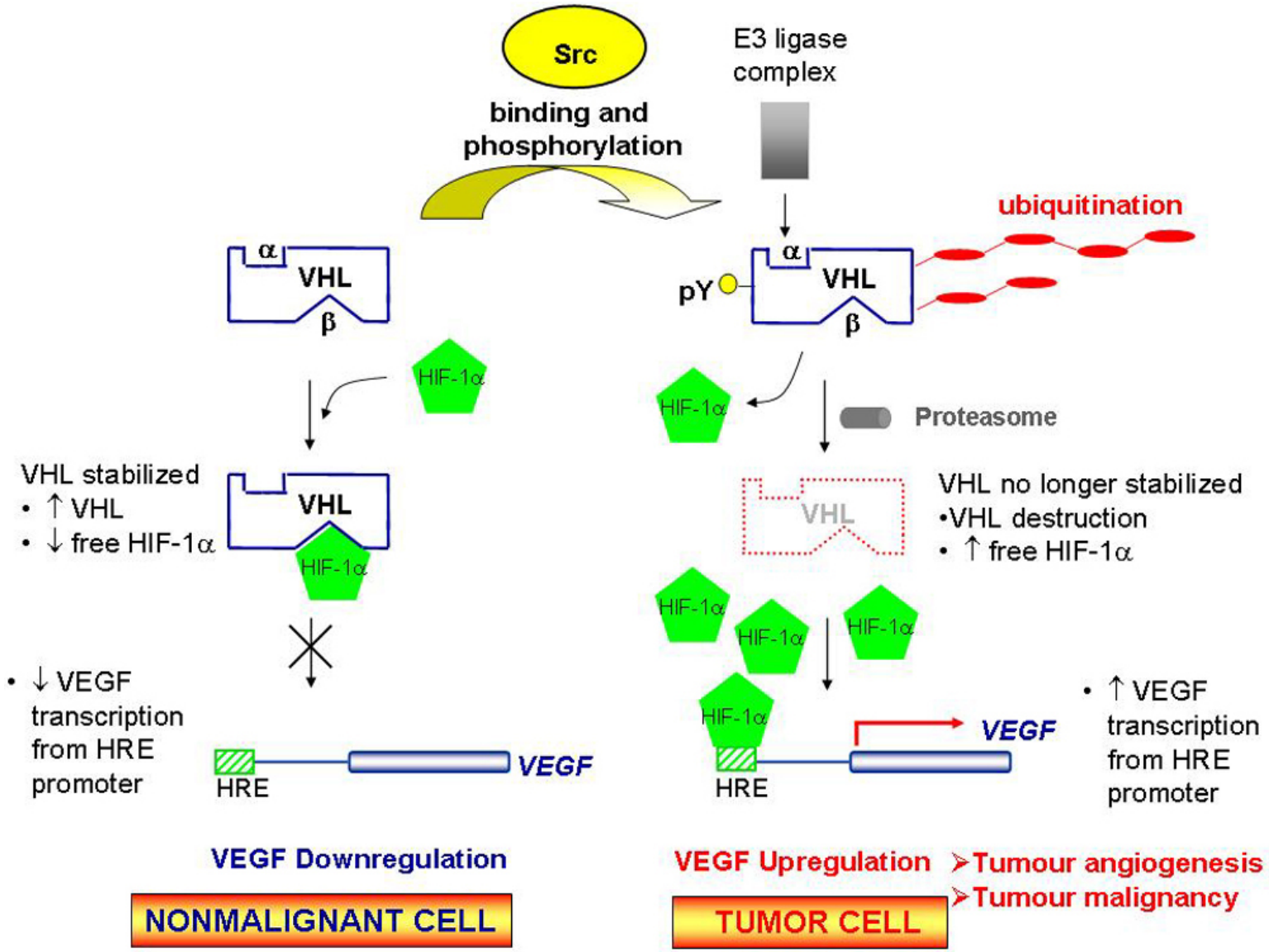
Src
binding and phosphorylation
E3 ligase complex
ubiquitination
α
VHL
β
pY
HIF-1α
Proteasome
VHL stabilized
• ↑ VHL
• ↓ free HIF-1α
VHL no longer stabilized
•VHL destruction
• ↑ free HIF-1α
• ↓ VEGF transcription from HRE promoter
HRE
VEGF
• ↑ VEGF transcription from HRE promoter
VEGF Downregulation
NONMALIGNANT CELL
VEGF Upregulation
➢Tumour angiogenesis
➢Tumour malignancy
TUMOR CELL

Figure 41. Model of Src downregulation of von Hippel-Lindau tumour suppressor protein and promotion of tumour angiogenesis and tumour progression.

Src-directed post-translational tyrosine phosphorylation modification of VHL allows tagging and recruitment of VHL for proteolysis by an E3 ligase complex. Also, post-translational modification of VHL may displace VHL from the VHL E3 ligase complex (thereby facilitating ubiquitin tagging and recruitment of VHL for proteolysis by E3 ligase complexes and/or facilitating VHL protein instability). Consequently, a build up of increased levels of HIF-1α upregulates VEGF production, and ultimately increases tumour angiogenesis, and increases the potential for tumour progression.

REFERENCES

Aiello,L.P., George,D.J., Cahill,M.T., Wong,J.S., Cavallerano,J., Hannah,A.L., Kaelin,W.G., Jr. (2002). Rapid and durable recovery of visual function in a patient with von hippel-lindau syndrome after systemic therapy with vascular endothelial growth factor receptor inhibitor su5416. Ophthalmology *109*, 1745-1751.

Alexandropoulos,K., Cheng,G., Baltimore,D. (1995). Proline-rich sequences that bind to Src homology 3 domains with individual specificities. Proc.Natl.Acad.Sci.U.S.A *92*, 3110-3114.

Alonso,G., Koegl,M., Mazurenko,N., Courtneidge,S.A. (1995). Sequence requirements for binding of Src family tyrosine kinases to activated growth factor receptors. J.Biol.Chem. *270*, 9840-9848.

An,J., Rettig,M.B. (2005). Mechanism of von Hippel-Lindau protein-mediated suppression of nuclear factor kappa B activity. Mol.Cell Biol. *25*, 7546-7556.

Baba,M., Hirai,S., Kawakami,S., Kishida,T., Sakai,N., Kaneko,S., Yao,M., Shuin,T., Kubota,Y., Hosaka,M., Ohno,S. (2001). Tumor suppressor protein VHL is induced at high cell density and mediates contact inhibition of cell growth. Oncogene *20*, 2727-2736.

Bao,J., Gur,G., Yarden,Y. (2003). Src promotes destruction of c-Cbl: implications for oncogenic synergy between Src and growth factor receptors. Proc.Natl.Acad.Sci.U.S.A *100*, 2438-2443.

Bergers,G., Javaherian,K., Lo,K.M., Folkman,J., Hanahan,D. (1999). Effects of angiogenesis inhibitors on multistage carcinogenesis in mice. Science *284*, 808-812.

Bishop,T., Lau,K.W., Epstein,A.C., Kim,S.K., Jiang,M., O'Rourke,D., Pugh,C.W., Gleadle,J.M., Taylor,M.S., Hodgkin,J., Ratcliffe,P.J. (2004). Genetic analysis of pathways regulated by the von Hippel-Lindau tumor suppressor in Caenorhabditis elegans. PLoS.Biol. *2*, e289.

Bjorge,J.D., Pang,A., Fujita,D.J. (2000). Identification of protein-tyrosine phosphatase 1B as the major tyrosine phosphatase activity capable of dephosphorylating and activating c-Src in several human breast cancer cell lines. J.Biol.Chem. *275*, 41439-41446.

Blankenship,C., Naglich,J.G., Whaley,J.M., Seizinger,B., Kley,N. (1999). Alternate choice of initiation codon produces a biologically active product of the von Hippel Lindau gene with tumor suppressor activity. Oncogene *18*, 1529-1535.

Bolen,J.B., Veillette,A., Schwartz,A.M., DeSeau,V., Rosen,N. (1987a). Activation of pp60c-src protein kinase activity in human colon carcinoma. Proc.Natl.Acad.Sci.U.S.A *84*, 2251-2255.

Bolen,J.B., Veillette,A., Schwartz,A.M., DeSeau,V., Rosen,N. (1987b). Analysis of pp60c-src in human colon carcinoma and normal human colon mucosal cells. Oncogene Res. *1*, 149-168.

Bonicalzi,M.E., Groulx,I., de Paulsen,N., Lee,S. (2001). Role of exon 2-encoded beta -domain of the von Hippel-Lindau tumor suppressor protein. J.Biol.Chem. *276*, 1407-1416.

Boyce,B.F., Yoneda,T., Lowe,C., Soriano,P., Mundy,G.R. (1992). Requirement of pp60c-src expression for osteoclasts to form ruffled borders and resorb bone in mice. J.Clin.Invest *90*, 1622-1627.

Brown,M.T., Cooper,J.A. (1996). Regulation, substrates and functions of src. Biochim.Biophys.Acta *1287*, 121-149.

Caldwell,M.C., Hough,C., Furer,S., Linehan,W.M., Morin,P.J., Gorospe,M. (2002). Serial analysis of gene expression in renal carcinoma cells reveals VHL-dependent sensitivity to TNFalpha cytotoxicity. Oncogene *21*, 929-936.

Carmeliet,P. (2000). Mechanisms of angiogenesis and arteriogenesis. Nat.Med. *6*, 389-395.

Cartwright,C.A., Meisler,A.I., Eckhart,W. (1990). Activation of the pp60c-src protein kinase is an early event in colonic carcinogenesis. Proc.Natl.Acad.Sci.U.S.A *87*, 558-562.

Cavallaro,U., Christofori,G. (2000). Molecular mechanisms of tumor angiogenesis and tumor progression. J.Neurooncol. *50*, 63-70.

Chen,F., Kishida,T., Yao,M., Hustad,T., Glavac,D., Dean,M., Gnarra,J.R., Orcutt,M.L., Duh,F.M., Glenn,G., . (1995). Germline mutations in the von Hippel-Lindau disease tumor suppressor gene: correlations with phenotype. Hum.Mutat. *5*, 66-75.

Cicchetti,P., Mayer,B.J., Thiel,G., Baltimore,D. (1992). Identification of a protein that binds to the SH3 region of Abl and is similar to Bcr and GAP-rho. Science *257*, 803-806.

Cohen,A.J., Li,F.P., Berg,S., Marchetto,D.J., Tsai,S., Jacobs,S.C., Brown,R.S. (1979). Hereditary renal-cell carcinoma associated with a chromosomal translocation. N.Engl.J.Med. *301*, 592-595.

Corless,C.L., Kibel,A.S., Iliopoulos,O., Kaelin,W.G., Jr. (1997). Immunostaining of the von Hippel-Lindau gene product in normal and neoplastic human tissues. Hum.Pathol. *28*, 459-464.

Courtneidge,S.A., Fumagalli,S., Koegl,M., Superti-Furga,G., Twamley-Stein,G.M. (1993). The Src family of protein tyrosine kinases: regulation and functions. Dev.Suppl 57-64.

Crossey,P.A., Richards,F.M., Foster,K., Green,J.S., Prowse,A., Latif,F., Lerman,M.I., Zbar,B., Affara,N.A., Ferguson-Smith,M.A., . (1994). Identification of intragenic mutations in the von Hippel-Lindau disease tumour suppressor gene and correlation with disease phenotype. Hum.Mol.Genet. *3*, 1303-1308.

Czernilofsky,A.P., Levinson,A.D., Varmus,H.E., Bishop,J.M., Tischer,E., Goodman,H.M. (1980). Nucleotide sequence of an avian sarcoma virus oncogene (src) and proposed amino acid sequence for gene product. Nature *287*, 198-203.

Dames,S.A., Martinez-Yamout,M., De Guzman,R.N., Dyson,H.J., Wright,P.E. (2002). Structural basis for Hif-1 alpha /CBP recognition in the cellular hypoxic response. Proc.Natl.Acad.Sci.U.S.A *99*, 5271-5276.

Davidowitz,E.J., Schoenfeld,A.R., Burk,R.D. (2001). VHL induces renal cell differentiation and growth arrest through integration of cell-cell and cell-extracellular matrix signaling. Mol.Cell Biol. *21*, 865-874.

Ding,Q., Stewart,J., Jr., Olman,M.A., Klobe,M.R., Gladson,C.L. (2003). The pattern of enhancement of Src kinase activity on platelet-derived growth factor stimulation of glioblastoma cells is affected by the integrin engaged. J.Biol.Chem. *278*, 39882-39891.

Edgell,C.J., McDonald,C.C., Graham,J.B. (1983). Permanent cell line expressing human factor VIII-related antigen established by hybridization. Proc.Natl.Acad.Sci.U.S.A *80*, 3734-3737.

Egan,C., Pang,A., Durda,D., Cheng,H.C., Wang,J.H., Fujita,D.J. (1999). Activation of Src in human breast tumor cell lines: elevated levels of phosphotyrosine phosphatase activity that preferentially recognizes the Src carboxy terminal negative regulatory tyrosine 530. Oncogene *18*, 1227-1237.

Eickelberg,O., Seebach,F., Riordan,M., Thulin,G., Mann,A., Reidy,K.H., Van Why,S.K., Kashgarian,M., Siegel,N. (2002). Functional activation of heat shock factor and hypoxia-inducible factor in the kidney. J.Am.Soc.Nephrol. *13*, 2094-2101.

Ellis,L.M., Staley,C.A., Liu,W., Fleming,R.Y., Parikh,N.U., Bucana,C.D., Gallick,G.E. (1998). Down-regulation of vascular endothelial growth factor in a human colon carcinoma cell line transfected with an antisense expression vector specific for c-src. J.Biol.Chem. *273*, 1052-1057.

Esteban-Barragan,M.A., Avila,P., Alvarez-Tejado,M., Gutierrez,M.D., Garcia-Pardo,A., Sanchez-Madrid,F., Landazuri,M.O. (2002). Role of the von Hippel-Lindau tumor suppressor gene in the formation of beta1-integrin fibrillar adhesions. Cancer Res. *62*, 2929-2936.

Ferri,C., Pittoni,V., Piccoli,A., Laurenti,O., Cassone,M.R., Bellini,C., Properzi,G., Valesini,G., De Mattia,G., Santucci,A. (1995). Insulin stimulates endothelin-1 secretion from human endothelial cells and modulates its circulating levels in vivo. J.Clin.Endocrinol.Metab *80*, 829-835.

Fleming,R.Y., Ellis,L.M., Parikh,N.U., Liu,W., Staley,C.A., Gallick,G.E. (1997). Regulation of vascular endothelial growth factor expression in human colon carcinoma cells by activity of src kinase. Surgery *122*, 501-507.

Folkman,J. (1995). Angiogenesis in cancer, vascular, rheumatoid and other disease. Nat.Med. *1*, 27-31.

Fujita,Y., Krause,G., Scheffner,M., Zechner,D., Leddy,H.E., Behrens,J., Sommer,T., Birchmeier,W. (2002). Hakai, a c-Cbl-like protein, ubiquitinates and induces endocytosis of the E-cadherin complex. Nat.Cell Biol. *4*, 222-231.

Galban,S., Fan,J., Martindale,J.L., Cheadle,C., Hoffman,B., Woods,M.P., Temeles,G., Brieger,J., Decker,J., Gorospe,M. (2003). von Hippel-Lindau protein-mediated repression of tumor necrosis factor alpha translation revealed through use of cDNA arrays. Mol.Cell Biol. *23*, 2316-2328.

Girmens,J.F., Erginay,A., Massin,P., Scigalla,P., Gaudric,A., Richard,S. (2003). Treatment of von Hippel-Lindau retinal hemangioblastoma by the vascular endothelial growth factor receptor inhibitor SU5416 is more effective for associated macular edema than for hemangioblastomas. Am.J.Ophthalmol. *136*, 194-196.

Gnarra,J.R., Ward,J.M., Porter,F.D., Wagner,J.R., Devor,D.E., Grinberg,A., Emmert-Buck,M.R., Westphal,H., Klausner,R.D., Linehan,W.M. (1997). Defective placental vasculogenesis causes embryonic lethality in VHL-deficient mice. Proc.Natl.Acad.Sci.U.S.A *94*, 9102-9107.

Gnarra,J.R., Zhou,S., Merrill,M.J., Wagner,J.R., Krumm,A., Papavassiliou,E., Oldfield,E.H., Klausner,R.D., Linehan,W.M. (1996). Post-transcriptional regulation of vascular endothelial growth factor mRNA by the product of the VHL tumor suppressor gene. Proc.Natl.Acad.Sci.U.S.A *93*, 10589-10594.

Groulx,I., Bonicalzi,M.E., Lee,S. (2000). Ran-mediated nuclear export of the von Hippel-Lindau tumor suppressor protein occurs independently of its assembly with cullin-2. J.Biol.Chem. *275*, 8991-9000.

Groulx,I., Lee,S. (2002). Oxygen-dependent ubiquitination and degradation of hypoxia-inducible factor requires nuclear-cytoplasmic trafficking of the von Hippel-Lindau tumor suppressor protein. Mol.Cell Biol. *22*, 5319-5336.

Guillemin,K., Krasnow,M.A. (1997). The hypoxic response: huffing and HIFing. Cell *89*, 9-12.

Hakak,Y., Martin,G.S. (1999). Ubiquitin-dependent degradation of active Src. Curr.Biol. *9*, 1039-1042.

Harris,K.F., Shoji,I., Cooper,E.M., Kumar,S., Oda,H., Howley,P.M. (1999). Ubiquitin-mediated degradation of active Src tyrosine kinase. Proc.Natl.Acad.Sci.U.S.A *96*, 13738-13743.

Hergovich,A., Lisztwan,J., Barry,R., Ballschmieter,P., Krek,W. (2003). Regulation of microtubule stability by the von Hippel-Lindau tumour suppressor protein pVHL. Nat.Cell Biol. *5*, 64-70.

Hershko,A., Heller,H., Elias,S., Ciechanover,A. (1983). Components of ubiquitin-protein ligase system. Resolution, affinity purification, and role in protein breakdown. J.Biol.Chem. *258*, 8206-8214.

Hoffman,M.A., Ohh,M., Yang,H., Klco,J.M., Ivan,M., Kaelin,W.G., Jr. (2001). von Hippel-Lindau protein mutants linked to type 2C VHL disease preserve the ability to downregulate HIF. Hum.Mol.Genet. *10*, 1019-1027.

Horne,W.C., Neff,L., Chatterjee,D., Lomri,A., Levy,J.B., Baron,R. (1992). Osteoclasts express high levels of pp60c-src in association with intracellular membranes. J.Cell Biol. *119*, 1003-1013.

Huang,L.E., Gu,J., Schau,M., Bunn,H.F. (1998). Regulation of hypoxia-inducible factor 1alpha is mediated by an O2-dependent degradation domain via the ubiquitin-proteasome pathway. Proc.Natl.Acad.Sci.U.S.A *95*, 7987-7992.

Hunter,T., Cooper,J.A. (1985). Protein-tyrosine kinases. Annu.Rev.Biochem. *54*, 897-930.

Iliopoulos,O., Kibel,A., Gray,S., Kaelin,W.G., Jr. (1995). Tumour suppression by the human von Hippel-Lindau gene product. Nat.Med. *1*, 822-826.

Iliopoulos,O., Ohh,M., Kaelin,W.G., Jr. (1998). pVHL19 is a biologically active product of the von Hippel-Lindau gene arising from internal translation initiation. Proc.Natl.Acad.Sci.U.S.A *95*, 11661-11666.

Irby,R.B., Mao,W., Coppola,D., Kang,J., Loubeau,J.M., Trudeau,W., Karl,R., Fujita,D.J., Jove,R., Yeatman,T.J. (1999). Activating SRC mutation in a subset of advanced human colon cancers. Nat.Genet. *21*, 187-190.

Isner,J.M., Asahara,T. (1999). Angiogenesis and vasculogenesis as therapeutic strategies for postnatal neovascularization. J.Clin.Invest *103*, 1231-1236.

Ivan,M., Kondo,K., Yang,H., Kim,W., Valiando,J., Ohh,M., Salic,A., Asara,J.M., Lane,W.S., Kaelin,W.G., Jr. (2001). HIFalpha targeted for VHL-mediated destruction by proline hydroxylation: implications for O2 sensing. Science *292*, 464-468.

Iwai,K., Yamanaka,K., Kamura,T., Minato,N., Conaway,R.C., Conaway,J.W., Klausner,R.D., Pause,A. (1999). Identification of the von Hippel-lindau tumor-suppressor protein as part of an active E3 ubiquitin ligase complex. Proc.Natl.Acad.Sci.U.S.A *96*, 12436-12441.

Jaakkola,P., Mole,D.R., Tian,Y.M., Wilson,M.I., Gielbert,J., Gaskell,S.J., Kriegsheim,A., Hebestreit,H.F., Mukherji,M., Schofield,C.J., Maxwell,P.H., Pugh,C.W., Ratcliffe,P.J. (2001). Targeting of HIF-alpha to the von Hippel-Lindau ubiquitylation complex by O2-regulated prolyl hydroxylation. Science *292*, 468-472.

Jove,R., Hanafusa,H. (1987). Cell transformation by the viral src oncogene. Annu.Rev.Cell Biol. *3*, 31-56.

Jung,C.R., Hwang,K.S., Yoo,J., Cho,W.K., Kim,J.M., Kim,W.H., Im,D.S. (2006). E2-EPF UCP targets pVHL for degradation and associates with tumor growth and metastasis. Nat.Med. *12*, 809-816.

Kaelin,W.G., Jr. (2002). Molecular basis of the VHL hereditary cancer syndrome. Nat.Rev.Cancer *2*, 673-682.

Kaelin,W.G., Jr. (2004). The von Hippel-Lindau tumor suppressor gene and kidney cancer. Clin.Cancer Res. *10*, 6290S-6295S.

Kaelin,W.G., Jr. (2007). The von Hippel-Lindau tumor suppressor protein and clear cell renal carcinoma. Clin.Cancer Res. *13*, 680s-684s.

Kaelin,W.G., Jr. (2008). The von Hippel-Lindau tumour suppressor protein: O2 sensing and cancer. Nat.Rev.Cancer *8*, 865-873.

Kamura,T., Brower,C.S., Conaway,R.C., Conaway,J.W. (2002). A molecular basis for stabilization of the von Hippel-Lindau (VHL) tumor suppressor protein by components of the VHL ubiquitin ligase. J.Biol.Chem. *277*, 30388-30393.

Kamura,T., Koepp,D.M., Conrad,M.N., Skowyra,D., Moreland,R.J., Iliopoulos,O., Lane,W.S., Kaelin,W.G., Jr., Elledge,S.J., Conaway,R.C., Harper,J.W., Conaway,J.W. (1999). Rbx1, a component of the VHL tumor suppressor complex and SCF ubiquitin ligase. Science *284*, 657-661.

Kanda,S., Kanetake,H., Miyata,Y. (2007). Role of Src in angiopoietin 1-induced capillary morphogenesis of endothelial cells: Effect of chronic hypoxia on Src inhibition by PP2. Cell Signal. *19*, 472-480.

Kaplan,K.B., Swedlow,J.R., Morgan,D.O., Varmus,H.E. (1995). c-Src enhances the spreading of src-/- fibroblasts on fibronectin by a kinase-independent mechanism. Genes Dev. *9*, 1505-1517.

Karni,R., Dor,Y., Keshet,E., Meyuhas,O., Levitzki,A. (2002). Activated pp60c-Src leads to elevated hypoxia-inducible factor (HIF)-1alpha expression under normoxia. J.Biol.Chem. *277*, 42919-42925.

Kmiecik,T.E., Shalloway,D. (1987). Activation and suppression of pp60c-src transforming ability by mutation of its primary sites of tyrosine phosphorylation. Cell *49*, 65-73.

Knudson,A.G., Jr. (1971). Mutation and cancer: statistical study of retinoblastoma. Proc.Natl.Acad.Sci.U.S.A *68*, 820-823.

Kurban,G., Hudon,V., Duplan,E., Ohh,M., Pause,A. (2006). Characterization of a von Hippel Lindau pathway involved in extracellular matrix remodeling, cell invasion, and angiogenesis. Cancer Res. *66*, 1313-1319.

Kwon,M., Yoon,C.S., Fitzpatrick,S., Kassam,G., Graham,K.S., Young,M.K., Waisman,D.M. (2001). p22 is a novel plasminogen fragment with antiangiogenic activity. Biochemistry *40*, 13246-13253.

Laemmli,U.K. (1970). Cleavage of structural proteins during the assembly of the head of bacteriophage T4. Nature *227*, 680-685.

Lando,D., Peet,D.J., Gorman,J.J., Whelan,D.A., Whitelaw,M.L., Bruick,R.K. (2002). FIH-1 is an asparaginyl hydroxylase enzyme that regulates the transcriptional activity of hypoxia-inducible factor. Genes Dev. *16*, 1466-1471.

Latif,F., Tory,K., Gnarra,J., Yao,M., Duh,F.M., Orcutt,M.L., Stackhouse,T., Kuzmin,I., Modi,W., Geil,L., . (1993). Identification of the von Hippel-Lindau disease tumor suppressor gene. Science *260*, 1317-1320.

LaVallee,T.M., Prudovsky,I.A., McMahon,G.A., Hu,X., Maciag,T. (1998). Activation of the MAP kinase pathway by FGF-1 correlates with cell proliferation induction while activation of the Src pathway correlates with migration. J.Cell Biol. *141*, 1647-1658.

Levitzki,A. (1996). SRC as a target for anti-cancer drugs. Anticancer Drug Des *11*, 175-182.

Levy,J.B., Iba,H., Hanafusa,H. (1986). Activation of the transforming potential of p60c-src by a single amino acid change. Proc.Natl.Acad.Sci.U.S.A *83*, 4228-4232.

Li,Z., Na,X., Wang,D., Schoen,S.R., Messing,E.M., Wu,G. (2002). Ubiquitination of a novel deubiquitinating enzyme requires direct binding to von Hippel-Lindau tumor suppressor protein. J.Biol.Chem. *277*, 4656-4662.

Li,Z., Wang,D., Na,X., Schoen,S.R., Messing,E.M., Wu,G. (2003). The VHL protein recruits a novel KRAB-A domain protein to repress HIF-1alpha transcriptional activity. EMBO J. *22*, 1857-1867.

Lisztwan,J., Imbert,G., Wirbelauer,C., Gstaiger,M., Krek,W. (1999). The von Hippel-Lindau tumor suppressor protein is a component of an E3 ubiquitin-protein ligase activity. Genes Dev. *13*, 1822-1833.

Lolkema,M.P., Gervais,M.L., Snijckers,C.M., Hill,R.P., Giles,R.H., Voest,E.E., Ohh,M. (2005). Tumor suppression by the von Hippel-Lindau protein requires phosphorylation of the acidic domain. J.Biol.Chem. *280*, 22205-22211.

Lowell,C.A., Niwa,M., Soriano,P., Varmus,H.E. (1996). Deficiency of the Hck and Src tyrosine kinases results in extreme levels of extramedullary hematopoiesis. Blood *87*, 1780-1792.

Lubensky,I.A., Gnarra,J.R., Bertheau,P., Walther,M.M., Linehan,W.M., Zhuang,Z. (1996). Allelic deletions of the VHL gene detected in multiple microscopic clear cell renal lesions in von Hippel-Lindau disease patients. Am.J.Pathol. *149*, 2089-2094.

Luttrell,D.K., Lee,A., Lansing,T.J., Crosby,R.M., Jung,K.D., Willard,D., Luther,M., Rodriguez,M., Berman,J., Gilmer,T.M. (1994). Involvement of pp60c-src with two major signaling pathways in human breast cancer. Proc.Natl.Acad.Sci.U.S.A *91*, 83-87.

Lutz,M.P., Esser,I.B., Flossmann-Kast,B.B., Vogelmann,R., Luhrs,H., Friess,H., Buchler,M.W., Adler,G. (1998). Overexpression and activation of the tyrosine kinase Src in human pancreatic carcinoma. Biochem.Biophys.Res.Commun. *243*, 503-508.

Maa,M.C., Leu,T.H., McCarley,D.J., Schatzman,R.C., Parsons,S.J. (1995). Potentiation of epidermal growth factor receptor-mediated oncogenesis by c-Src: implications for the etiology of multiple human cancers. Proc.Natl.Acad.Sci.U.S.A *92*, 6981-6985.

Madhusudan,S., Deplanque,G., Braybrooke,J.P., Cattell,E., Taylor,M., Price,P., Tsaloumas,M.D., Moore,N., Huson,S.M., Adams,C., Frith,P., Scigalla,P., Harris,A.L. (2004). Antiangiogenic therapy for von Hippel-Lindau disease. JAMA *291*, 943-944.

Maher,E.R., Kaelin,W.G., Jr. (1997). von Hippel-Lindau disease. Medicine (Baltimore) *76*, 381-391.

Mao,W., Irby,R., Coppola,D., Fu,L., Wloch,M., Turner,J., Yu,H., Garcia,R., Jove,R., Yeatman,T.J. (1997). Activation of c-Src by receptor tyrosine kinases in human colon cancer cells with high metastatic potential. Oncogene *15*, 3083-3090.

Masaki,T., Okada,M., Tokuda,M., Shiratori,Y., Hatase,O., Shirai,M., Nishioka,M., Omata,M. (1999). Reduced C-terminal Src kinase (Csk) activities in hepatocellular carcinoma. Hepatology *29*, 379-384.

Maxwell,P.H., Wiesener,M.S., Chang,G.W., Clifford,S.C., Vaux,E.C., Cockman,M.E., Wykoff,C.C., Pugh,C.W., Maher,E.R., Ratcliffe,P.J. (1999). The tumour suppressor protein VHL targets hypoxia-inducible factors for oxygen-dependent proteolysis. Nature *399*, 271-275.

Maynard,M.A., Ohh,M. (2004). Von Hippel-Lindau tumor suppressor protein and hypoxia-inducible factor in kidney cancer. Am.J.Nephrol. *24*, 1-13.

Mekhail,K., Gunaratnam,L., Bonicalzi,M.E., Lee,S. (2004). HIF activation by pH-dependent nucleolar sequestration of VHL. Nat.Cell Biol. *6*, 642-647.

Mekhail,K., Khacho,M., Carrigan,A., Hache,R.R., Gunaratnam,L., Lee,S. (2005). Regulation of ubiquitin ligase dynamics by the nucleolus. J.Cell Biol. *170*, 733-744.

Mori,S., Ronnstrand,L., Yokote,K., Engstrom,A., Courtneidge,S.A., Claesson-Welsh,L., Heldin,C.H. (1993). Identification of two juxtamembrane autophosphorylation sites in the PDGF beta-receptor; involvement in the interaction with Src family tyrosine kinases. EMBO J. *12*, 2257-2264.

Mukhopadhyay,D., Tsiokas,L., Zhou,X.M., Foster,D., Brugge,J.S., Sukhatme,V.P. (1995). Hypoxic induction of human vascular endothelial growth factor expression through c-Src activation. Nature *375*, 577-581.

Na,X., Duan,H.O., Messing,E.M., Schoen,S.R., Ryan,C.K., di Sant'Agnese,P.A., Golemis,E.A., Wu,G. (2003). Identification of the RNA polymerase II subunit hsRPB7 as a novel target of the von Hippel-Lindau protein. EMBO J. *22*, 4249-4259.

Neufeld,G., Kessler,O., Vadasz,Z., Gluzman-Poltorak,Z. (2001). The contribution of proangiogenic factors to the progression of malignant disease: role of vascular endothelial growth factor and its receptors. Surg.Oncol.Clin.N.Am. *10*, 339-56, ix.

Neumann,H.P., Bender,B.U. (1998). Genotype-phenotype correlations in von Hippel-Lindau disease. J.Intern.Med. *243*, 541-545.

Ohh,M., Kaelin,W.G., Jr. (2003). VHL and kidney cancer. Methods Mol.Biol. *222*, 167-183.

Ohh,M., Park,C.W., Ivan,M., Hoffman,M.A., Kim,T.Y., Huang,L.E., Pavletich,N., Chau,V., Kaelin,W.G. (2000). Ubiquitination of hypoxia-inducible factor requires direct binding to the beta-domain of the von Hippel-Lindau protein. Nat.Cell Biol. *2*, 423-427.

Ohh,M., Takagi,Y., Aso,T., Stebbins,C.E., Pavletich,N.P., Zbar,B., Conaway,R.C., Conaway,J.W., Kaelin,W.G., Jr. (1999). Synthetic peptides define critical contacts

between elongin C, elongin B, and the von Hippel-Lindau protein. J.Clin.Invest *104*, 1583-1591.

Ohh,M., Yauch,R.L., Lonergan,K.M., Whaley,J.M., Stemmer-Rachamimov,A.O., Louis,D.N., Gavin,B.J., Kley,N., Kaelin,W.G., Jr., Iliopoulos,O. (1998). The von Hippel-Lindau tumor suppressor protein is required for proper assembly of an extracellular fibronectin matrix. Mol.Cell *1*, 959-968.

Okuda,H., Hirai,S., Takaki,Y., Kamada,M., Baba,M., Sakai,N., Kishida,T., Kaneko,S., Yao,M., Ohno,S., Shuin,T. (1999). Direct interaction of the beta-domain of VHL tumor suppressor protein with the regulatory domain of atypical PKC isotypes. Biochem.Biophys.Res.Commun. *263*, 491-497.

Okuda,H., Saitoh,K., Hirai,S., Iwai,K., Takaki,Y., Baba,M., Minato,N., Ohno,S., Shuin,T. (2001). The von Hippel-Lindau tumor suppressor protein mediates ubiquitination of activated atypical protein kinase C. J.Biol.Chem. *276*, 43611-43617.

Ottenhoff-Kalff,A.E., Rijksen,G., van Beurden,E.A., Hennipman,A., Michels,A.A., Staal,G.E. (1992). Characterization of protein tyrosine kinases from human breast cancer: involvement of the c-src oncogene product. Cancer Res. *52*, 4773-4778.

Parsons,J.T., Weber,M.J. (1989). Genetics of src: structure and functional organization of a protein tyrosine kinase. Curr.Top.Microbiol.Immunol. *147*, 79-127.

Pause,A., Lee,S., Lonergan,K.M., Klausner,R.D. (1998). The von Hippel-Lindau tumor suppressor gene is required for cell cycle exit upon serum withdrawal. Proc.Natl.Acad.Sci.U.S.A *95*, 993-998.

Pawson,T., Gish,G.D. (1992). SH2 and SH3 domains: from structure to function. Cell *71*, 359-362.

Peng,Z.Y., Cartwright,C.A. (1995). Regulation of the Src tyrosine kinase and Syp tyrosine phosphatase by their cellular association. Oncogene *11*, 1955-1962.

Petrella,B.L., Lohi,J., Brinckerhoff,C.E. (2005). Identification of membrane type-1 matrix metalloproteinase as a target of hypoxia-inducible factor-2 alpha in von Hippel-Lindau renal cell carcinoma. Oncogene *24*, 1043-1052.

Piwnica-Worms,H., Saunders,K.B., Roberts,T.M., Smith,A.E., Cheng,S.H. (1987). Tyrosine phosphorylation regulates the biochemical and biological properties of pp60c-src. Cell *49*, 75-82.

Potente,M., Urbich,C., Sasaki,K.I., Hofmann,W.K., Heeschen,C., Aicher,A., Kollipara,R., Depinho,R.A., Zeiher,A.M., Dimmeler,S. (2005). Involvement of Foxo transcription factors in angiogenesis and postnatal neovascularization. J.Clin.Invest *115*, 2382-2392.

Qi,H., Ohh,M. (2003). The von Hippel-Lindau tumor suppressor protein sensitizes renal cell carcinoma cells to tumor necrosis factor-induced cytotoxicity by suppressing the nuclear factor-kappaB-dependent antiapoptotic pathway. Cancer Res. *63*, 7076-7080.

Rahimi,N., Hung,W., Tremblay,E., Saulnier,R., Elliott,B. (1998). c-Src kinase activity is required for hepatocyte growth factor-induced motility and anchorage-independent growth of mammary carcinoma cells. J.Biol.Chem. *273*, 33714-33721.

Rankin,E.B., Tomaszewski,J.E., Haase,V.H. (2006). Renal cyst development in mice with conditional inactivation of the von Hippel-Lindau tumor suppressor. Cancer Res. *66*, 2576-2583.

Ren,R., Mayer,B.J., Cicchetti,P., Baltimore,D. (1993). Identification of a ten-amino acid proline-rich SH3 binding site. Science *259*, 1157-1161.

Resh,M.D. (1994). Myristylation and palmitylation of Src family members: the fats of the matter. Cell *76*, 411-413.

Richard,S., Croisille,L., Yvart,J., Casadeval,N., Eschwege,P., Aghakhani,N., David,P., Gaudric,A., Scigalla,P., Hermine,O. (2002). Paradoxical secondary polycythemia in von Hippel-Lindau patients treated with anti-vascular endothelial growth factor receptor therapy. Blood *99*, 3851-3853.

Richards,F.M. (2001). Molecular pathology of von HippelLindau disease and the VHL tumour suppressor gene. Expert.Rev.Mol.Med. *2001*, 1-27.

Roe,J.S., Kim,H., Lee,S.M., Kim,S.T., Cho,E.J., Youn,H.D. (2006). p53 stabilization and transactivation by a von Hippel-Lindau protein. Mol.Cell *22*, 395-405.

Rosenkranz,S., Ikuno,Y., Leong,F.L., Klinghoffer,R.A., Miyake,S., Band,H., Kazlauskas,A. (2000). Src family kinases negatively regulate platelet-derived growth factor alpha receptor-dependent signaling and disease progression. J.Biol.Chem. *275*, 9620-9627.

Ruegg,C., Yilmaz,A., Bieler,G., Bamat,J., Chaubert,P., Lejeune,F.J. (1998). Evidence for the involvement of endothelial cell integrin alphaVbeta3 in the disruption of the tumor vasculature induced by TNF and IFN-gamma. Nat.Med. *4*, 408-414.

Schoenfeld,A., Davidowitz,E.J., Burk,R.D. (1998). A second major native von Hippel-Lindau gene product, initiated from an internal translation start site, functions as a tumor suppressor. Proc.Natl.Acad.Sci.U.S.A *95*, 8817-8822.

Schoenfeld,A.R., Davidowitz,E.J., Burk,R.D. (2000a). Elongin BC complex prevents degradation of von Hippel-Lindau tumor suppressor gene products. Proc.Natl.Acad.Sci.U.S.A *97*, 8507-8512.

Schoenfeld,A.R., Parris,T., Eisenberger,A., Davidowitz,E.J., De Leon,M., Talasazan,F., Devarajan,P., Burk,R.D. (2000b). The von Hippel-Lindau tumor suppressor gene protects cells from UV-mediated apoptosis. Oncogene *19*, 5851-5857.

Schwartzberg,P.L., Xing,L., Hoffmann,O., Lowell,C.A., Garrett,L., Boyce,B.F., Varmus,H.E. (1997). Rescue of osteoclast function by transgenic expression of kinase-deficient Src in src-/- mutant mice. Genes Dev. *11*, 2835-2844.

Semenza,G.L. (1999). Perspectives on oxygen sensing. Cell *98*, 281-284.

Semenza,G.L. (2000). Expression of hypoxia-inducible factor 1: mechanisms and consequences. Biochem.Pharmacol. *59*, 47-53.

Semenza,G.L., Wang,G.L. (1992). A nuclear factor induced by hypoxia via de novo protein synthesis binds to the human erythropoietin gene enhancer at a site required for transcriptional activation. Mol.Cell Biol. *12*, 5447-5454.

Smart,J.E., Oppermann,H., Czernilofsky,A.P., Purchio,A.F., Erikson,R.L., Bishop,J.M. (1981). Characterization of sites for tyrosine phosphorylation in the transforming protein of Rous sarcoma virus (pp60v-src) and its normal cellular homologue (pp60c-src). Proc.Natl.Acad.Sci.U.S.A *78*, 6013-6017.

Songyang,Z., Carraway,K.L., III, Eck,M.J., Harrison,S.C., Feldman,R.A., Mohammadi,M., Schlessinger,J., Hubbard,S.R., Smith,D.P., Eng,C., . (1995). Catalytic specificity of protein-tyrosine kinases is critical for selective signalling. Nature *373*, 536-539.

Songyang,Z., Shoelson,S.E., Chaudhuri,M., Gish,G., Pawson,T., Haser,W.G., King,F., Roberts,T., Ratnofsky,S., Lechleider,R.J., . (1993). SH2 domains recognize specific phosphopeptide sequences. Cell *72*, 767-778.

Soriano,P., Montgomery,C., Geske,R., Bradley,A. (1991). Targeted disruption of the c-src proto-oncogene leads to osteopetrosis in mice. Cell *64*, 693-702.

Stebbins,C.E., Kaelin,W.G., Jr., Pavletich,N.P. (1999). Structure of the VHL-ElonginC-ElonginB complex: implications for VHL tumor suppressor function. Science *284*, 455-461.

Stehelin,D., Varmus,H.E., Bishop,J.M., Vogt,P.K. (1976). DNA related to the transforming gene(s) of avian sarcoma viruses is present in normal avian DNA. Nature *260*, 170-173.

Stickle,N.H., Chung,J., Klco,J.M., Hill,R.P., Kaelin,W.G., Jr., Ohh,M. (2004). pVHL modification by NEDD8 is required for fibronectin matrix assembly and suppression of tumor development. Mol.Cell Biol. *24*, 3251-3261.

Stratmann,R., Krieg,M., Haas,R., Plate,K.H. (1997). Putative control of angiogenesis in hemangioblastomas by the von Hippel-Lindau tumor suppressor gene. J.Neuropathol.Exp.Neurol. *56*, 1242-1252.

Summy,J.M., Trevino,J.G., Baker,C.H., Gallick,G.E. (2005). c-Src regulates constitutive and EGF-mediated VEGF expression in pancreatic tumor cells through activation of phosphatidyl inositol-3 kinase and p38 MAPK. Pancreas *31*, 263-274.

Tang,N., Mack,F., Haase,V.H., Simon,M.C., Johnson,R.S. (2006). pVHL function is essential for endothelial extracellular matrix deposition. Mol.Cell Biol. *26*, 2519-2530.

Tanimoto,K., Makino,Y., Pereira,T., Poellinger,L. (2000). Mechanism of regulation of the hypoxia-inducible factor-1 alpha by the von Hippel-Lindau tumor suppressor protein. EMBO J. *19*, 4298-4309.

Thomas,S.M., Brugge,J.S. (1997). Cellular functions regulated by Src family kinases. Annu.Rev.Cell Dev.Biol. *13*, 513-609.

Tice,D.A., Biscardi,J.S., Nickles,A.L., Parsons,S.J. (1999). Mechanism of biological synergy between cellular Src and epidermal growth factor receptor. Proc.Natl.Acad.Sci.U.S.A *96*, 1415-1420.

Troyanovsky,B., Levchenko,T., Mansson,G., Matvijenko,O., Holmgren,L. (2001). Angiomotin: an angiostatin binding protein that regulates endothelial cell migration and tube formation. J.Cell Biol. *152*, 1247-1254.

van der,H.E., de Krijger,R.R., Dinjens,W.N., Weeks,L.E., Bonjer,H.J., Bruining,H.A., Lamberts,S.W., Koper,J.W. (1998). Germline mutations in the vhl gene in patients presenting with phaeochromocytomas. Int.J.Cancer *77*, 337-340.

Verbeek,B.S., Vroom,T.M., Adriaansen-Slot,S.S., Ottenhoff-Kalff,A.E., Geertzema,J.G., Hennipman,A., Rijksen,G. (1996). c-Src protein expression is increased in human breast cancer. An immunohistochemical and biochemical analysis. J.Pathol. *180*, 383-388.

Visser,C.J., Rijksen,G., Woutersen,R.A., de Weger,R.A. (1996). Increased immunoreactivity and protein tyrosine kinase activity of the protooncogene pp60c-src in preneoplastic lesions in rat pancreas. Lab Invest *74*, 2-11.

Weis,S., Shintani,S., Weber,A., Kirchmair,R., Wood,M., Cravens,A., McSharry,H., Iwakura,A., Yoon,Y.S., Himes,N., Burstein,D., Doukas,J., Soll,R., Losordo,D., Cheresh,D. (2004). Src blockade stabilizes a Flk/cadherin complex, reducing edema and tissue injury following myocardial infarction. J.Clin.Invest *113*, 885-894.

Weissenberger,J., Loeffler,S., Kappeler,A., Kopf,M., Lukes,A., Afanasieva,T.A., Aguzzi,A., Weis,J. (2004). IL-6 is required for glioma development in a mouse model. Oncogene *23*, 3308-3316.

Wiener,J.R., Nakano,K., Kruzelock,R.P., Bucana,C.D., Bast,R.C., Jr., Gallick,G.E. (1999). Decreased Src tyrosine kinase activity inhibits malignant human ovarian cancer tumor growth in a nude mouse model. Clin.Cancer Res. *5*, 2164-2170.

Yokouchi,M., Kondo,T., Sanjay,A., Houghton,A., Yoshimura,A., Komiya,S., Zhang,H., Baron,R. (2001). Src-catalyzed phosphorylation of c-Cbl leads to the interdependent ubiquitination of both proteins. J.Biol.Chem. *276*, 35185-35193.

Zbar,B., Kishida,T., Chen,F., Schmidt,L., Maher,E.R., Richards,F.M., Crossey,P.A., Webster,A.R., Affara,N.A., Ferguson-Smith,M.A., Brauch,H., Glavac,D., Neumann,H.P., Tisherman,S., Mulvihill,J.J., Gross,D.J., Shuin,T., Whaley,J., Seizinger,B., Kley,N., Olschwang,S., Boisson,C., Richard,S., Lips,C.H., Lerman,M., . (1996). Germline mutations in the Von Hippel-Lindau disease (VHL) gene in families from North America, Europe, and Japan. Hum.Mutat. *8*, 348-357.

Zhu,H., Bunn,H.F. (2001). Signal transduction. How do cells sense oxygen? Science *292*, 449-451.

Zhu,S., Bjorge,J.D., Fujita,D.J. (2007). PTP1B contributes to the oncogenic properties of colon cancer cells through Src activation. Cancer Res. *67*, 10129-10137.

Zia,M.K., Rmali,K.A., Watkins,G., Mansel,R.E., Jiang,W.G. (2007). The expression of the von Hippel-Lindau gene product and its impact on invasiveness of human breast cancer cells. Int.J.Mol.Med. *20*, 605-611.

APPENDIX

Publications

Chou, M.T.-H., Anthony, J., Bjorge, J.D., and Fujita, D.J. Src-mediated Destabilization of the VHL Tumour Suppressor Protein Upregulates VEGF Synthesis. In preparation, submission to *Cancer Research*.

Published Absracts

CBCRA Reasons for Hope Breast Cancer conference 2008, Vancouver, BC. --- Poster presentation and abstract: "Destabilization of the von Hippel-Lindau (VHL) Tumour Suppressor Protein by Src results in Upregulation of Vascular Endothelial Growth Factor Synthesis: Implications for Tumour Angiogenesis and Breast Cancer Metastasis." (April 25-28, 2008.)

Alberta Cancer Research Institute/Alberta Cancer Board meeting, Banff, AB. --- Invited seminar presentation, poster presentation, and abstract:: "Src-Mediated Destabilization of the von Hippel-Lindau Tumour Suppressor Protein Upregulates Vascular Endothelial Growth Factor Synthesis: Implications for Tumour Angiogenesis and Breast Cancer Metastasis" (Nov 6-8, 2007.)

Mechanisms & Models of Cancer meeting, Salk Institute, La Jolla, California. --- Poster presentation and abstract: "Src-Mediated Destabilization of the von Hippel-Lindau (VHL) Tumour Suppressor Protein Upregulates VEGF Synthesis." (Aug 8-12, 2007.)

Canadian Breast Cancer Research Alliance (CBCRA) Reasons for Hope Breast Cancer Conference 2006, Montreal, Quebec. --- Poster presentation and abstract: "Src-mediated Destabilization of the VHL Tumour Suppressor Protein Upregulates VEGF Synthesis." (May 6-8, 2006.)

19th Meeting on Oncogenes, Frederick, Maryland. --- Poster presentation and abstract: "Multiple Roles of Src in VEGF-Related Angiogenesis and Tumourigenesis." (Jun 18-21, 2003.)

Division of labour

Mary Chou planned the project, designed and conducted all experiments. In the cases of collaboration, MC cooperated in all design, conducting experiments, and data analysis. Thank you to Dr. Josephine Anthony for her collaborations and helpful discussions in the experimental studies to locate the Src phosphorylation site on VHL. JA was a post-doctoral fellow in Dr. Fujita's lab for the latter 8 months of 2008. Dr. Don Fujita provided scientific and technical guidance, and mentorship. DF cooperated in project/experimental planning design, and data analysis. DF mentored and supervised MC and JA.

The work presented in this thesis is currently being prepared for publication. The work in Chapter Three to Four and the work in Chapter Five are being prepared for submission as two papers respectively, for submission to Cancer Research.